

CYTOTOXIC EFFECTS OF MANSONONE G AND ETHOXY MANSONONE G FROM
MANSONIA GAGEI DRUMM IN NON-SMALL CELL LUNG CANCER



A Thesis Submitted in Partial Fulfillment of the Requirements
for the Degree of Master of Science in Pharmacology
Inter-Department of Pharmacology
Graduate School
Chulalongkorn University
Academic Year 2019
Copyright of Chulalongkorn University

ฤทธิ์ต้านมะเร็งของแมนโซโนนจีและอนุพันธ์ของสารแมนโซโนนจีที่สกัดได้จากต้นจันทน์ชะมดต่อ
มะเร็งปอดชนิดไม่ใช่เซลล์เล็ก



วิทยานิพนธ์นี้เป็นส่วนหนึ่งของการศึกษาตามหลักสูตรปริญญาวิทยาศาสตรมหาบัณฑิต
สาขาวิชาเภสัชวิทยา สหสาขาวิชาเภสัชวิทยา
บัณฑิตวิทยาลัย จุฬาลงกรณ์มหาวิทยาลัย
ปีการศึกษา 2562
ลิขสิทธิ์ของจุฬาลงกรณ์มหาวิทยาลัย

อรรชวิภา วรณโชติ : ฤทธิ์ต้านมะเร็งของแมนโซโนนจีและอนุพันธ์ของสารแมนโซโนนจีที่สกัดได้
จากต้นจันทน์ชะมดต่อมะเร็งปอดชนิดไม่ใช่เซลล์เล็ก. (CYTOTOXIC EFFECTS OF
MANSONONE G AND ETHOXY MANSONONE G FROM *MANSONIA GAGEI* DRUMM IN
NON-SMALL CELL LUNG CANCER) อ.ที่ปรึกษาหลัก : ผศ. ดร.ปิยนุช วงศ์อนันต์, อ.ที่ปรึกษา
ร่วม : ผศ. ดร.วัชรวิ ลิมปนสิทธิกุล, ผศ. ดร.วรินทร์ ขวศิริ

Monsonone เป็นสารในกลุ่ม naphthoquinone ที่สกัดมาจากเนื้อไม้ของต้น *Mansonia gagei* Drumm หรือต้นจันทน์ชะมด และพบว่าฤทธิ์ทางเภสัชวิทยาที่หลากหลาย ได้แก่ ฤทธิ์ต้านเชื้อราและเชื้อแบคทีเรีย ฤทธิ์ต้านอนุมูลอิสระ ฤทธิ์ต้านฮอร์โมนเอสโตรเจน ฤทธิ์ต้านเซลล์ไขมัน และฤทธิ์ต้านมะเร็ง จากการศึกษาที่ผ่านมาพบว่าอนุพันธ์ของสาร mansonone G (MG) ในกลุ่มเอเทอร์นั้นมีฤทธิ์ต้านเชื้อแบคทีเรียและฤทธิ์ต้านเซลล์ไขมันได้ดีกว่า MG ซึ่งเป็นไปได้ว่าอนุพันธ์ของสารแมนโซโนนจีนั้นอาจมีฤทธิ์ทางชีวภาพดีกว่าสาร MG อย่างไรก็ตามยังไม่เคยมีรายงานถึงการศึกษาฤทธิ์ต้านมะเร็งและกลไกการออกฤทธิ์ของสาร MG และอนุพันธ์ของสาร ได้แก่ ethoxy mansonone G (EMG) ในเซลล์มะเร็งปอดมาก่อน ในงานวิจัยนี้จึงสนใจที่จะศึกษาฤทธิ์ต้านมะเร็งของสาร MG และ EMG ในเซลล์มะเร็งปอดชนิดไม่ใช่เซลล์เล็ก ได้แก่ เซลล์ A549 ที่มี EGFR ปกติและเซลล์ H1975 ที่มีการกลายพันธุ์ของ EGFR ผลการศึกษาพบว่า MG และ EMG สามารถยับยั้งการรอดชีวิตของเซลล์มะเร็ง A549 และ H1975 โดยพบว่า EMG มีความเป็นพิษต่อเซลล์มะเร็งปอดมากกว่า MG และมีความเป็นพิษต่อเซลล์ปกติ PCS201-010 น้อยกว่าเซลล์มะเร็งปอด จากการศึกษาในระดับกลไกพบว่า EMG สามารถยับยั้งการเจริญเติบโตของเซลล์ A549 ผ่านการชักนำให้วัฏจักรเซลล์หยุดที่ระยะ G₁ แต่ไม่มีผลให้เกิดการสะสมของเซลล์ H1975 ในระยะใดระยะหนึ่งในวัฏจักรของเซลล์ นอกจากนี้ EMG สามารถเหนี่ยวนำให้เซลล์ A549 และ H1975 เกิดการตายแบบอะพอพโทซิสผ่านการสร้างอนุมูลอิสระโดยที่ *N*-acetyl cysteine (NAC) สามารถลดผลของ EMG ต่อการตายของเซลล์แบบอะพอพโทซิสทั้งในเซลล์ A549 และ H1975 และผลการศึกษาในระดับโปรตีนแสดงให้เห็นว่า EMG ลดการแสดงออกของโปรตีน Bcl-X_L และ Bcl-2 และเพิ่มการแสดงออกของ BAK และ BAX ในเซลล์ทั้งสองชนิด นอกจากนี้ EMG ยังสามารถกระตุ้นการทำงานของวิถีสัญญาณ AKT และ ERK1/2 ในเซลล์ A549 และยับยั้งการทำงานของวิถีสัญญาณ AKT และ ERK1/2 ในเซลล์ H1975 จากผลการศึกษาแสดงให้เห็นว่า EMG มีความเป็นพิษต่อเซลล์มะเร็งปอดชนิดไม่ใช่เซลล์เล็กผ่านการยับยั้งวัฏจักรเซลล์ ชักนำให้เกิดการตายแบบอะพอพโทซิส เหนี่ยวนำการสร้างอนุมูลอิสระ และปรับเปลี่ยนวิถีสัญญาณ AKT และ ERK1/2 ซึ่งชี้ให้เห็นว่า EMG อาจจะสามารถถูกพัฒนาให้เป็นยาต้านมะเร็งปอดในอนาคต

สาขาวิชา	เภสัชวิทยา	ลายมือชื่อ นิสิต
ปีการศึกษา	2562	ลายมือชื่อ อ.ที่ปรึกษาหลัก
		ลายมือชื่อ อ.ที่ปรึกษาร่วม
		ลายมือชื่อ อ.ที่ปรึกษาร่วม

5887269020 : MAJOR PHARMACOLOGY

KEYWORD: ETHOXY MANSONONE G, LUNG CANCER, CYTOTOXICITY, APOPTOSIS, CELL
CYCLE ARREST, ROS

Arachawipa Wannachote : CYTOTOXIC EFFECTS OF MANSONONE G AND ETHOXY
MANSONONE G FROM *MANSONIA GAGEI* DRUMM IN NON-SMALL CELL LUNG CANCER.
Advisor: Asst. Prof. PIYANUCH WONGANAN, Ph.D. Co-advisor: Asst. Prof. WACHAREE
LIMPANASITHIKUL, Ph.D., Asst. Prof. WARINTHORN CHAVASIRI, Ph.D.

Mansonones are naphthoquinone-containing compounds extracted from the heartwood of *Mansonia gagei*. Several studies have reported that mansonones have various pharmacological activities such as antibacterial, antifungal, antioxidant, antiestrogenic, antiadipogenic and anticancer effects. A previous study reported that ether analogues of mansonone G (MG), a major compound isolated from *Mansonia gagei* Drumm, displayed higher antibacterial and antiadipogenic activities than parent MG. However, the anticancer activities of MG and ethoxy MG (EMG) on lung cancer cells have never been investigated. This study aimed to determine cytotoxic activities of MG and EMG and the underlying mechanism(s) in two non-small cell lung cancer cell lines, EGFR wild-type A549 cells and EGFR mutant H1975 cells. The present study demonstrated that MG and EMG significantly inhibited the viability of A549 and H1975 cells in a concentration dependent manner. It should be noted that EMG displayed higher cytotoxicity than MG in both A549 and H1975 cells. Notably, EMG was more toxic to NSCLC cells than PCS201-010 normal cells. Mechanistic studies demonstrated that EMG induced cell cycle arrest at G₁ phase in A549 cells but did not induce cell cycle arrest at any phase of cell cycle in H1975 cells. Additionally, EMG induced apoptosis through ROS generation in both A549 and H1975 cells and this effect was abolished by *N*-acetyl cysteine (NAC). Western blotting revealed that EMG downregulated the expression of Bcl-X_L and Bcl-2 and upregulated the expression of BAK and BAX in both A549 and H1975 cells. EMG activated the phosphorylation of ERK1/2 and AKT in A549 cells whereas it inhibited the phosphorylation of ERK1/2 and AKT in H1975 cells. Taken together, the results of this study suggest that the cytotoxicity of EMG is mediated via induction of cell cycle arrest and apoptosis, generation of ROS and modulation of PI3K/AKT and MAPK/ERK signaling pathways in NSCLC cells. These results suggest that EMG is a promising anticancer agent for lung cancer.

Field of Study: Pharmacology

Student's Signature

Academic Year: 2019

Advisor's Signature

Co-advisor's Signature

Co-advisor's Signature

ACKNOWLEDGEMENTS

This study would not have been successfully completed without the support of many people. Firstly, I would like to express my deepest gratitude to my thesis advisor, Assistant Professor Dr. Piyanuch Wonganan and my thesis co-advisor Assistant Professor Dr. Wacharee Limpanasithikul, at the Department of Pharmacology, Faculty of Medicine for the patient guidance and dedication they provided me, all the way throughout my years of study and through the process of researching and writing this thesis. They have always been accommodating and lend a helping hand. They have supported me in everything I have done and encouraged me when I doubted myself. So, I am grateful to them.

I would like to thank my co-advisor, Assistant Professor Dr. Warinthorn Chavasiri at the Department of Chemistry, Faculty of Science, Chulalongkorn University for kindly providing plant extracts, MG and EMG.

I would like to gratefully acknowledge Assistant Professor Dr. Wannarasmi Ketchart at the Department of Pharmacology, Professor Dr. Apiwat Mutirangura at the Department of Anatomy, Faculty of Medicine, Chulalongkorn University and Miss Nalinee Pradubayat at the Department of Pharmacology, Faculty of Pharmacy, Rangsit University for providing non-small cell lung cancer cells and primary dermal fibroblasts cells. My thanks also go to Dr. Supranee Buranapraditkun at the Cellular Immunology Laboratory, Allergy and Clinical Immunology Unit, Department of Medicine, Faculty of Medicine, Chulalongkorn University for her technical assistance on flow cytometry.

I would like to thank all the lovely staffs at the Department of Pharmacology, Faculty of Medicine for their advice and assistance. Also, thanks to all Ph.D. and master's student at the Cell Culture Laboratory for encouragement and helpful suggestions about many cell culture techniques.

Finally, I would not forget to thank my parents who have supported me, encourage me and believed in me. They kept me going and this work would not have been possible without their support. Thank you.

Arachawipa Wannachote

TABLE OF CONTENTS

	Page
ABSTRACT (THAI).....	iii
ABSTRACT (ENGLISH)	iv
ACKNOWLEDGEMENTS.....	v
TABLE OF CONTENTS.....	vi
LIST OF TABLES.....	1
LIST OF FIGURES	2
LIST OF ABBREVIATIONS.....	4
CHAPTER I INTRODUCTION.....	8
1.1 Background and rationale.....	8
1.2 Objectives	10
1.3 Hypothesis	10
1.4 Conceptual framework.....	11
CHAPTER II LITERATURE REVIEWS	12
2.1 Lung cancer	12
2.1.1 Types of lung cancer.....	12
2.1.2 Risk factors of lung cancer	13
2.1.3 Treatment of lung cancer	13
2.2 Cell cycle.....	15
2.3 Apoptosis	16
2.3.1 Death-receptor-induced extrinsic apoptosis pathway	16
2.3.2 Mitochondrial-apoptosome-mediated intrinsic apoptosis pathway	17

2.4 Reactive oxygen species.....	18
2.5 Epidermal growth factor receptor cell proliferation signaling pathways.....	19
2.5.1 MAPK/ERK signaling pathway	19
2.5.2 PI3K/AKT signaling pathway.....	20
2.6 Mansonone and its derivative	21
CHAPTER III MATERIALS AND METHODS	25
3.1 Equipment.....	25
3.2 Materials.....	25
3.3 Reagents	25
3.4 Methods	27
3.4.1 Preparation of test compound stock solutions	27
3.4.2 Cell culture.....	27
3.4.3 Cytotoxicity assay.....	28
3.4.4 Analysis of cell cycle progression.....	28
3.4.5 Detection of apoptosis using Annexin-V/PI staining assay	29
3.4.6 ROS generation assay.....	29
3.4.7 Evaluation of protein expression using western blotting	30
CHAPTER IV RESULTS	32
4.1 Effect of mansonone G (MG), ethoxy mansonone G (EMG) and cisplatin (CDDP) on viability of non-small cell lung cancer and normal cells	32
4.2 Effect of EMG on ROS generation in A549 cells	35
4.3 Effect of EMG on cell cycle distribution in A549 cells	37
4.4 Effect of EMG on apoptosis induction in A549 cells	38

4.5 Effect of EMG on the expression of Bcl-2 family proteins in A549 cells	40
4.6 Apoptosis-inducing effect of EMG through ROS generation in A549 cells	43
4.7 Effect of EMG on MAPK/ERK and PI3K/AKT signaling pathways in A549 cells....	44
4.8 Effect of EMG on ROS generation in H1975 cells	46
4.9 Effect of EMG on cell cycle distribution in H1975 cells.....	48
4.10 Effect of EMG on apoptosis induction in H1975 cells	49
4.11 Effect of EMG on the expression of Bcl-2 family proteins in H1975 cells	52
4.12 Apoptosis-inducing effect of EMG through ROS generation in H1975 cells	55
4.13 Effect of EMG on MAPK/ERK and PI3K/AKT signaling pathways in H1975 cells	56
CHAPTER V DISCUSSION AND CONCLUSION	58
APPENDIX A PREPARATION OF REAGENTS	63
APPENDIX B RESULTS	67
REFERENCES.....	73
VITA	84

LIST OF TABLES

	Page
Table 1 IC_{50} and selectivity index values of MG, EMG and CDDP on A549, H1975 and PCS201-010 cells	35



LIST OF FIGURES

	Page
Figure 1 The cell cycle phases and their associated cyclin-dependent kinases (CDK)/cyclin complexes.....	16
Figure 2 Extrinsic and intrinsic apoptotic signaling pathways	18
Figure 3 MAPK/ERK signaling pathway	20
Figure 4 PI3K/AKT signaling pathway	21
Figure 5 Structures of mansonones C, E, F, G, H, I, N, O, P, Q and S	22
Figure 6 Structure of EMG	24
Figure 7 Effects of MG, EMG and CDDP on viability of A549 and H1975 cells.....	33
Figure 8 Effects of MG, EMG and CDDP on viability of PCS201-010 cells.	34
Figure 9 Effect of EMG on ROS generation in A549 cells.....	36
Figure 10 Effect of EMG on cell cycle distribution of A549 cells.	37
Figure 11 Apoptosis-inducing effect of EMG on A549 cells.	38
Figure 12 Effect of EMG on PARP cleavage in A549 cells.....	39
Figure 13 Effects of EMG on the expression of pro-apoptotic Bcl-2 family proteins in A549 cells.....	41
Figure 14 Effect of EMG on the expression of anti-apoptotic Bcl-2 family proteins in A549 cells.....	42
Figure 15 Apoptosis-inducing effect of EMG was mediated through ROS generation in A549 cells.....	43
Figure 16 Effects of EMG on MAPK/ERK and PI3K/AKT signaling pathways in A549 cells.....	45
Figure 17 Effect of EMG on ROS generation in H1975 cells.....	47
Figure 18 Effect of EMG on cell cycle distribution of H1975 cells.	48

Figure 19 Apoptosis-inducing effect of EMG on H1975 cells.	50
Figure 20 Effect of EMG on PARP cleavage in H1975 cells.	51
Figure 21 Effect of EMG on the expression of pro-apoptotic Bcl-2 family proteins in H1975 cells.....	53
Figure 22 Effect of EMG on the expression of anti-apoptotic Bcl-2 family proteins in H1975 cells.....	54
Figure 23 Apoptosis-inducing effect of EMG is mediated through ROS generation in H1975 cells.....	55
Figure 24 Effect of EMG on MAPK/ERK and PI3K/AKT signaling pathways in H1975 cells.....	57



LIST OF ABBREVIATIONS

%	Percentage
µg	Microgram
µM	Micromolar
ANOVA	Analysis of variance
APAF-1	Apoptotic protease-activating factor-1
ATCC	American Type Culture Collection
ATP	Adenosine triphosphate
BAK	Bcl-2 antagonist killer
BAX	Bcl-2 associated X protein
Bcl-2	B-cell lymphoma-2
Bcl-X _L	B-cell lymphoma-extra large
BH domain	Bcl-2 homology domain
Caspase	Cysteine aspartic acid specific protease
CDDP	Cisplatin
CDK	Cyclin dependent protein kinases
CO ₂	Carbon dioxide
COPD	Chronic obstructive pulmonary disease
cPARP	Cleaved poly (ADP-ribose) polymerase
DCF	Dichlorofluorescein
DCFH	Dichlorodihydrofluorescein
DCFH-DA	Dichloro-dihydro-fluorescein diacetate
DIABLO	Direct inhibitor of apoptosis-binding protein binding protein with a low isoelectric point
DISC	Death-inducing signaling complex
DMEM	Dulbecco's Modified Eagle Medium
DMSO	Dimethyl sulfoxide
DNA	Deoxyribonucleic acid

E2F	E2 factor
EGF	Epidermal growth factor
EGFR	Epidermal growth factor receptor
EMG	Ethoxy mansonone G
Endo G	Endonuclease G
ERK	Extracellular signal-regulated kinase
ER α	Estrogen receptor alpha
FADD	Fas-associated death domain
FasL	Fas Ligand
FasR	Fas receptor
FBS	Fetal bovine serum
FITC	Fluorescein conjugate
g/mol	Gram per mole
GAPDH	Glyceraldehyde 3-phosphase dehydrogenase
GDP	Guanosine diphosphate
GEF	Guanine nucleotide exchange factor
Grb2	Growth factor receptor-bound protein 2
GSH	Glutathione
GTP	Guanosine-5'-triphosphate
h	Hour
H ₂ O ₂	Hydrogen peroxide
HBSS	Hank's buffered salt solution
HO [•]	Hydroxyl radical
HRP	Horseradish peroxidase
IAP	Inhibitors of apoptosis protein
IARC	International Agency for Research on Cancer
IC ₅₀	Half inhibitory concentration
LSD	Least square difference
MAPK	Mitogen-activated protein kinase

MBC	Minimum bactericidal concentration
Mek	Mitogen-activated protein kinase
MG	Mansonone G
MIC	Minimum inhibitory concentration
mL	Milliliter
MPTP	Mitochondrial permeability transition pore
MTT	3-(4,5-dimethylthiazol-2-yl)-2,5-diphenyltetrazolium bromide
NAC	<i>N</i> -acetylcystein
NaOH	Sodium hydroxide
NCI	The National Cancer Institute of Thailand
NFDM	Non-fat dry milk
nm	nanometer
NSCLC	Non-small cell lung cancer
O ₂ ⁻	Superoxide anion
p53	Tumor suppressor protein 53
p-AKT	phospho-AKT
PARP	Poly (ADP-ribose) polymerase
PBS	Phosphate buffer saline
PDK1	Phosphoinositide-dependent kinase 1
p-ERK	phospho-ERK1/2
PH domain	Pleckstrin-homology domains
PI	Propidium iodide
PI3K	Phosphatidylinositol 3-kinase
PIP2	Phosphatidylinositol 4,5-bisphosphate
PIP3	Phosphatidylinositol-3,4,5-trisphosphate
PKB (AKT)	Protein kinase B
PPAR	Peroxisome proliferator-activated receptor
PS	Phosphatidyl serine

RAF	Rapidly accelerates fibrosarcoma
RAS	Rat sarcoma viral oncogene homolog
Rb	Retinoblastoma
RIPA	Radioimmunoprecipitation assay
RNase A	Ribonuclease A
ROS	Reactive oxygen species
rpm	Round per minutes
RPMI	Roswell Park Memorial Institute
SCLC	Small cell lung cancer
SDS	Sodium dodecyl sulfate
SEM	Standard error of mean
SI	Selective index
SMAC	Second mitochondria-derived activator of caspases
SOD	Superoxide dismutase
SOS	Son of sevenless
SPSS	Statistical package for the social sciences
TB	Tuberculosis
TBST	Tris-buffered saline containing 0.1% Tween 20
TEMED	<i>N,N,N,N</i> -tetramethyl ethylenediamine
TKI	Tyrosine kinase inhibitor
TNFR1	TNF-related apoptosis-inducing ligand receptor1
TNFR1	Tumor necrosis factor receptor 1
TNF- α	Tumor necrosis factor- α
TRADD	TNFR-associated death domain
TRAIL	TNF-related apoptosis-inducing ligand
VEGF	Vascular endothelial growth factor
VEGFR	Vascular endothelial growth factor receptor

CHAPTER I

INTRODUCTION

1.1 Background and rationale

Lung cancer is the leading cause of cancer deaths worldwide (1). In 2018, the International Agency for Research on Cancer (IARC) has reported that lung cancer is the most common cancer and the leading cause of death (2). The National Cancer Institute of Thailand (NCI) reported that in 2017, lung cancer has been the fourth most commonly diagnosed cancer in Thais after breast cancer, liver cancer, and colorectal cancer, respectively (3). Non-small cell lung cancer (NSCLC) is the most common form of lung cancer, accounting for approximately 80% of all cases. Treatment options for lung cancer include surgery, radiotherapy, chemotherapy, and targeted therapy (4). Chemotherapy is the most common treatment options for patients with advanced stage NSCLC. The chemotherapeutic drugs most often used for lung cancer are cisplatin, carboplatin and paclitaxel (5). Although chemotherapeutic agents have been commonly used to treat lung cancer patients, serious side effects often limit their clinical application. Mutations of epidermal growth factor receptor (EGFR) have been implicated in the pathogenesis of several cancers (6) and NSCLC patients with exon 19 deletion and exon 21 L858R substitution mutations can be effectively treated with first- and second-small molecule generation tyrosine kinase inhibitors (TKIs) such as gefitinib and afatinib (7-9). However, the use of EGFR TKIs are limited by the mechanisms of tumor resistance, such as the gatekeeper EGFR-T790M mutation, and bypass activation of signaling cascades (10). Given the fact that chemotherapeutic agents cause many serious side effects and NSCLC cells rapidly acquire resistance to EGFR TKIs; therefore, new compounds with high anticancer activity and low toxicity are critically needed.

Reactive oxygen species (ROS), such as superoxide anion ($O_2^{\cdot-}$), hydrogen peroxide (H_2O_2), and hydroxyl radical (HO^{\cdot}), are essential for various biological processes in normal and cancer cells (11). It is commonly known that increase in ROS level are

detected in cancer cells compared to normal cells due to high metabolic rate and mitochondrial dysfunction. However, excess cellular levels of ROS cause damage to proteins, nucleic acids, lipid membranes and organelles, leading to apoptotic cell death (7, 8). In fact, some commonly used chemotherapeutic drugs such as cisplatin, carboplatin, oxaliplatin and doxorubicin generate ROS in cancer cells (12). Therefore, inducing ROS production is a very promising therapeutic strategy for cancer treatment.

Mansonones are naphthoquinone-containing compounds extracted from the heartwood of *Mansonia gagei* (13). Several studies have reported that mansonones have various pharmacological activities such as antibacterial, antifungal, antioxidant, antiestrogenic, antiadipogenic and antitumor effects (14-17). A previous study demonstrated that mansonones E and F, isolated from the dried root bark of *Ulmus pumila*, exhibited anticancer activity against several types of cancer such as melanoma (A375-S2), cervical cancer (HeLa), breast cancer (MCF-7) and lymphoma (U937) cells (18). Similarly, mansonone E, isolated from *Thespesia populnea*, was found to significantly inhibit the growth of four cancer cell lines, including breast cancer (MCF-7), cervical cancer (HeLa), colon cancer (HT-29), and oral cavity cancer (KB). Moreover, it was shown that mansonone E induced apoptosis in HeLa cells by inducing oligonucleosomal fragmentation, activating caspase-3, downregulating expression of anti-apoptotic proteins, Bcl-X_L and Bcl-2 and upregulating expression of a proapoptotic protein, BAX (19).

Previously, Hairani *et al.* demonstrated that mansonone G (MG), a major compound isolated from *Mansonia gagei* Drumm, exhibited a good antibacterial activity. It however should be noted that ether analogues of MG, had higher antibacterial activity than the parent MG (13). In addition to antibacterial activity, a recent study has shown that the ether analogues of MG displayed higher antiadipogenic activity than the parent MG (20). Since the anticancer activities of MG and ethoxy MG (EMG) on lung cancer cells have never been investigated, the present study aimed to determine cytotoxic activities

of MG and EMG and the underlying mechanism(s) in two non-small cell lung cancer cell lines, EGFR wild-type A549 cells and EGFR mutant H1975 cells.

1.2 Objectives

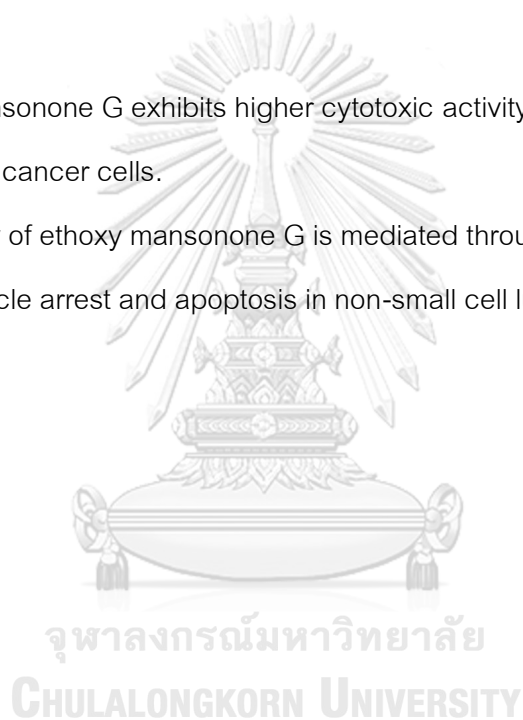
To study the cytotoxic activities of mansonone G and ethoxy mansonone G in non-small cell lung cancer cells.

To investigate mechanisms underlying cytotoxicity of mansonone G or ethoxy mansonone G in non-small cell lung cancer cells

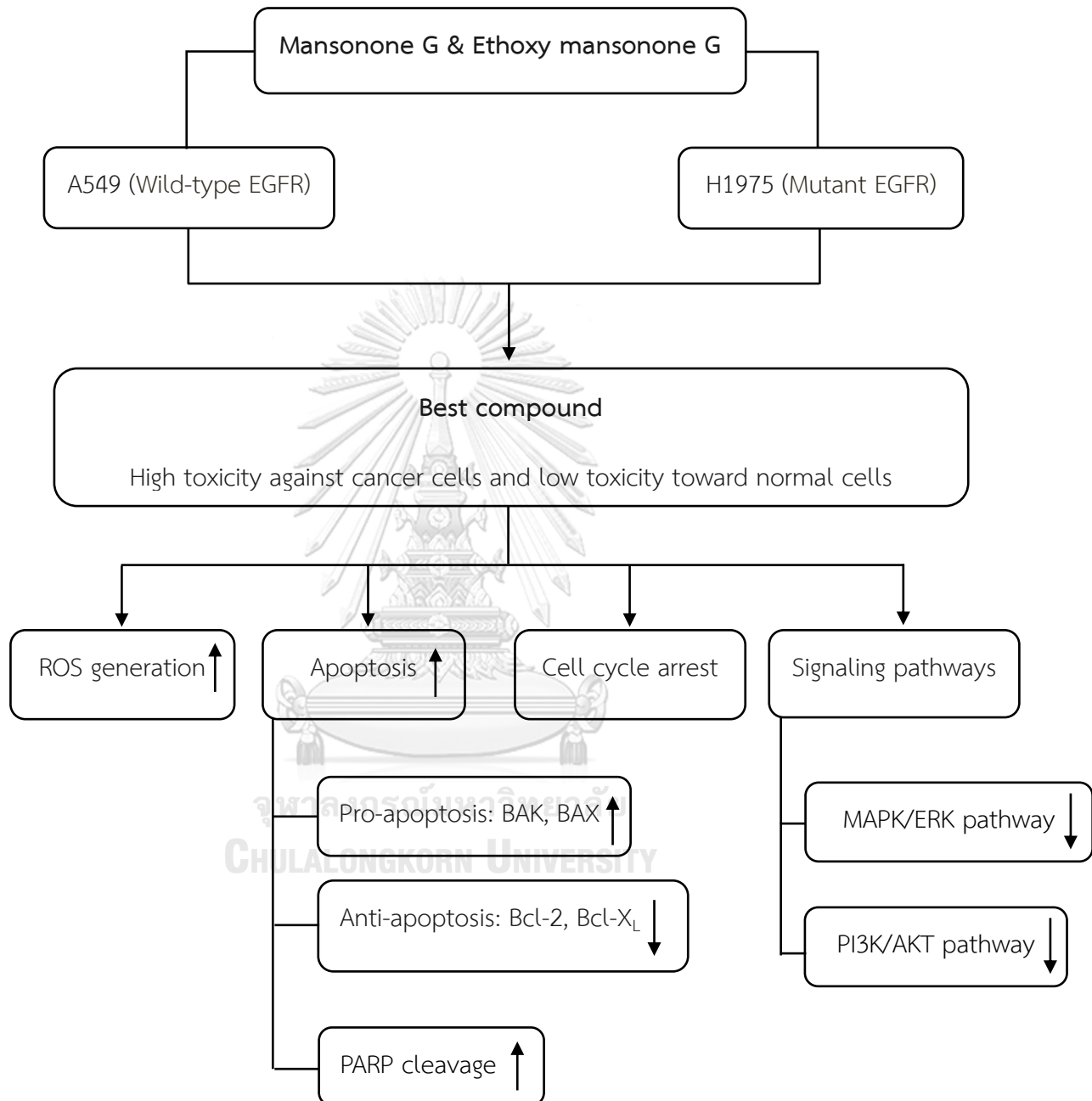
1.3 Hypothesis

Ethoxy mansonone G exhibits higher cytotoxic activity than mansonone G in non-small cell lung cancer cells.

Cytotoxicity of ethoxy mansonone G is mediated through production of ROS and induction of cell cycle arrest and apoptosis in non-small cell lung cancer cells.



1.4 Conceptual framework



CHAPTER II

LITERATURE REVIEWS

2.1 Lung cancer

Lung cancer is one of the most common human cancers and represents the leading cause of cancer mortality worldwide for both men and women. The American Cancer Society estimates that in 2019, approximately 228,150 new cases of lung cancer will be diagnosed (116,440 in men and 111,710 in women) and there will be an estimated 142,670 deaths from lung cancer (76,650 in men and 66,020 among women), accounting for about 23% of all cancer deaths in the United States (21). The National Cancer Institute of Thailand reported that in 2017, lung cancer has been the fourth most commonly diagnosed cancer in Thais after breast cancer, liver cancer, and colorectal cancer, respectively (3).

2.1.1 Types of lung cancer

Lung cancer can be mainly divided into 2 types including small cell lung cancer (SCLC) and non-small cell lung cancer (NSCLC).

i) **SCLC** accounts for 10%-15% of lung cancers. This type of lung cancer is the most aggressive form of lung cancer. SCLC grows and metastasizes rapidly to many sites within the body and is often diagnosed after cancer cells have extensively spread to other organs. SCLC is strongly related to cigarette smoking.

ii) **NSCLC** is the most common type of lung cancer, accounting for about 80% of all lung cancer. It usually grows and spreads more slowly than SCLC. NSCLC can be divided into several main types that are named based upon the type of cells found in the tumor.

(1) **Adenocarcinoma**, which accounts for about 40%, is the most common type of NSCLC and usually starts in cells that would normally secrete substances such as mucus. It is commonly found in the outer or peripheral areas of the lungs.

(2) **Squamous cell carcinoma**, which accounts for about 25-30%, generally starts in squamous cells, which are flat cells that line inside the airways of the lungs

(3) **Large cell carcinoma** accounts for about 10%-15%. It tends to grow and spread quickly, making it harder to treat.

(4) **Other subtypes** such as adenosquamous carcinoma and sarcomatoid carcinoma, are much less common (4).

2.1.2 Risk factors of lung cancer

- **Smoking** is by far the leading risk factor of lung cancer. It is shown that about 80% of lung cancer deaths results from smoking. The risk for lung cancer among smokers is many times higher than among non-smokers. Moreover, lung cancer is caused by exposure to secondhand smoke.

- **Personal or family history of lung cancer** People with a parent, sibling or child with lung cancer have an increased risk of this disease.

- **Exposure to other cancer-causing agents in the workplace or environment** For example, asbestos, radon, arsenic, uranium, beryllium, vinyl chloride, nickel chromates, coal products, mustard gas, chloromethyl ethers, gasoline, diesel exhaust, and some forms of silica and chromium can increase the risk of developing lung cancer

- **People with a history of lung disease** Chronic obstructive pulmonary disease (COPD), asthma, pneumonia and tuberculosis (TB) can be risk factors for developing lung cancer (22, 23).

2.1.3 Treatment of lung cancer

There are many treatment options for lung cancer, depending on the type of lung cancer and stage of the disease. Patients with SCLC are usually treated with chemotherapy and radiation therapy while patients with NSCLC can be treated with surgery, chemotherapy, radiation therapy, targeted therapy, or a combination of these treatments (24). Surgery is the most common therapeutic option for the early stage of NSCLC but rarely used as part of the main treatment of SCLC. Radiation therapy may be given as adjuvant therapy in combination with surgery or chemotherapy to kill any

remaining cancer cells in order to prolong survival (25). Chemotherapy is the most common treatment options for SCLC and NSCLC patients with advanced stage. The chemotherapeutic drugs most often used for lung cancer are cisplatin, carboplatin and paclitaxel (5, 26).

Cisplatin and carboplatin are two of the most common types of platinum-based chemotherapeutic agents. Mechanism of action of platinum compounds is binding covalently to the N⁷ position of guanine on DNA to form intra-strand and inter-strand DNA crosslinks which cause an unwinding and bending of the DNA, resulting in single- or double-strand DNA breaks, inhibiting DNA replication and transcription (27, 28). Common side effects of platinum compounds include hair loss, mouth sores, nausea, vomiting, fatigue, anemia, bleeding and infection. The main side effects of cisplatin and carboplatin are nephrotoxicity and myelosuppression, respectively (29-31).

Paclitaxel (taxol), a microtubule-stabilizing drug in the taxane class of chemotherapeutic agents, is used for various types of cancers. Taxol strongly binds to the N-terminal region of the β -subunit of tubulin and promotes the formation of highly stable microtubules, preventing depolymerization, thus inhibiting cell division and arresting the cell cycle at the G₂/M phase. The main side effects of this drug are arthralgia/myalgia, cardiovascular effects and hypersensitivity reactions (32, 33).

Unfortunately, chemotherapeutic drugs can also affect normal cells, resulting in unwanted side effects. This has led to the development of targeted cancer therapy. The drugs generally target proteins that found more specifically in cancer cells than normal cells. Several targeted agents have been approved for treatment of lung cancer such as bevacizumab (Avastin[®]) and erlotinib (Tarceva[®])

Bevacizumab, a monoclonal antibody, specifically binds to circulating vascular endothelial growth factor (VEGF)-A to prevent interaction with VEGF receptors (VEGFRs) on the surface of endothelial cells and thereby inhibiting the process of angiogenesis (34, 35). The common side effects of bevacizumab include proteinuria, hypertension, and hemorrhagic events. In addition, bevacizumab can cause serious side effects include gastrointestinal perforation, fistula formation, serious bleeding, arterial thromboembolic

events, nephrotic syndrome, hypertensive crisis, or hypertensive encephalopathy (35, 36).

Erlotinib is a small molecule that binds to the adenosine triphosphate (ATP) binding site of the epidermal growth factor receptors (EGFRs), inhibiting downstream signaling pathways (37, 38). The common side effects of erlotinib are rash, diarrhea and fatigue. Moreover, this drug can cause serious side effects, including severe rash, severe paronychia, interstitial pneumonia, myocardial ischemia and acute hepatitis (39, 40).

2.2 Cell cycle

Cell cycle is a process involved in the growth and proliferation of cells. The eukaryotic cell cycle is divided into four stages, including G_1 (gap 1), S (synthesis), G_2 (gap 2), and M (mitosis). In the first G_1 phase, the cell is preparing for DNA replication. S phase is the phase of the cell cycle in which DNA is replicated. The G_2 phase is the second gap phase which proteins are synthesized in preparation for mitosis while the M phase is the phase involves chromosome segregation and cell division (41-43). The cell can stop cycling after division and enters a state of quiescence (G_0). The cell can remain in this phase for a long time until it is stimulated by appropriate stimuli such as growth factors (44).

The cell cycle is regulated by two protein families: the cyclins and the cyclin-dependent protein kinases (CDKs). CDK activity depends on the presence of activating cyclin subunit which are synthesized and degraded in a cell cycle. Cyclin D/CDK4 or cyclin D/CDK6 complexes initiate phosphorylation of retinoblastoma (Rb) protein, resulting in release of E2F transcription factors, enabling the expression of genes required for G_1 to S phase transition. In late G_1 , cyclin E/CDK2 reinforce RB1 phosphorylation to irreversibly initiate the gene expression program of the S phase. In addition to cyclin E, cyclin A accumulates at the G_1/S phase transition and persists through S phase where it initially associates with CDK2 and then associates with CDK1 in late S phase. During the G_2/M transition, the cyclin A/CDK1 complex is activated to initiate mitosis. Finally, cyclin B/CDK1 complexes are activated to allow the progression through the M phase (45, 46).

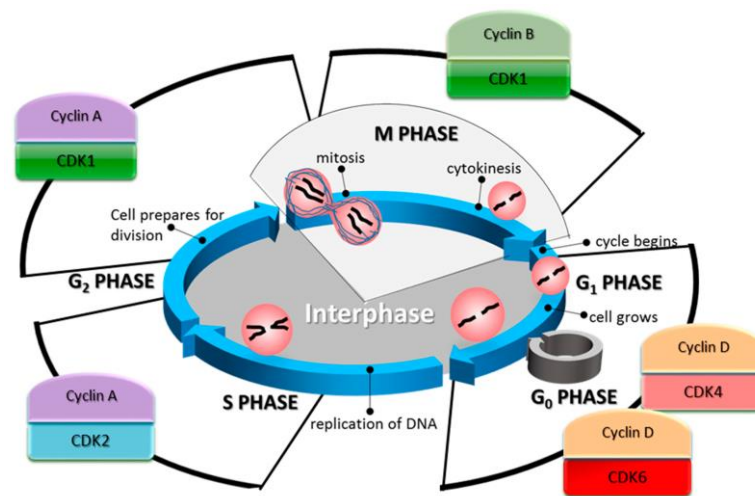


Figure 1 The cell cycle phases and their associated cyclin-dependent kinases (CDK)/cyclin complexes(47)

2.3 Apoptosis

Apoptosis or programmed cell death is a key regulator of physiological growth control and tissue homeostasis. Several cancer therapy approaches, including, chemotherapy, radiation therapy and immunotherapy, primarily exert their antitumor effect by triggering apoptosis in cancer cells (48). Apoptosis is characterized by typical morphological and biochemical hallmarks, including cell shrinkage, nuclear DNA fragmentation and membrane blebbing. There are two main apoptotic pathways including, the extrinsic and the intrinsic pathways (49).

2.3.1 Death-receptor-induced extrinsic apoptosis pathway

The extrinsic signaling pathway, that initiates apoptosis, is triggered by binding of a death ligand to a death receptor, such as tumor necrosis factor- α (TNF- α)/ tumor necrosis factor receptor 1(TNFR1), Fas Ligand (FasL)/ Fas receptor (FasR), TNF-related apoptosis-inducing ligand (TRAIL)/TNF-related apoptosis-inducing ligand receptor1 (TNFR1). Binding of the ligand induces a conformational change of the death domain in the receptor, recruiting adaptor proteins such as TNFR-associated death domain (TRADD), Fas-associated death domain (FADD), to form death-inducing signaling

complex (DISC). Recruitment of procaspase-8 to DISC leads to cleavage of procaspase-8, resulting in activation of caspase-8 and initiation of apoptosis by direct cleavage of downstream effector caspases (49-51).

2.3.2 Mitochondrial-apoptosome-mediated intrinsic apoptosis pathway

Most chemotherapeutic drugs kill tumor cells through intrinsic apoptotic pathway. The pathway is initiated by various extra- and intra-cellular stimuli including ultraviolet, irradiation, growth factor withdrawal, oxidative stress, and chemotherapeutic drugs (52). All of these stimuli cause changes in the inner mitochondrial membrane that results in an opening of the mitochondrial permeability transition (MPT) pore, loss of the mitochondrial transmembrane potential and release of apoptogenic factors such as endonuclease G (Endo G), second mitochondria-derived activator of caspases/direct IAP binding protein with a low iso-electric point (SMAC/DIABLO), Omi and cytochrome c into the cytosol. SMAC/DIABLO and Omi are reported to promote apoptosis by inhibiting activity of inhibitors of apoptosis proteins (IAPs) whereas endonuclease G is responsible for DNA degradation, chromatin condensation, and DNA fragmentation. Cytochrome c binds to APAF-1, which oligomerizes to form apoptosome. Once formed, this complex, comprising of APAF-1–cytochrome c–procaspase 9, triggers the activation of procaspase 9 to caspase 9. This initiator caspase starts the hydrolytic cascade that stimulates the effector caspases, leading to apoptosis (53, 54).

Regulation of intrinsic apoptosis pathway occur through members of the Bcl-2 family of proteins, which can be divided into three groups including,

- I. **Anti-apoptotic Bcl-2 proteins** (such as Bcl-2, Bcl-X_L) consist of BH1, BH2, BH3 and BH4 domains. These proteins preserve outer mitochondrial membrane integrity by inhibiting the pro-apoptotic members.
- II. **Pro-apoptotic Bcl-2 effector proteins** (such as BAK, BAX) consist of BH1, BH2 and BH3 domains. These proteins promote apoptosis by forming oligomers on the cytosolic side of the outer mitochondrial membrane, creating pores that permeabilize the mitochondrial membrane and allowing the release of apoptogenic factors to the cytosol.

- III. BH3 only pro-apoptotic Bcl-2 protein (such as BAD, Bid, Bim) These proteins promote apoptosis by inhibiting anti-apoptotic proteins or activating anti-apoptotic members (54-56).

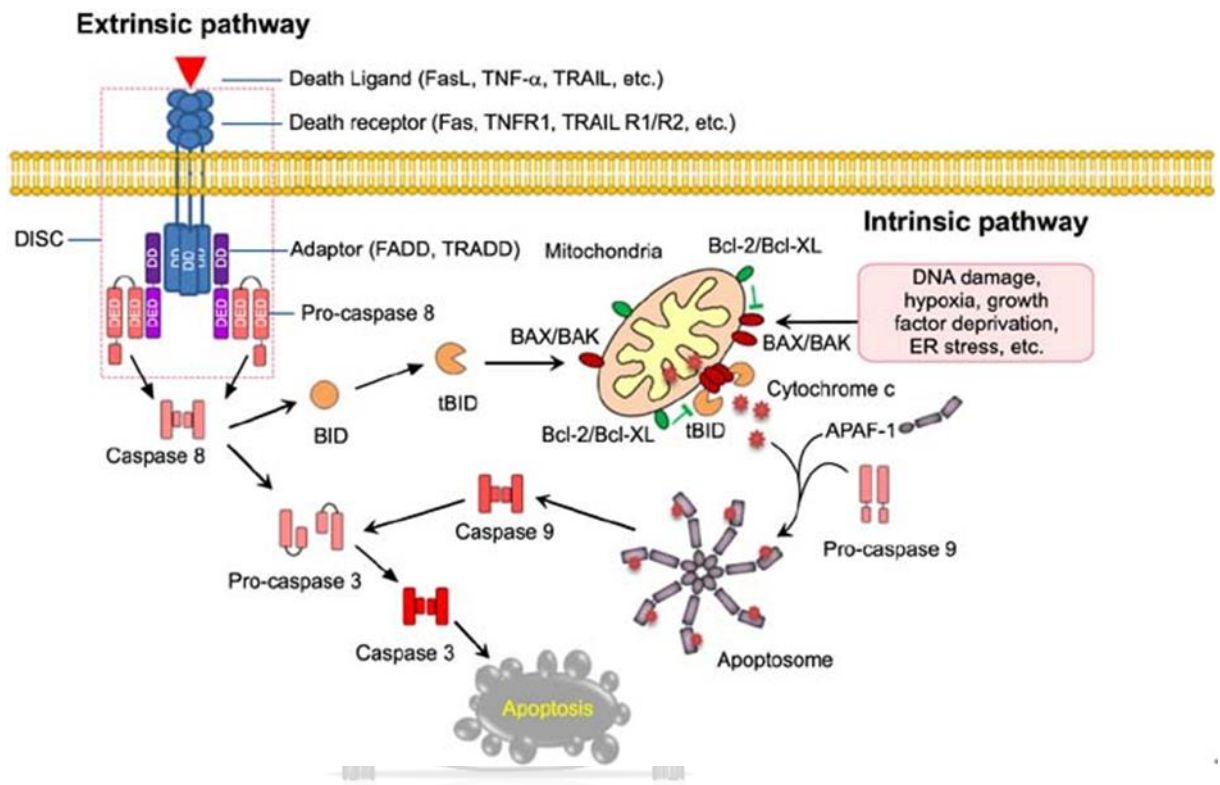


Figure 2 Extrinsic and intrinsic apoptotic signaling pathways (57)

2.4 Reactive oxygen species

Reactive oxygen species (ROS) are small molecules that are short-lived and highly reactive. ROS include oxygen (O_2), superoxide anion (O_2^-), hydroxyl free radicals (HO^-) and hydrogen peroxide (H_2O_2). The generation of ROS in cells exists in equilibrium with a wide variety of antioxidants. These include enzymatic scavengers such as superoxide dismutase (SOD), catalase, glutathione peroxidase (GPx) and peroxiredoxins, as well as non-enzymatic scavengers such as vitamins C and E, glutathione (GSH), lipoic acid and carotenoids (58). Low level of ROS plays an important role in regulating normal physiological functions involved in development such as cell cycle progression, proliferation, differentiation, migration and cell death. However, high level of ROS caused

by the imbalance between ROS generation and antioxidant can lead to oxidative damage that could trigger cell death. It is now known that cancer cells have higher ROS level compared to normal cells due to high metabolic rate and mitochondrial dysfunction. Thus, excessive accumulation of ROS in cancer cells can induce apoptosis through oxidative stress (58-62). In fact, there are many commonly used chemotherapeutic drugs such as cisplatin, carboplatin, oxaliplatin and doxorubicin that have been known to increase the level of ROS (63-65). Moreover, several studies reported that natural compounds such as curcumin, catechins, plumbagin, shikonin and resveratrol exhibited anticancer activity by inducing cell death through ROS generation (66-69).

2.5 Epidermal growth factor receptor cell proliferation signaling pathways

The epidermal growth factor receptor (EGFR) is a receptor tyrosine kinase that is commonly upregulated in various types of cancers such as non-small-cell lung cancer, metastatic colorectal cancer, glioblastoma, head and neck cancer, pancreatic cancer, and breast cancer (70). The EGFR-regulated cell proliferation and survival are mediated through two major signaling pathways, including MAPK/ERK and PI3K/AKT pathways (71).

2.5.1 MAPK/ERK signaling pathway

The signal starts when receptor tyrosine kinases such as EGFR are activated by extracellular ligands, such as epidermal growth factor (EGF), resulting in receptor dimerization which promotes autophosphorylation of tyrosine residues in the intracellular domain of the receptor. These phosphorylated residues serve as specific binding sites for intracellular signaling proteins containing SH2 domain such as growth factor receptor-bound protein 2 (Grb2). Consequently, son of sevenless (SOS), a guanine nucleotide exchange factor (GEF), is recruited to the plasma membrane as a result of its interaction with Grb2. Then, SOS stimulates Ras by switching from inactive GDP to active GTP bound form of Ras. Active Ras can bind with and activate Raf. Upon activation, Raf induces the phosphorylation of Mek1/2. Thereafter, activated Mek1/2 phosphorylates Erk1/2. Finally, active Erk1/2 translocates to the nucleus, where Erk phosphorylates and activates various

transcription factors that involve cellular processes such as proliferation, migration and differentiation (72-74).

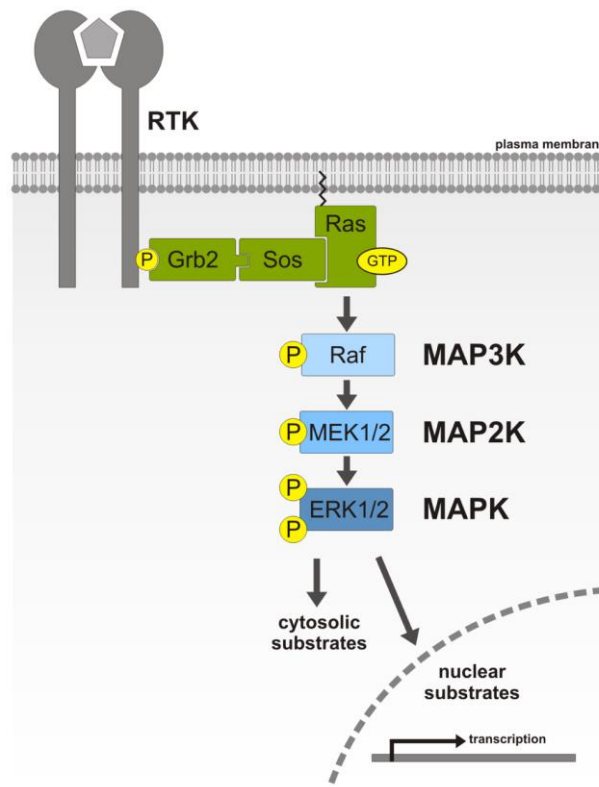


Figure 3 MAPK/ERK signaling pathway(75)

2.5.2 PI3K/AKT signaling pathway

Binding of the ligand to membrane receptor tyrosine kinases triggers activation of phosphatidylinositol 3-kinases (PI3K) which further converts phosphatidylinositol 4,5-bisphosphate (PIP₂) lipids to phosphatidylinositol-3,4,5-trisphosphate (PIP₃) at the membrane, providing docking sites for intracellular signaling proteins with pleckstrin-homology (PH) domains including the phosphoinositide-dependent kinase 1 (PDK1) and the serine-threonine kinase AKT (76, 77). Then, AKT is recruited to the plasma membrane along with PDK1, allowing PDK1 to phosphorylate and activate AKT. Once activated, AKT could translocate from the plasma membrane to the cytoplasm and nucleus to phosphorylate many target proteins, promoting cell proliferation, differentiation, apoptosis, angiogenesis and metabolism (78, 79).

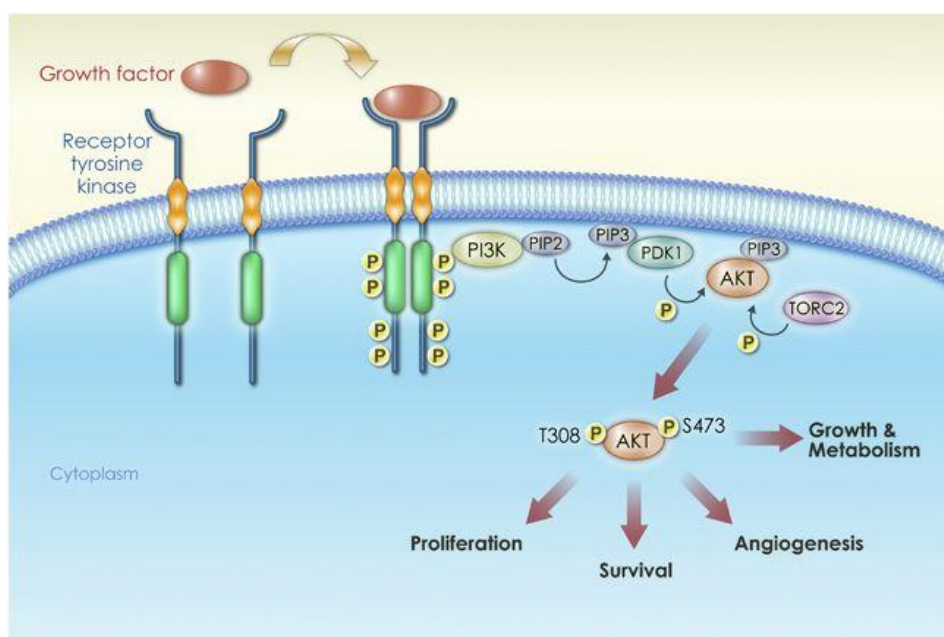


Figure 4 PI3K/AKT signaling pathway(80)

2.6 Mansonone and its derivative

Mansonones are naphthoquinone-containing compounds isolated from the heartwood of *Mansonia gagei* Drumm, a Thai plant in family Sterculiaceae. The common names in Thai are Chan-cha-mod, Chan-hom and Chan-pha-ma. The heartwood of this plant has been used in Thai traditional medicine as antidepressant, antiemetic, cardiac stimulant, and refreshment agents (81, 82). Previous studies have reported that the chemical constituents from heartwood of *Mansonia gagei* Drumm are mansonones C, E, F, G, H, I, N, O, P, Q and S (15, 82, 83).

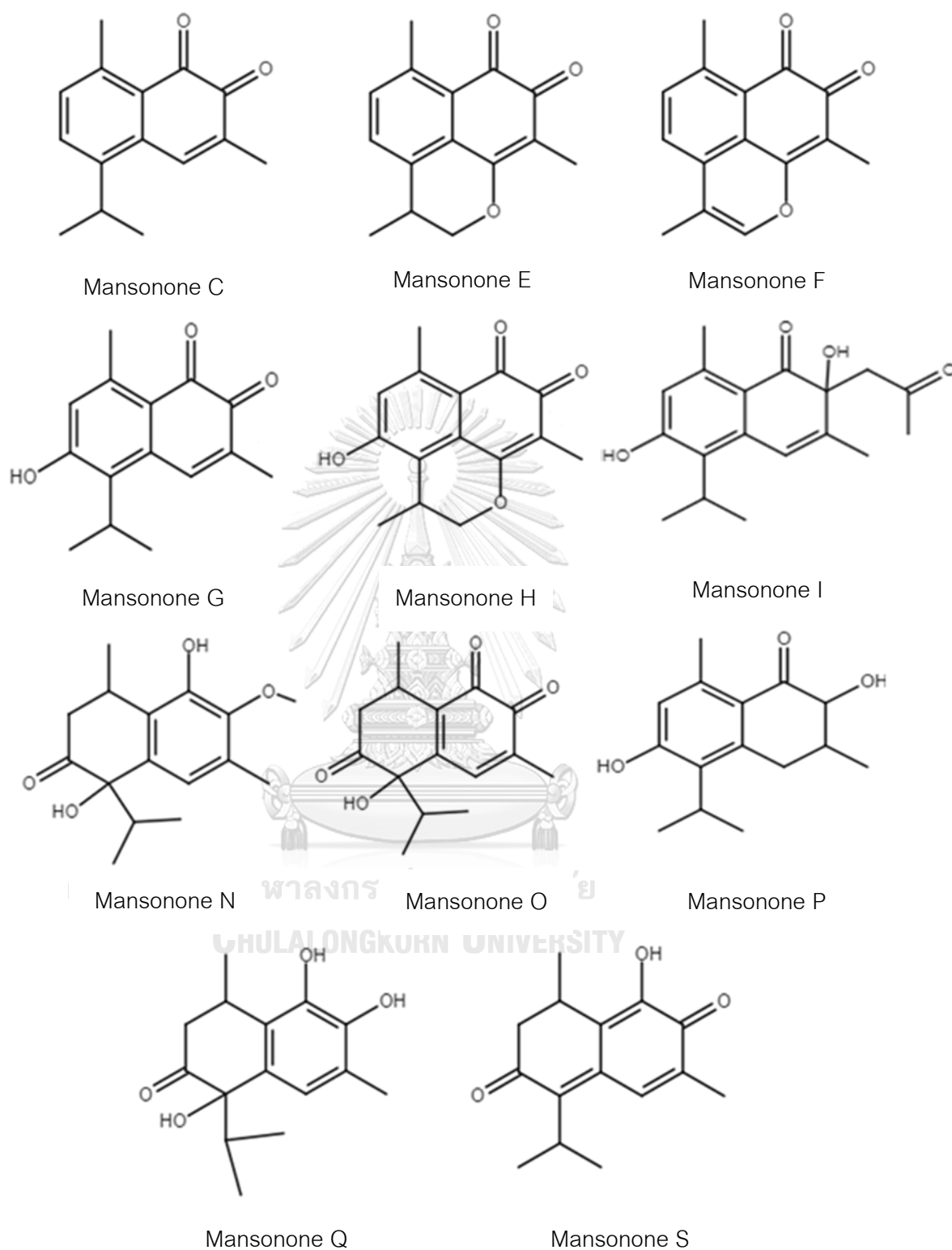


Figure 5 Structures of mansonones C, E, F, G, H, I, N, O, P, Q and S

Pharmacological effects of mansonones

Several studies reported that mansonones have various pharmacological activities such as antibacterial, antifungal, antiestrogenic, antiadipogenic and anticancer effects.

Antibacterial effect

Boonsri *et al.* demonstrated that mansonone E isolated from *Thespesia populnea* displayed antibacterial activity against *Bacillus subtilis* with minimum inhibitory concentration (MIC) of 4.69 $\mu\text{g}/\text{mL}$ (19). Moreover, mansonone E has shown to possess potent antibacterial activity against both *Xanthomonas oryzae* pv. *oryzae* (Xoo) and *Xanthomonas oryzae* pv. *oryzicola* (Xoc) with MIC and minimum bactericidal concentration (MBC) of 7.8 and $>500 \mu\text{g mL}^{-1}$, respectively (84).

Antifungal effect

Tiew P. *et al.* reported that mansonones C and E have antifungal activities against *Candida albicans* with a minimal amount of 1.5 μg and 2.5 μg , respectively. They also effectively inhibited *Cladosporium cucumerinum* growth with a minimal inhibitory amount of 0.6 μg , and 0.6 μg respectively (85). Additionally, mansonone E exhibited antifungal activity against *Phytophthora parasitica* with 94% inhibition at 1000 $\mu\text{g mL}^{-1}$. Similar to mansonone E, the growth of this fungus was significantly inhibited by mansonones C and G at concentration of 1000 $\mu\text{g mL}^{-1}$ with 81 and 84% inhibition, respectively (84).

Anti-estrogenic effect

In 2013, El-Halawany AM, *et al.* reported that acetyl mansonone G displayed a 10-fold increase in its binding ability to estrogen receptor alpha (ER α), when compared to mansonone G, with an IC₅₀ 630 μM . Moreover, acetyl mansonone G at 10 μM has shown to inhibit 17 β -estradiol-induced β -galactosidase activity in the yeast estrogen screen (YES) expressing ER- α and ER- β model (86).

Anti-adipogenic effect

A recent study reported that mansonones C and G suppressed differentiation of 3T3-L1 cells into adipocyte-like cells, with a 40% decrease in lipid accumulation via the suppression of peroxisome proliferator-activated receptor (PPAR)- γ activity (20).

Anticancer effect

Wang D. *et al.* demonstrated the anticancer activities of mansonones E and F isolated from the dried root bark of *Ulmus pumila*. The IC_{50} values of mansonone E were 2.2, 7.9, 3.1, and 0.9 μM while the IC_{50} values of mansonone F were 13.3, 30.5, 29.4, and 3.0 μM in melanoma (A375-S2), cervical cancer (HeLa), breast cancer (MCF-7) and lymphoma (U937) cells, respectively. Similarly, mansonone E, isolated from *Thespesia populnea*, has significantly inhibited the growth of four cancer cell lines including breast cancer (MCF-7), cervical cancer (HeLa), colon cancer (HT-29), and oral cavity cancer (KB) with IC_{50} of 0.05, 0.55, 0.18 and 0.4 μM , respectively (59). Moreover, it was reported that mansonone E induces apoptosis in HeLa cells by inducing oligonucleosomal fragmentation, activating caspase-3, downregulating expressions of anti-apoptotic proteins, Bcl-X_L and Bcl-2 and upregulating expression of proapoptotic protein, Bax (17).

In 2016, Hairani R, *et al.* isolated several mansonones, including mansonones C (77 mg), E (207 mg), G (10 g) and H (196 mg), from heartwood of *Mansonia gagei* Drumm and evaluated for their antibacterial activities. The results revealed that mansonones E and G displayed antibacterial activity against *Staphylococcus aureus*, *Streptococcus mutans*, *Streptococcus sobrinus* higher than the others (13). Since mansonone G exhibited good antibacterial activity and could be obtained in the highest yield, its ether and ester analogues were synthesized. Notably, ether analogues of mansonone G, had higher antibacterial activity than the parent mansonone G (87). In addition to antibacterial activity, a recent study has shown that the ether analogues of mansonone G displayed higher antiadipogenic activity than the parent MG (20).

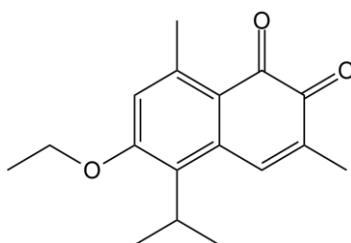


Figure 6 Structure of EMG

CHAPTER III

MATERIALS AND METHODS

3.1 Equipment

- Analytical balance 0.001 g (Mettler Toledo, Switzerland)
- Analytical balance 0.00001 g (Sartorius, Germany)
- Autoclave (Sanyo, Japan)
- Autopipette (Brand, Germany)
- Biohazard laminar flow hood (Labconco, USA)
- Centrifuge (Hettich, Germany)
- CO₂ incubator (Thermo, USA)
- Controller pipette (Gilson, USA)
- Electrophoresis system (Bio-Rad, USA)
- Fluorescence microplate reader (Thermo, Finland)
- Fluorescence flow cytometer (BD Bioscience, USA)
- Light microscope (Nikon, Japan)
- Microplate reader (Thermo, Finland)
- Temperature control centrifuge (Eppendorf, Germany)
- Vortex mixer (Scientific Industries, USA)

3.2 Materials

- 6 well plate (Corning Inc., USA)
- 15 mL conical tube (Corning Inc., USA)
- 25 and 75 cm² rectangular cell culture flask (Corning Inc., USA)
- 96 well black polystyrene plate (Corning Inc., USA)
- 96 well plate (Corning Inc., USA)
- Nitrocellulose membrane (Bio-Rad, USA)

3.3 Reagents

- 0.4% Trypan blue dye (Sigma, USA)
- 2,7-dichloro-dihydro-fluorescein diacetate (Sigma, USA)

- Ammonium persulfate (Sigma, USA)
- Annexin V, fluorescein conjugate (FITC) (Invitrogen, USA)
- Anti-IgG, horseradish peroxidase (HRP)-linked antibody (Cell Signaling Technology, USA)
- Bromophenol blue (Sigma, USA)
- β -mercaptoethanol (Sigma, USA)
- *Cis*-diammineplatinum (II) dichloride (Sigma, USA)
- Dimethyl sulfoxide (DMSO) [analytical grade] (Merck, Thailand)
- Dimethyl sulfoxide (DMSO) [molecular grade] (Sigma, USA)
- Dulbecco's Modified Eagle Medium (DMEM) (Gibco, USA)
- Fetal bovine serum (Gibco, USA)
- Glycerol (Sigma, USA)
- Glycine (Sigma, USA)
- Hank's buffered salt solution (HBSS) (Sigma, USA)
- Western horseradish peroxidase substrate (Merck, Germany)
- *N,N,N,N*-tetramethyl ethylenediamine (TEMED) (Sigma, USA)
- *N*-acetylcysteine (Sigma, USA)
- Penicillin-streptomycin (Gibco, USA)
- Primary antibodies (Cell Signaling Technology, USA)
 - AKT (pan) rabbit monoclonal antibody
 - BAK rabbit monoclonal antibody
 - BAX rabbit monoclonal antibody
 - Bcl-2 rabbit monoclonal antibody
 - Bcl-X_L rabbit monoclonal antibody
 - GAPDH rabbit monoclonal antibody
 - p44/42 MAPK (Erk1/2) rabbit monoclonal antibody
 - PARP rabbit monoclonal antibody
 - phospho-AKT rabbit monoclonal antibody
 - Phospho-p44/42 MAPK (Erk1/2) rabbit monoclonal antibody

- Propidium iodide (BD Pharmingen, USA)
- Protease inhibitors (Sigma, USA)
- Protein assay kit (Bio-Rad, USA)
- Protogel (National Diagnostic, USA)
- RIPA lysis buffer (Thermo scientific, USA)
- Roswell Park Memorial Institute (RPMI)-1640 medium (Gibco, USA)
- Sodium dodecyl sulfate polyacrylamide gel (SDS) (EM science, USA)
- Thiazolyl blue tetrazolium bromide (MTT) (Sigma, USA)
- Tris base (Vivantis, USA)
- Triton X-100 (Sigma, USA)
- Trypsin/EDTA (Gibco, USA)
- Tween 20 (Sigma, USA)

3.4 Methods

3.4.1 Preparation of test compound stock solutions

Mansonone G (MG) was isolated from the heartwood of *Mansonia gagei* (*M.gagei*) whereas ethoxy mansonone G (EMG) was semi-synthesized according to the previous study (20). Stock solutions of MG, EMG and cisplatin were prepared in dimethyl sulfoxide (DMSO) at 50 mM and stored at 4°C until use. In the experiments, the stock solution was diluted in culture media to give appropriate final concentrations. The 0.2% DMSO was used as a vehicle control.

3.4.2 Cell culture

Human lung adenocarcinoma cell lines, A549 and H1975 were from American Type Culture Collection (ATCC, USA) and normal human primary dermal fibroblasts (PCS201-010) was kindly provided by Ms. Nalinee Pradubyat from College of Pharmacy, Rangsit University. A549 cells were maintained in Dulbecco's modified Eagle's medium (DMEM) supplemented with 10% fetal bovine serum (FBS) and 100 units/mL penicillin and 100 µg/mL streptomycin. H1975 cells were maintained in Roswell Park Memorial Institute

(RPMI) 1640 medium supplemented with 10% FBS, 100 U/mL penicillin and 100 µg/mL streptomycin. PCS201-010 cells were maintained in DMEM with high glucose supplemented with 10% FBS and 100 units/mL penicillin and 100 µg/mL streptomycin. The cells were maintained in 5% CO₂ humidified at 37°C.

3.4.3 Cytotoxicity assay

The cytotoxic effects of MG and EMG were determined by methyl thiazolyl tetrazolium (MTT) assay. Briefly, A549, H1975 and PCS201-010 cells were seeded at a density of 2.5×10^4 cells/mL in 96-well plates and incubated at 37°C and 5% CO₂ overnight. Cells were then treated with 2.5, 5, 10, 20 and 40 µM of MG, EMG or cisplatin (positive control) or 0.2% DMSO (vehicle control) for 48 h. After treatment, 15 µL of MTT (5 mg/mL) was added into each well and incubated at 37°C for 4 h. The formazan crystals created after incubation were dissolved in DMSO. The absorbance of obtained colored solution was measured at 570 nm using a microplate reader (Thermo, Finland). The percentage of cell viability was calculated using the following equation:

$$\% \text{ cell viability} = \left(\frac{\text{Absorbance}_{\text{Sample}}}{\text{Absorbance}_{\text{Untreated group}}} \right) \times 100$$

The half inhibitory concentration (IC₅₀) was obtained using GraphPad Prism 7 (GraphPad Software, USA).

The selective index (SI) which indicates the cytotoxic selectivity of a test compound against cancer cells was calculated from the IC₅₀ of the test compound in normal cells versus cancer cells.

3.4.4 Analysis of cell cycle progression

The proportion of cells within each stage of the cell cycle was detected by flow cytometry using propidium iodide (PI). Cells that are in the G₀/G₁ phase have a diploid DNA content (2n). During S phase (DNA synthesis), cells contain between 2n and 4n. Within G₂/M phase, cells have a tetraploid DNA content (4n).

A549 and H1975 cells were seeded at a density of 2.5×10^4 cells/mL in 6-well plates and incubated at 37°C and 5% CO₂ overnight. Cells were synchronized in G₀/G₁ phase

using serum starvation for 24 h. Then, the cells were treated with 5, 10 and 20 μM of EMG or 0.2% DMSO for 24 h. After that, the cells were washed with PBS, harvested by trypsinization, and centrifuged at 1,500 rpm for 5 min. Then, the cell pellets were collected, washed twice with cold PBS and fixed in 70% ethanol at -20°C for 15 min. The fixed cells were washed twice with cold PBS, resuspended with 300 μL of PBS and incubated with 2 μL of 4 mg/ml RNase A at room temperature for 30 min. The cells were then stained with 1 μL of 0.05 $\mu\text{g}/\text{mL}$ PI (BD Pharmingen, USA) at room temperature in the dark for 15 min. The stained cells were analyzed by flow cytometer (BD LSR II, Biosciences).

3.4.5 Detection of apoptosis using Annexin-V/PI staining assay

Apoptosis was detected by staining the cells with fluorescein isothiocyanate (FITC)-conjugated annexin V (annexin V-FITC) and PI solution followed by flow cytometry analysis. In early apoptotic cells, phosphatidyl serine (PS), which are normally located on the inner membrane, will redistribute to the outer membrane that can be detected with annexin V-FITC. However, in late apoptotic and necrotic cells, the integrity of the plasma and nuclear membranes are lost, allowing PI to pass through the membrane.

A549 and H1975 cells were seeded at a density of 2.5×10^4 cells/mL in 6-well plates and incubated at 37°C and 5% CO_2 overnight. Then, the cells were treated with 5, 10 and 20 μM of EMG for 24 h or 0.2% DMSO. After incubation, the cells were washed twice with cold PBS, harvested by trypsinization, and centrifuged at 1,500 rpm for 5 min. The cell pellets were re-suspended with 500 μL of assay buffer and stained with 1 μL of PI and 3 μL of annexin V-FITC (Invitrogen, USA) in the dark at room temperature for 15 min. The stained cells, including viable cells (annexin V⁻, PI⁻), early apoptotic cells (annexin V⁺, PI⁻), late apoptotic cells (annexin V⁺, PI⁺) and necrotic cells (annexin V⁻, PI⁺), were quantitatively analyzed using flow cytometer (BD LSR II, Biosciences).

3.4.6 ROS generation assay

The ROS levels in the cells were determined by dichloro-dihydro-fluorescein diacetate (DCFH-DA). DCFH-DA, a nonpolar dye, is deacetylated by cellular esterases to

a non-fluorescent dichlorodihydrofluorescein (DCFH). In the presence of cellular ROS, DCFH is oxidized to the highly fluorescent dichlorofluorescein (DCF).

A549 and H1975 cells were seeded at a density of 2.5×10^4 cells/mL in 96-well plates and incubated at 37°C and 5% CO₂ overnight. Then, the cells were incubated with 100 μ L of 10 μ M DCFH-DA (Sigma, USA) in Hank's buffered salt solution (Sigma, USA) at 37°C in the dark for 30 min. After incubation, buffer was removed and the cells were washed with PBS. Subsequently, the cells were treated with 5, 10 and 20 μ M of EMG, 200 μ M of H₂O₂ (positive control) or 0.2% DMSO for 1 h. After that, the cells were washed twice with cold PBS and 200 μ L of 1% triton-X (Sigma, USA) in 0.3 M NaOH was added. The levels of ROS were analyzed by measuring the DCF fluorescence intensity at an excitation wavelength of 502 nm and an emission wavelength of 523 nm using a fluorescence microplate reader (Thermo, Finland). The fluorescence intensity in each group were expressed in the percentage of control as calculated from following equation:

$$\% \text{ control} = F_{\text{Sample}} / F_{\text{Control}} \times 100$$

3.4.7 Evaluation of protein expression using western blotting

Effects of EMG on the expression of apoptosis-related proteins, including pro-apoptotic proteins (BAK, BAX), anti-apoptotic proteins (Bcl-2, Bcl-X_L) and poly (ADP-ribose) polymerase (PARP) and proteins involved in PI3K/AKT and MAPK/ERK signaling pathways, including AKT, phospho-AKT, MAPK (Erk1/2) and phospho-ERK1/2 were determined by western blotting using GAPDH as an internal control.

A549 and H1975 cells were seeded at a density of 2.5×10^4 cells/mL in 6-well plates and incubated at 37°C and 5% CO₂ overnight. Then, A549 cells were treated with EMG at concentrations of 5, 10 and 20 μ M while H1975 cells were treated with EMG at concentrations of 2.5, 5 and 10 μ M for 24 h. Subsequently, cells were lysed with RIPA buffer (Thermo scientific, USA) containing protease inhibitors (Sigma, USA) and phosphatase inhibitors (Sigma, USA) and centrifuged at 14,000 rpm for 30 min. The supernatants were collected and the protein concentrations were evaluated by Bio-Rad DC Protein assay reagents (Bio-Rad, USA) using bovine serum albumin as a standard.

Then, the protein samples were separated by 8% SDS-PAGE and transferred to nitrocellulose membranes. The membrane was incubated in 3% non-fat dry milk (NFDM) in 1X Tris-buffered saline containing 0.1% Tween 20 (TBST) at room temperature for 1 h, and then incubated with the primary antibodies specific to proteins of interest, including BAK, BAX, Bcl-2, Bcl-X_L, PARP, AKT, phospho-AKT, MAPK (Erk1/2), phospho-ERK1/2 (1:1000 dilution, Cell signaling, USA) at 4°C overnight. Then, the membrane was incubated with HRP-conjugated secondary antibody (1:2000 dilution, Cell signaling, USA) at room temperature for 2 h. The target proteins were detected by Luminata Crescendo Western HRP substrate (Merck, Germany) and analyzed by Image Studio software (LICOR, USA)

3.4.8 Statistical analysis

All data are presented as mean \pm standard error of mean (SEM) from three independent experiments performed in triplicate. Statistical analysis of data was performed by one-way analysis of variance (ANOVA) followed by LSD using SPSS statistics 21 software (IBM Corporation, USA). The difference was considered significant if *p* value was < 0.05.

CHAPTER IV

RESULTS

4.1 Effect of mansonone G (MG), ethoxy mansonone G (EMG) and cisplatin (CDDP) on viability of non-small cell lung cancer and normal cells

Initially, the cytotoxic effects of MG, EMG and CDDP on NSCLC cell lines expressing wild-type EGFR A549 and mutant EGFR H1975 and normal fibroblast PCS201-101 cells were determined. Cells were exposed to 2.5, 5, 10, 20 or 40 μM of MG, EMG or CDDP for 48 h and the cell viability was evaluated using MTT assays. As shown in Figures 7A-C, MG, EMG and CDDP significantly inhibited the growth of A549 and H1975 cells in a concentration dependent manner ($p < 0.001$). The values of half maximal inhibitory concentration (IC_{50}) of MG, EMG and CDDP were illustrated in Table 1. It, however, should be noted that EMG displayed the most potent cytotoxicity toward NSCLC cells, compared to MG and cisplatin. Similar to cancer cells, MG, EMG and CDDP significantly inhibited the growth of normal fibroblast PCS201-101 cells in a concentration dependent manner (Figures 8A-C, $p < 0.001$). Of all three compounds, EMG showed highest selectivity index (SI) values, which represents IC_{50} for normal cells/ IC_{50} for cancer cells for both NSCLC cell lines (Table 1). The SI values of EMG for A549 and H1975 cells were 2.76 and 3.60, respectively. Thus, EMG was selected for further studies.

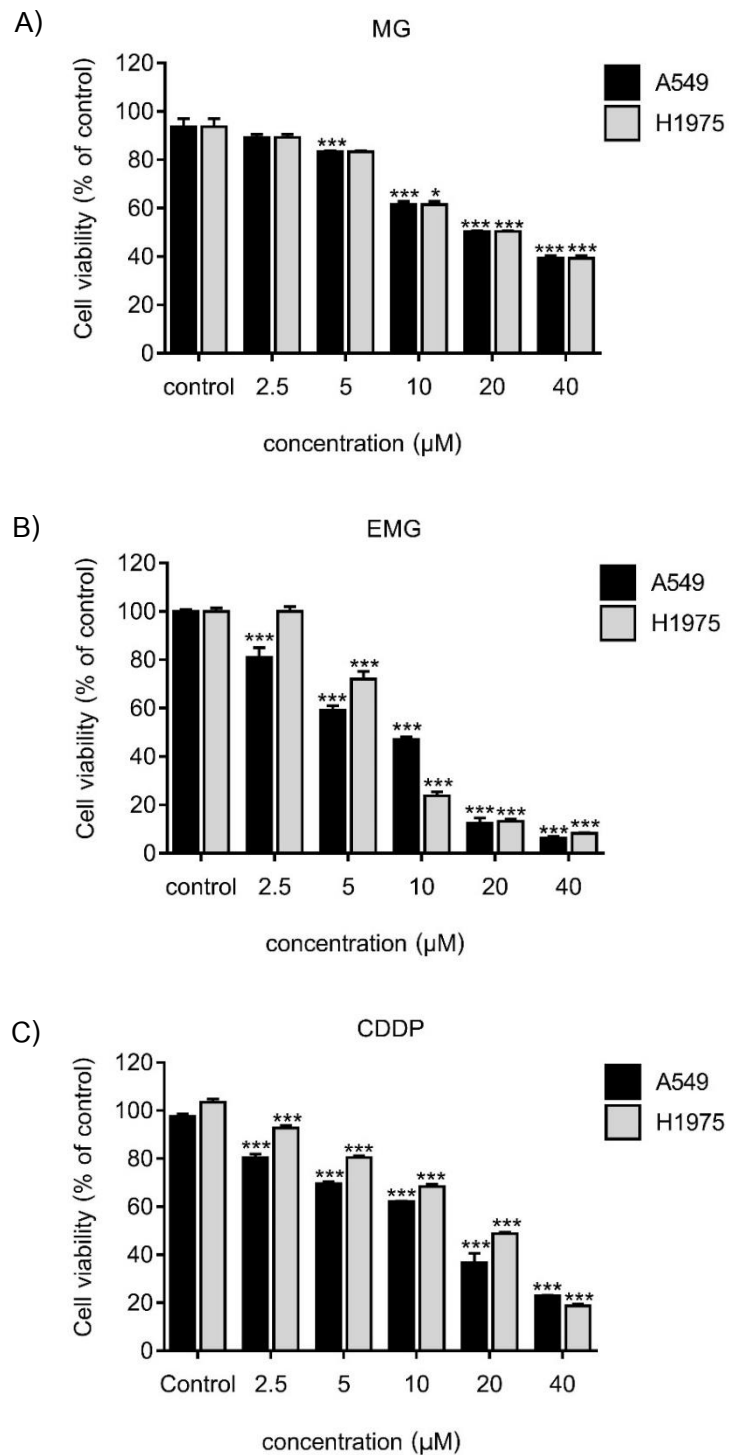


Figure 7 Effects of MG, EMG and CDDP on viability of A549 and H1975 cells. The cells were treated with MG, EMG or CDDP at 2.5, 5, 10, 20 or 40 μM for 48 h. Cell viability was evaluated using MTT assays. Each value is expressed as the mean \pm SEM (n=3). *P<0.05, **P<0.01, ***P<0.001 compared with vehicle control (0.2% DMSO).

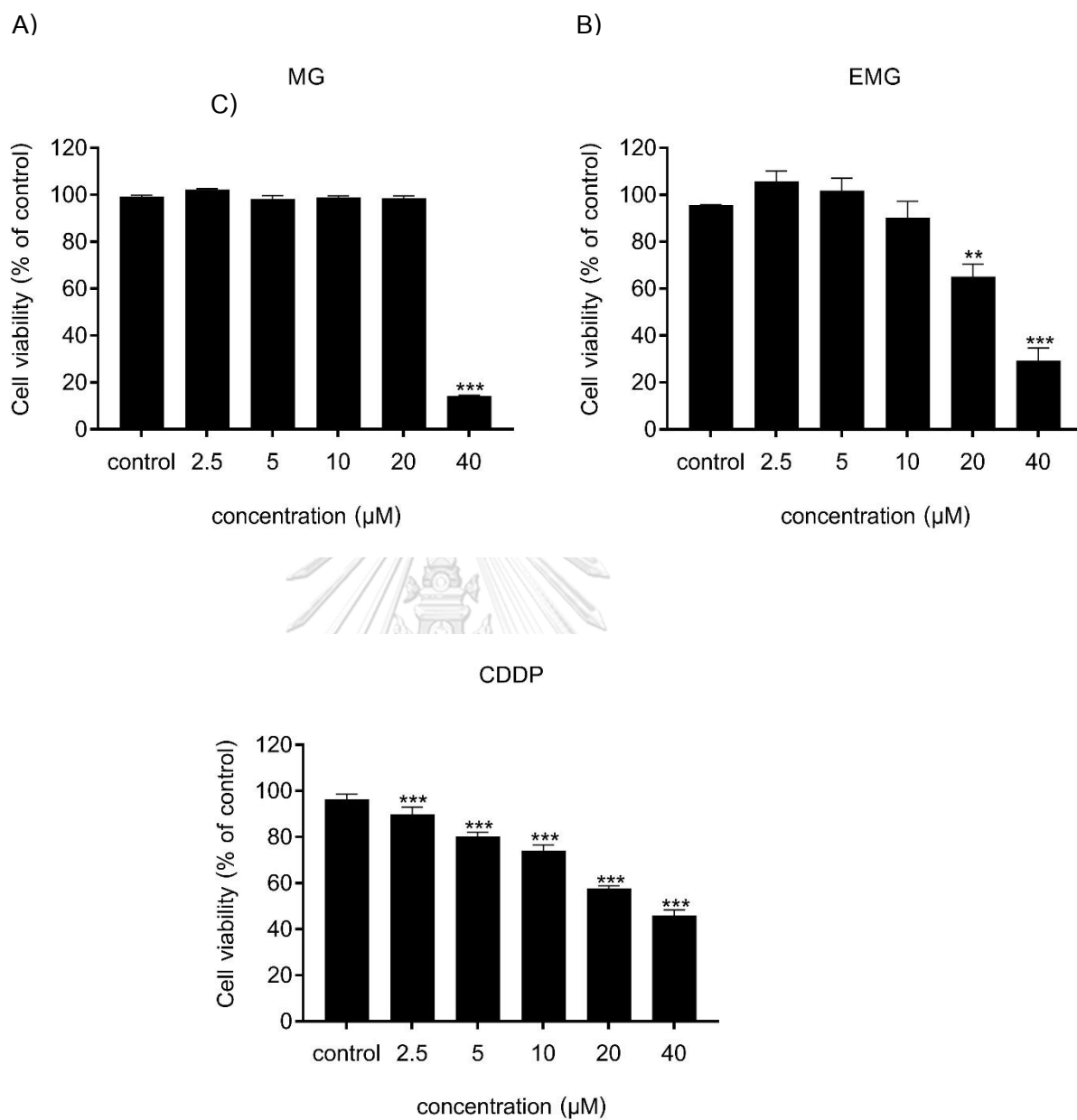


Figure 8 Effects of MG, EMG and CDDP on viability of PCS201-010 cells. The cells were treated with MG, EMG or CDDP at 2.5, 5, 10, 20 or 40 μM for 48 h. Cell viability was evaluated using MTT assays. Each value is expressed as the mean \pm SEM (n=3). **P<0.01, ***P<0.001 compared with vehicle control (0.2% DMSO).

Table 1 IC₅₀ and selectivity index values of MG, EMG and CDDP on A549, H1975 and PCS201-010 cells

Compounds	IC ₅₀ values (μM)			SI INDEX	
	A549	H1975	PCS201-010	A549	H1975
MG	20.88±0.44	30.03±1.84	27.59±1.99	1.32	0.92
EMG	9.49±0.58	7.27±0.26	26.19±1.31	2.76	3.60
CDDP	12.70±0.61	17.66±0.20	28.66±2.15	2.26	1.62

4.2 Effect of EMG on ROS generation in A549 cells

Several studies reported that natural naphthoquinones such as curcumin, plumbagin, shikonin and juglone induced oxidative stress via ROS generation in cancer cells (88). Thus, the effect of EMG on ROS generation in A549 cells was evaluated. Cells were treated with EMG at 5, 10 and 20 μM, CDDP at 10 μM or H₂O₂ at 200 μM for 1 h. The levels of ROS were determined by measuring the DCF fluorescence intensity. As shown in Figure 9A, EMG at 10 and 20 μM, CDDP at 10 μM and H₂O₂ at 200 μM significantly increased ROS levels from 100% to approximately 150%, 200%, 165% and 200%, respectively (P<0.05). To determine whether cytotoxicity of EMG is mediated through ROS generation in A549 cells, the cells were pre-treated with 5 mM *N*-acetylcysteine (NAC, a ROS scavenger) for 2 h and then incubated with 5, 10 and 20 μM of EMG or 10 μM of CDDP for additional 24 h. The cell viability was evaluated using MTT assays. The results showed that pretreatment with NAC significantly increased the viability of A549 cells by 1.2, 1.2, and 5.6 folds, when compared with the viability of the cells treated with EMG alone at 5, 10 and 20 μM, respectively (Figure 9B, P<0.01). Similarly, pretreatment with NAC prevented CDDP-induced cytotoxicity on A549 cells. These results suggest that cytotoxicity of EMG is partly mediated through ROS production in A549 cells.

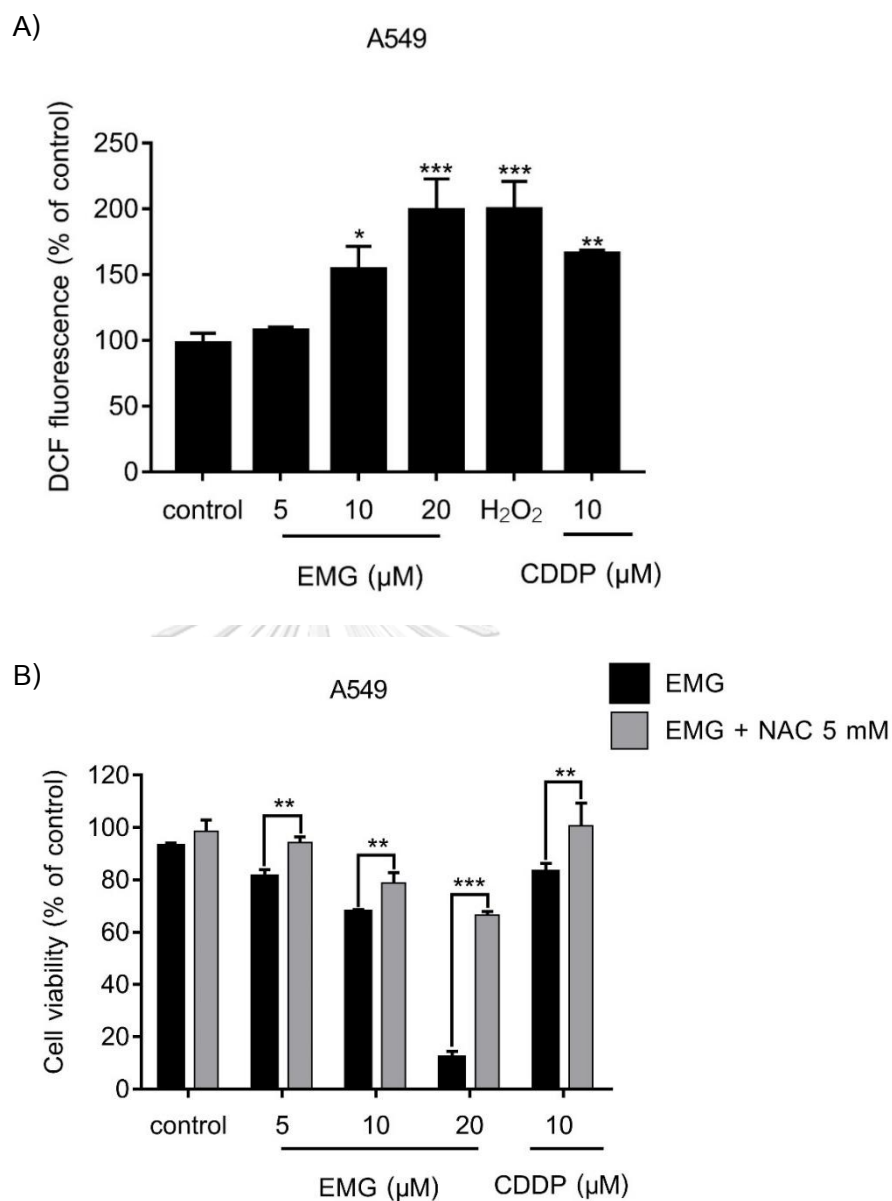


Figure 9 Effect of EMG on ROS generation in A549 cells. (A) Cells were treated with EMG at 5, 10 and 20 μM , CDDP at 10 μM or H_2O_2 at 200 μM for 1 h. The levels of ROS were determined by measuring the DCF fluorescence intensity using a fluorescence microplate reader. (B) Cells were treated with EMG at 5, 10 and 20 μM for 24 h in the presence or absence of 5 mM NAC. The cell viability was evaluated using MTT assays. Each value is expressed as the mean \pm SEM ($n=3$). * $P<0.05$, ** $P<0.01$, *** $P<0.001$ compared with vehicle control (0.2% DMSO).

4.3 Effect of EMG on cell cycle distribution in A549 cells

Some chemotherapeutic agents exerts their actions only during specific phase of the cell cycle while others exerts their actions at any point of the cell cycle (89, 90). Thus, the effect of EMG on cell cycle distribution of A549 cells was investigated. Initially, cells were synchronized in G_0/G_1 phase using serum starvation for 24 h before treatment with 5, 10 and 20 μM of EMG, 10 μM of CDDP or 0.2% DMSO for 24 h. Distribution of A549 cells in each phase of cell cycle after treatment was determined using PI staining, followed by fluorescence flow cytometry analysis. As shown in Figure 10, EMG at 5 and 10 μM significantly induced cell accumulation in the G_1 phase whereas CDDP at 10 μM significantly induced cell accumulation in the G_2/M phase in A549 cells ($P < 0.05$). These results suggest that EMG induced G_1 phase arrest in A549 cell.

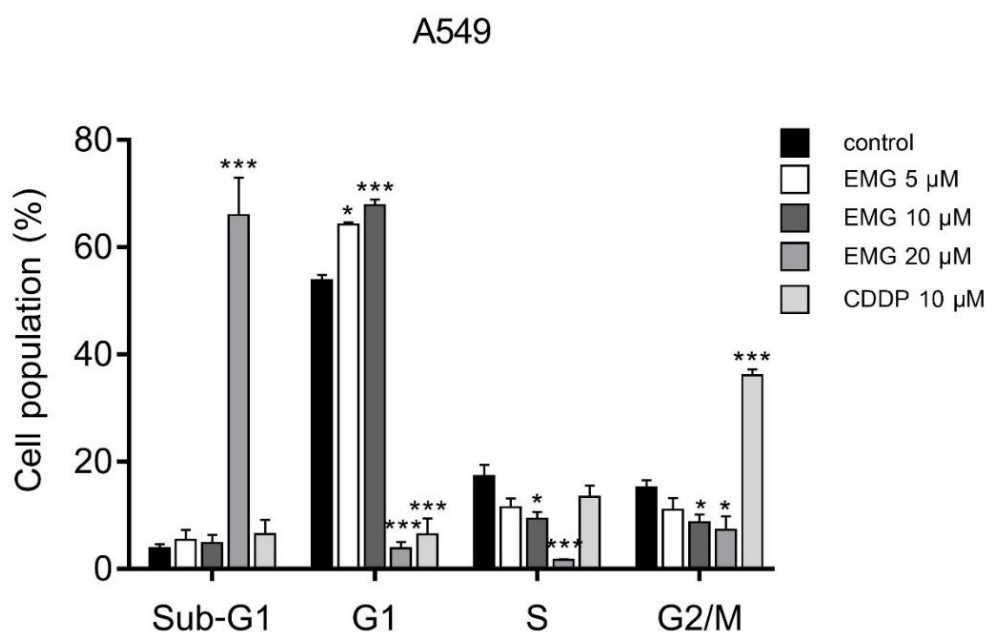


Figure 10 Effect of EMG on cell cycle distribution of A549 cells. Cells were synchronized in G_0/G_1 phase using serum starvation for 24 h. After serum starvation, the cells were treated with 5, 10 and 20 μM of EMG, 10 μM of CDDP, or 0.2% DMSO for 24 h. Flow cytometry analysis of PI-stained cells was used to determine cell cycle distribution. Each value is expressed as the mean \pm SEM ($n=3$). * $P < 0.05$, *** $P < 0.001$ compared with vehicle control (0.2% DMSO).

4.4 Effect of EMG on apoptosis induction in A549 cells

Most approved chemotherapeutic drugs induce cancer cells to undergo apoptosis via the mitochondrial pathway (91, 92). Thus, the apoptosis-inducing effect of EMG was evaluated in A549 cells. The cells were treated with 5, 10 and 20 μM of EMG and 10 μM of CDDP for 24 h. After annexin V-FITC/PI staining, apoptotic cells were identified by flow cytometry analysis. As shown in Figure 11, EMG induced A549 cells to undergo apoptosis. Treatment of A549 cells with EMG at 20 μM significantly increased apoptosis cell death by approximately 6-fold greater than the vehicle control ($P < 0.001$) whereas apoptotic A549 cells after treatment with CDDP at 10 μM were twice that of the vehicle control ($P < 0.01$).

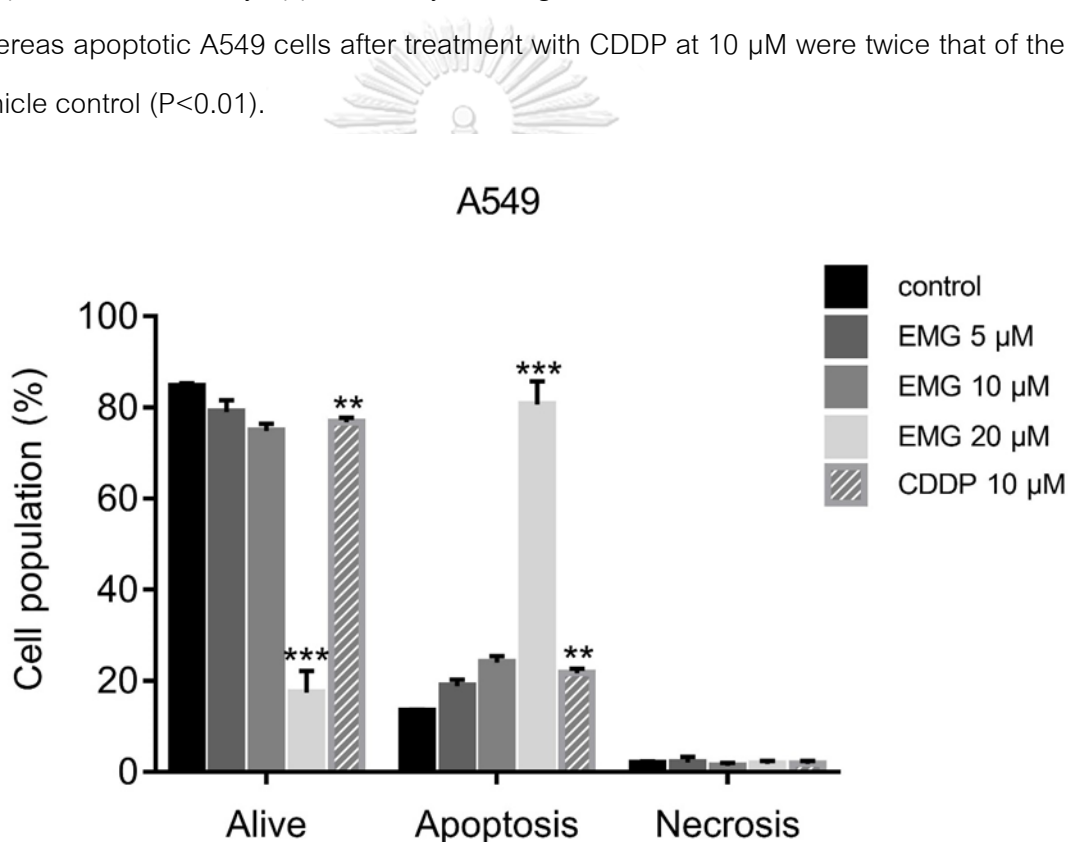


Figure 11 Apoptosis-inducing effect of EMG on A549 cells. Cells were treated with EMG at 5, 10 and 20 μM , CDDP at 10 μM or 0.2% DMSO for 24 h. Following treatment, apoptotic cells or necrotic cells were identified using annexin V-FITC/PI, followed by flow cytometry. Each value is expressed as the mean \pm SEM ($n=3$). ** $P < 0.01$, *** $P < 0.001$ compared with vehicle control (0.2% DMSO).

During apoptosis, poly (ADP-ribose) polymerase (PARP) is cleaved by caspase-3, resulting in DNA fragmentation (93). To confirm the apoptosis-inducing effect of EMG on A549 cells, the expression of cleaved PARP was determined using western blotting. The results showed that EMG at 20 μM as well as CDDP at 10 μM significantly induced PARP cleavage in A549 cells (Figure 12, $p < 0.01$). Taken together, these results suggest that cytotoxic effect of EMG is partly mediated via apoptosis induction in A549 cells.

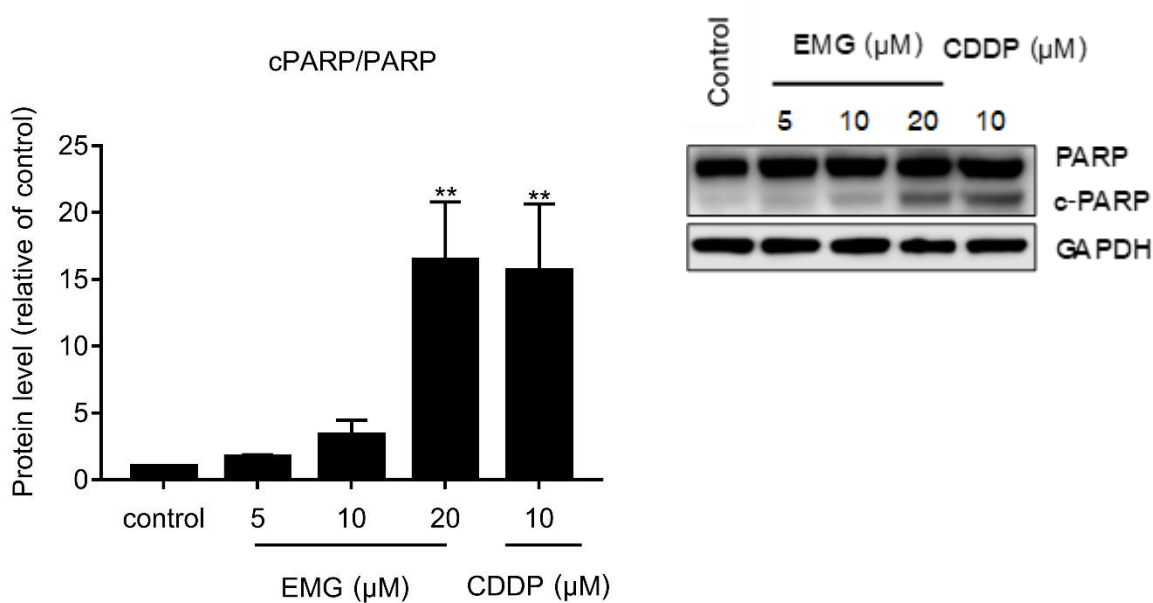
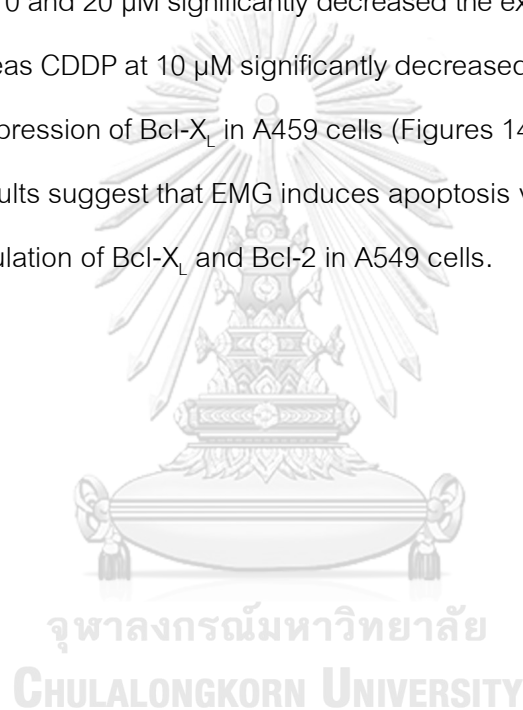


Figure 12 Effect of EMG on PARP cleavage in A549 cells. Cells were treated with EMG at 5, 10 and 20 μM or CDDP at 10 μM for 24 h. The protein expression of cleaved PARP and PARP were determined by western blotting. Each value is expressed as the mean \pm SEM (n=3). ** $P < 0.01$ compared with vehicle control (0.2% DMSO).

4.5 Effect of EMG on the expression of Bcl-2 family proteins in A549 cells

The mitochondrial or intrinsic apoptotic pathway is regulated by the Bcl-2 family proteins. In this study, the expression of Bcl-2 family proteins, including pro-apoptotic proteins (BAK, BAX) and anti-apoptotic proteins (Bcl-2, Bcl-X_L), was assessed using western blotting after the cells were treated with 5, 10 and 20 μ M of EMG, 10 μ M of CDDP or 0.2% DMSO for 24 h. As shown in Figures 13A and 13B, EMG at 20 μ M and CDDP at 10 μ M significantly increased the expression of BAK and BAX in A549 cells ($P < 0.05$). Moreover, EMG at 10 and 20 μ M significantly decreased the expression of Bcl-X_L and Bcl-2 in A549 cells whereas CDDP at 10 μ M significantly decreased the expression of Bcl-2 but did not alter the expression of Bcl-X_L in A459 cells (Figures 14A and 14B, $P < 0.05$). Taken together, these results suggest that EMG induces apoptosis via upregulation of BAK and BAX and downregulation of Bcl-X_L and Bcl-2 in A549 cells.



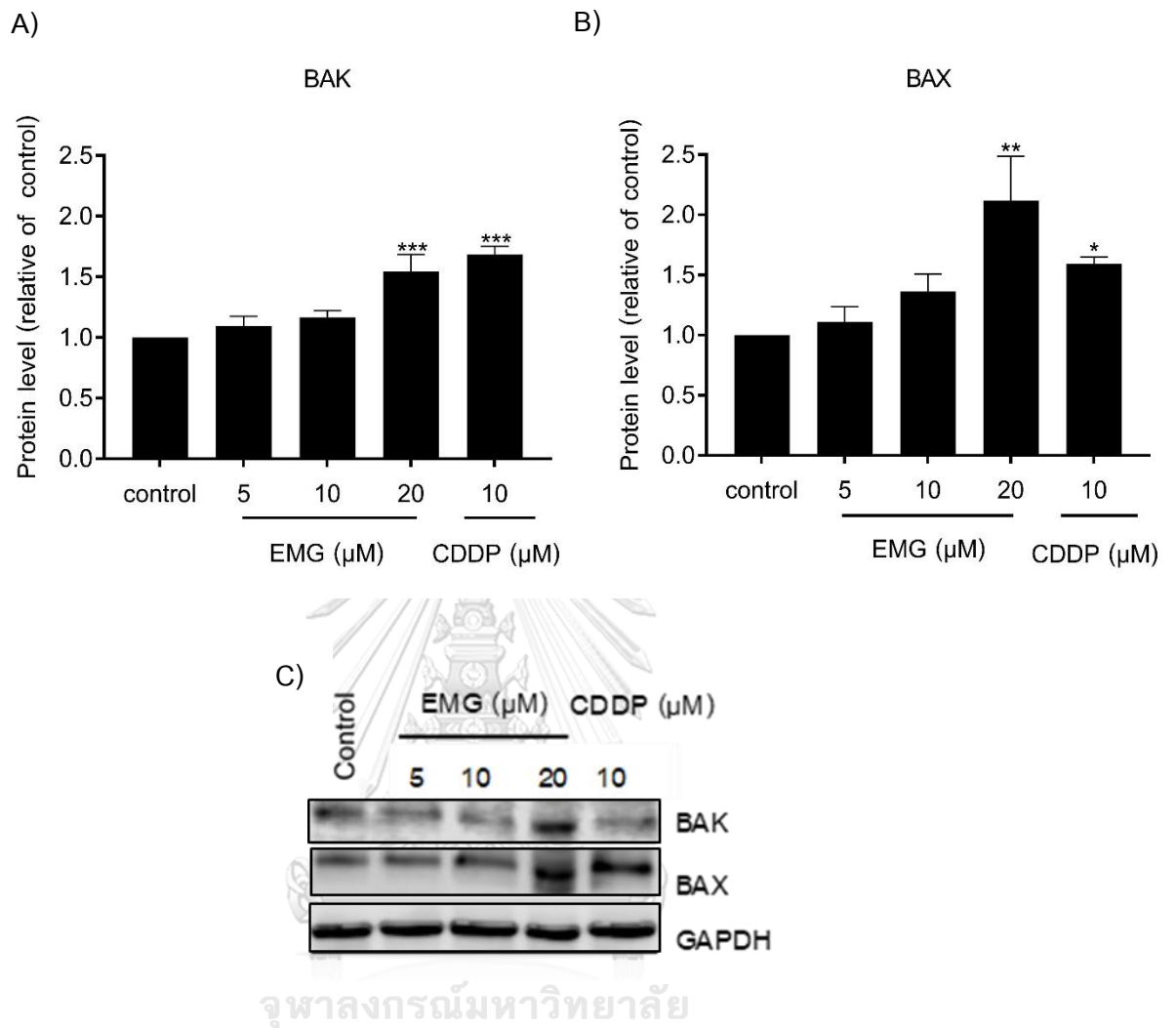


Figure 13 Effects of EMG on the expression of pro-apoptotic Bcl-2 family proteins in A549 cells. Cells were treated with EMG at 5 ,10 and 20 μM or CDDP at 10 μM for 24 h. The levels of pro-apoptotic proteins including (A) BAK (B) BAX were determined by western blot analysis. (C) Representative immunoblot images of BAK and BAX. The values are shown as fold change relative to the vehicle control. Each value is expressed as the mean ± SEM (n=3). *P<0.05, **P<0.01, ***P<0.001 compared with vehicle control (0.2% DMSO).

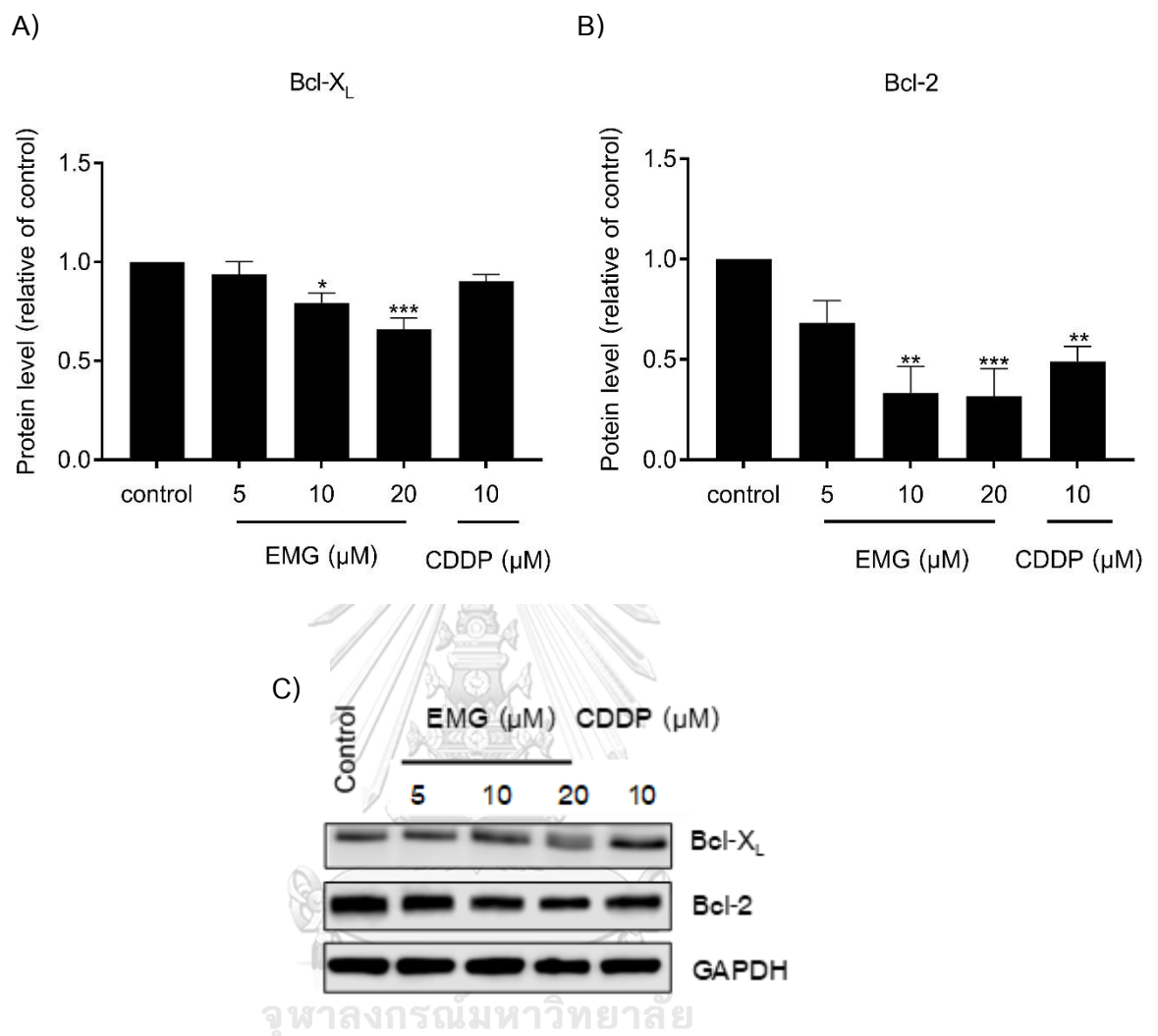


Figure 14 Effect of EMG on the expression of anti-apoptotic Bcl-2 family proteins in A549 cells. Cells were treated with EMG at 5, 10 and 20 μM or CDDP at 10 μM for 24 h. The levels of anti-apoptotic proteins including (A) Bcl-X_L and (B) Bcl-2 were determined by western blot. (C) Representative immunoblot images of Bcl-X_L and Bcl-2. The values are shown as fold change relative to the vehicle control. Each value is expressed as the mean ± SEM (n=3). *P<0.05, **P<0.01, ***P<0.001 compared with vehicle control (0.2% DMSO).

4.6 Apoptosis-inducing effect of EMG through ROS generation in A549 cells

To determine whether ROS is involved in apoptosis-inducing effect of EMG in A549 cells, the cells were pretreated with or without NAC for 2 h followed by EMG at 5, 10 and 20 μM or CDDP at 10 μM for 24 h. Then, the cells were stained with annexin V-FITC/PI and analyzed by flow cytometry. As shown in Figure 15, NAC prevented EMG-induced apoptosis in A549 cells. The percentage of apoptotic cell significantly decreased when the cells were pretreated with NAC by 3.2 and 1.1 folds, compared with cells treated with EMG at 20 μM and CDDP at 10 μM alone, respectively ($P < 0.05$). These results suggest that EMG-induced apoptosis is partly mediated through ROS generation in A549 cells.

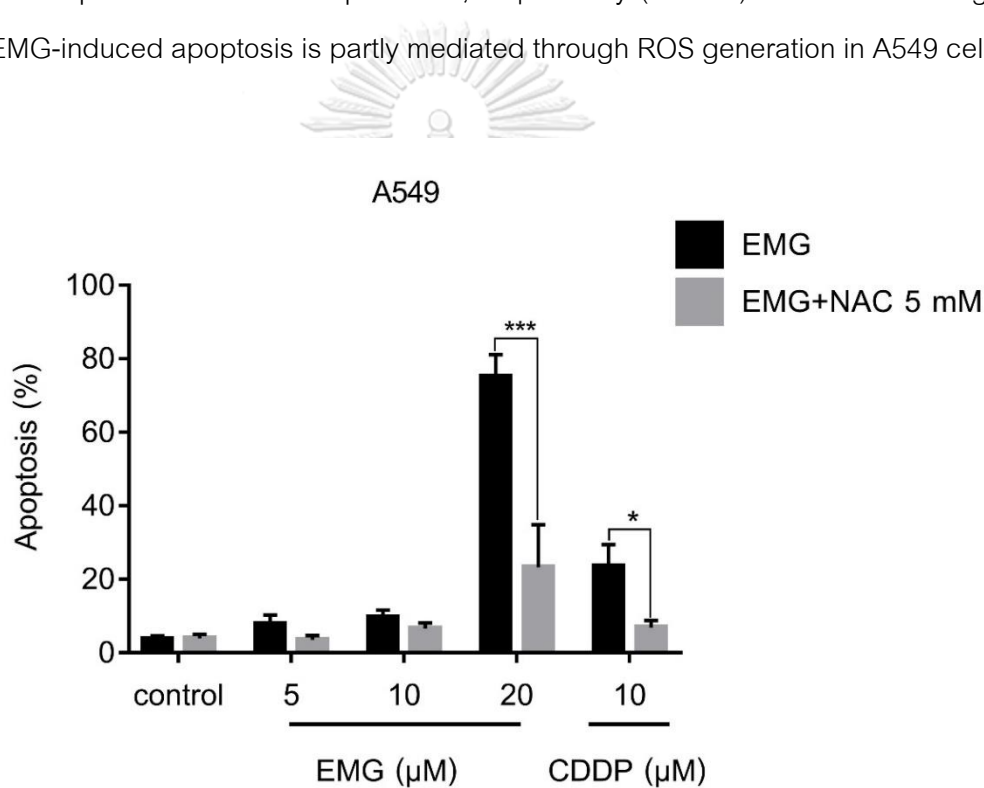


Figure 15 Apoptosis-inducing effect of EMG was mediated through ROS generation in A549 cells. Cells were treated with EMG at 5, 10 and 20 μM or CDDP at 10 μM for 24 h in the presence or absence of 5 mM NAC. Apoptotic and necrotic cells were identified by flow cytometry analysis using annexin V-FITC/PI staining method. Each value is expressed as the mean \pm SEM ($n=3$). * $P < 0.05$, *** $P < 0.001$ compared with EMG-treated cells.

4.7 Effect of EMG on MAPK/ERK and PI3K/AKT signaling pathways in A549 cells

It is commonly known that EGFR activation induces cell proliferation through two major signalling pathways, the MAPK/ERK and PI3K/AKT (94). Thus, the effects of EMG on the MAPK/ERK and PI3K/AKT signaling pathways in A549 cells were investigated. Cells were treated with EMG at 5, 10 and 20 μM , CDDP at 10 μM or 0.2% DMSO for 24 h and the expression of AKT, phospho(p)-AKT, ERK1/2 and p-ERK1/2 proteins was determined by western blotting. As shown in Figures 16A and 16B, EMG at 20 μM significantly increased the phosphorylation of AKT and ERK1/2 whereas CDDP at 10 μM did not alter the phosphorylation of ERK1/2 and AKT in A549 cells ($P < 0.01$). These results suggest that cytotoxicity of EMG may be mediated via activation of the MAPK/ERK and PI3K/AKT pathways in A549 cells.



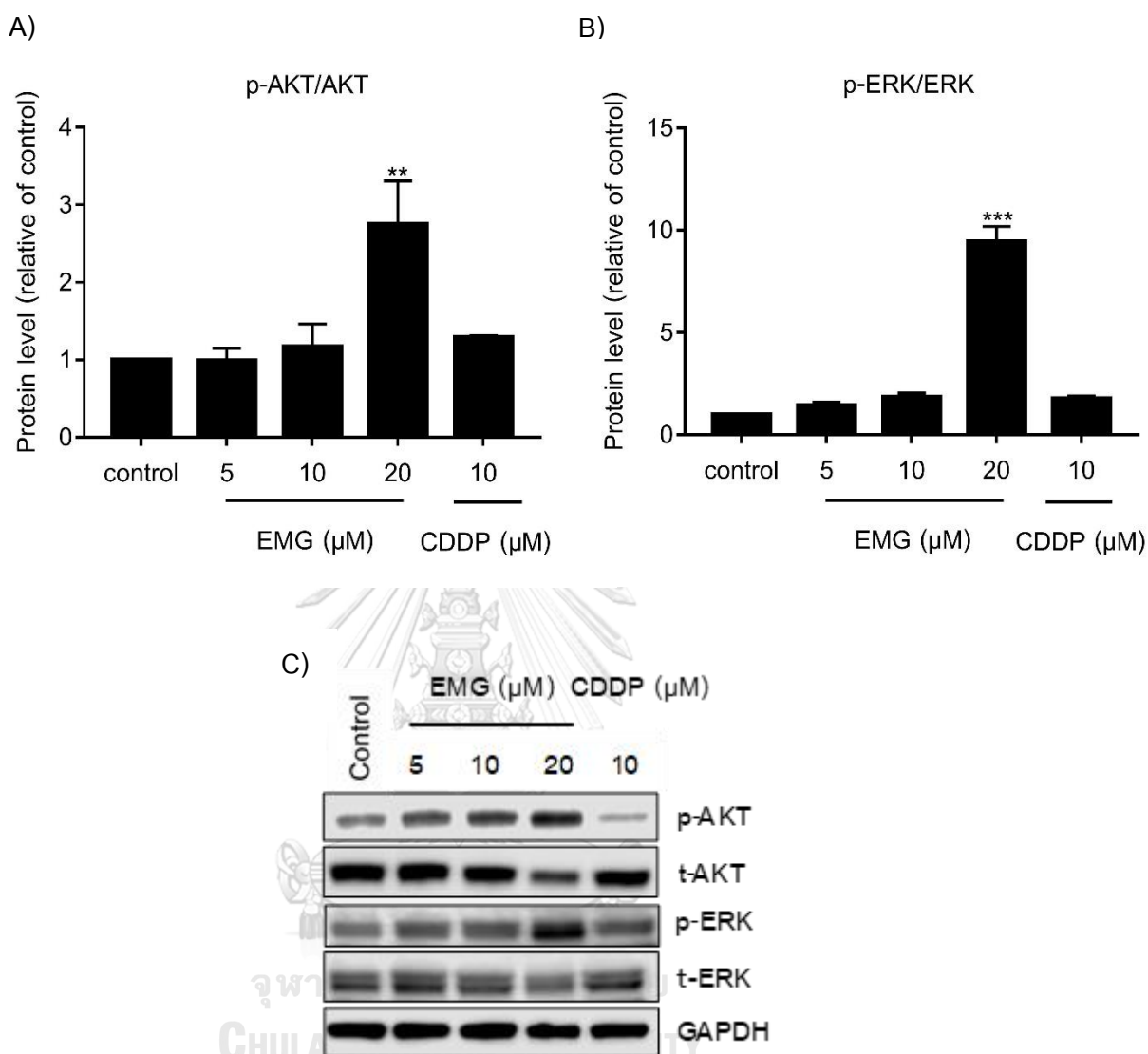
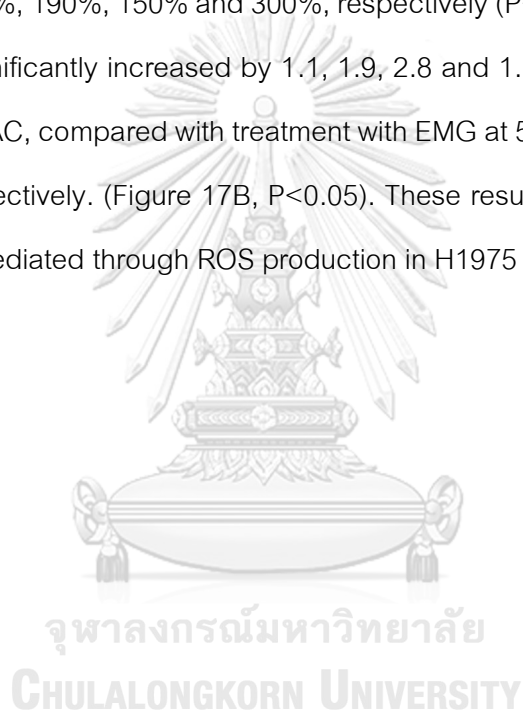


Figure 16 Effects of EMG on MAPK/ERK and PI3K/AKT signaling pathways in A549 cells. Cells were treated with EMG at 5, 10 and 20 μM , CDDP at 10 μM or 0.2% DMSO for 24 h. The protein levels were determined by western blotting. (A) The ratio of phospho-AKT/total-AKT (p-AKT/t-AKT) (B) The ratio of phospho-ERK1/2/total-ERK1/2 (p-ERK1/2/t-ERK1/2) (C) Representative immunoblot images of p-AKT, t-AKT, p-ERK1/2 and t-ERK1/2. The values are shown as fold change relative to the vehicle control. Each value is expressed as the mean \pm SEM (n=3). **P<0.01, ***P<0.001 compared with vehicle control (0.2% DMSO).

4.8 Effect of EMG on ROS generation in H1975 cells

Mutations of EGFR have been reported and implicated in the pathogenesis of several cancers, including NSCLC (6). Thus, the effect of EMG on ROS generation was evaluated in EGFR mutant H1975 cells. Cells were treated with EMG at 5, 10 and 20 μM , CDDP at 20 μM or H_2O_2 at 200 μM for 1 h and the levels of ROS were determined by measuring the DCF fluorescence intensity. As shown in Figure 17A, EMG at 10 and 20 μM , CDDP at 10 μM and H_2O_2 at 200 μM significantly increased ROS levels from 100% to approximately 155%, 190%, 150% and 300%, respectively ($P < 0.05$). Notably, the viability of H1975 cells significantly increased by 1.1, 1.9, 2.8 and 1.3 folds when the cells were pre-treated with NAC, compared with treatment with EMG at 5, 10 and 20 μM or CDDP at 20 μM alone, respectively. (Figure 17B, $P < 0.05$). These results suggest that cytotoxicity of EMG is partly mediated through ROS production in H1975 cells.



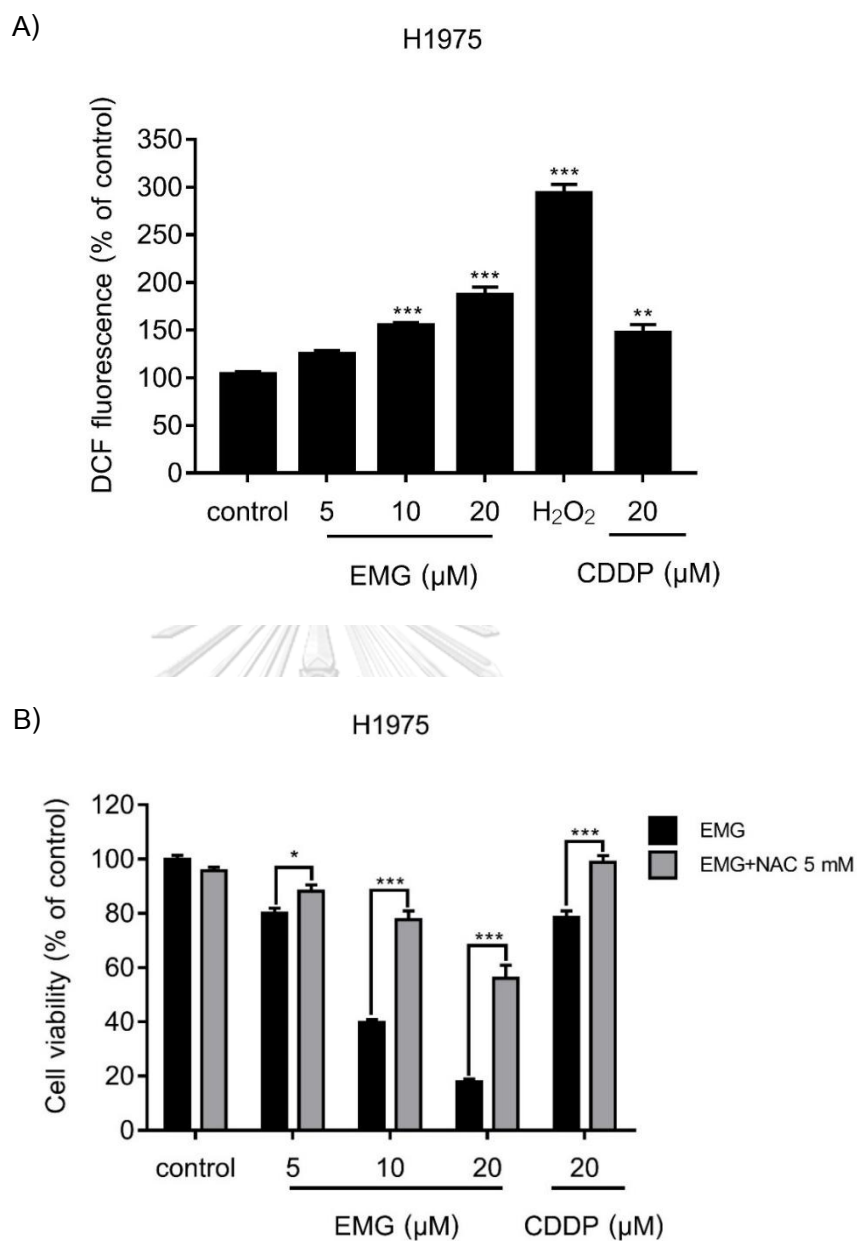


Figure 17 Effect of EMG on ROS generation in H1975 cells. (A) Cells were treated with EMG at 5, 10, 20 μM , CDDP at 20 μM or H₂O₂ at 200 μM for 1 h. The levels of ROS were determined by measuring the DCF fluorescence intensity using a fluorescence microplate reader. (B) Cells were treated with EMG at 5, 10 and 20 μM or CDDP at 20 μM for 24 h, in the presence or absence of 5 mM NAC. The cell viability was evaluated using MTT assays. Each value is expressed as the mean \pm SEM (n=3). *P<0.05, ** P<0.01, ***P<0.001 compared with vehicle control (0.2% DMSO).

4.9 Effect of EMG on cell cycle distribution in H1975 cells

To investigate the effect of EMG on H1975 cells in each phase of the cell cycle, the cells were initially synchronized in G₀/G₁ phase using serum starvation for 24 h. Then, cells were treated with 5, 10 and 20 μM of EMG, 20 μM of CDDP or 0.2% DMSO for 24 h. Distribution of PI-stained cells was identified by fluorescence flow cytometry. The result showed that EMG and CDDP did not induce significant accumulation of H1975 cells in a certain phase. Treatment with EMG at 5, 10 and 20 μM significantly decreased cell accumulation in the G₁, S and G₂/M phase when compared with vehicle control. However, EMG at 10 and 20 μM significantly induced accumulation of H1975 cells in the sub-G₁ phase, a good indicator of apoptosis. (Figure 18, P<0.05). These results suggest that EMG likely exerts its action on H1975 cells during any phase of the cell cycle.

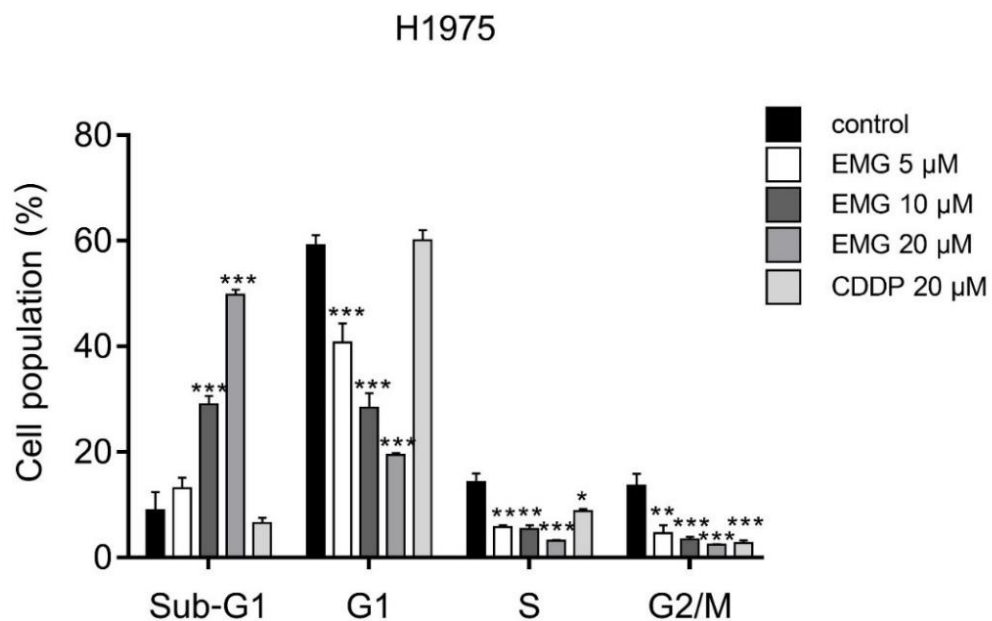


Figure 18 Effect of EMG on cell cycle distribution of H1975 cells. After serum starvation for 24 h, cells were treated with 5, 10 and 20 μM of EMG, 20 μM of CDDP, or 0.2% DMSO for 24 h. Cell cycle distribution was determined by flow cytometry analysis after PI staining. Each value is expressed as the mean ± SEM (n=3). *P<0.05, **P<0.01, ***P<0.001 compared with vehicle control (0.2% DMSO).

4.10 Effect of EMG on apoptosis induction in H1975 cells

To determine the apoptosis-inducing effect of EMG in H1975 cells, the cells were treated with 5, 10 and 20 μM of EMG, 20 μM of CDDP, or 0.2% DMSO for 24 h. Apoptotic cells death were determined using flow cytometry analysis of annexin V-FITC/PI-stained cells. As shown in Figure 19, EMG induced H1975 cells to undergo apoptosis. Treatment of H1975 cells with EMG at 5, 10 and 20 μM significantly increased apoptosis cell death in a concentration-dependent manner by approximately 45.9%, 62.9% and 79.2%, respectively, whereas CDDP at 10 μM significantly increased apoptosis cell death by approximately 21.9% ($P < 0.05$). To determine the effect of EMG on PARP cleavage in H1975 cells, the expression of cleaved PARP was measured after treatment with EMG at 2.5, 5 and 10 μM as well as CDDP at 20 μM . The results showed that EMG and CDDP significantly induced PARP cleavage in H1975 cells (Figure 20, $p < 0.001$). These results suggest that cytotoxic effect of EMG is partly mediated via apoptosis induction in H1975 cells.

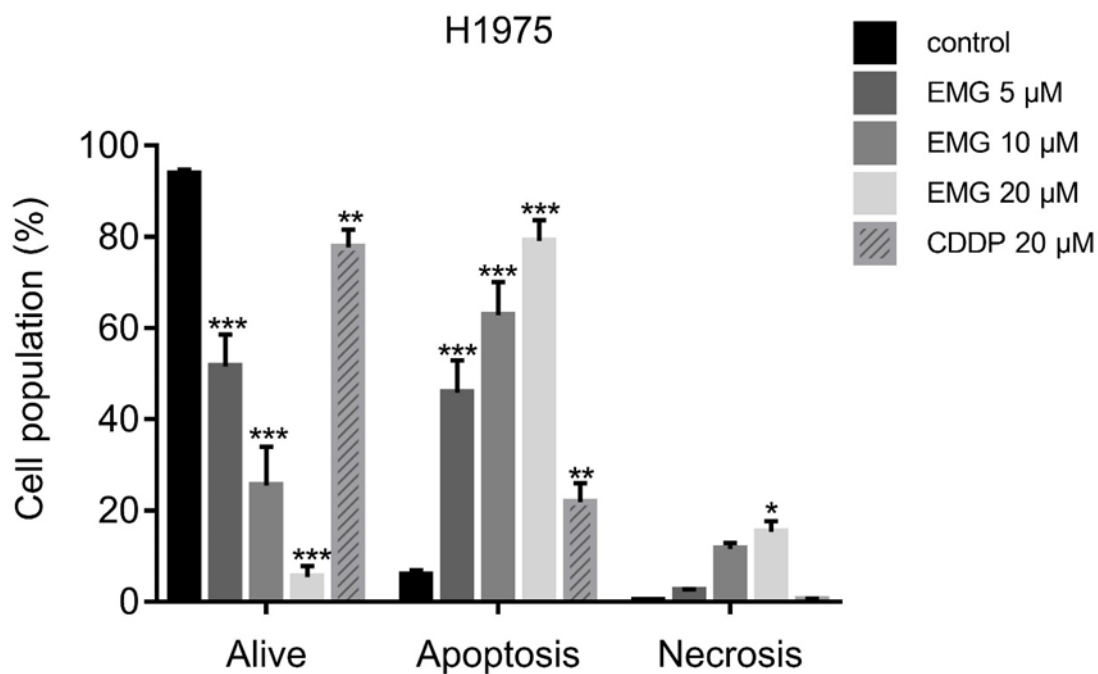


Figure 19 Apoptosis-inducing effect of EMG on H1975 cells. Cells were treated with EMG at 5, 10 and 20 μM and CDDP at 20 μM for 24 h. Following treatment, cells were analysed for apoptotic cells or necrotic cells by staining with annexin V-FITC/PI and examined by flow cytometry. Each value is expressed as the mean \pm SEM (n=3). *P<0.05, **P<0.01, ***P<0.001 compared with vehicle control (0.2% DMSO).

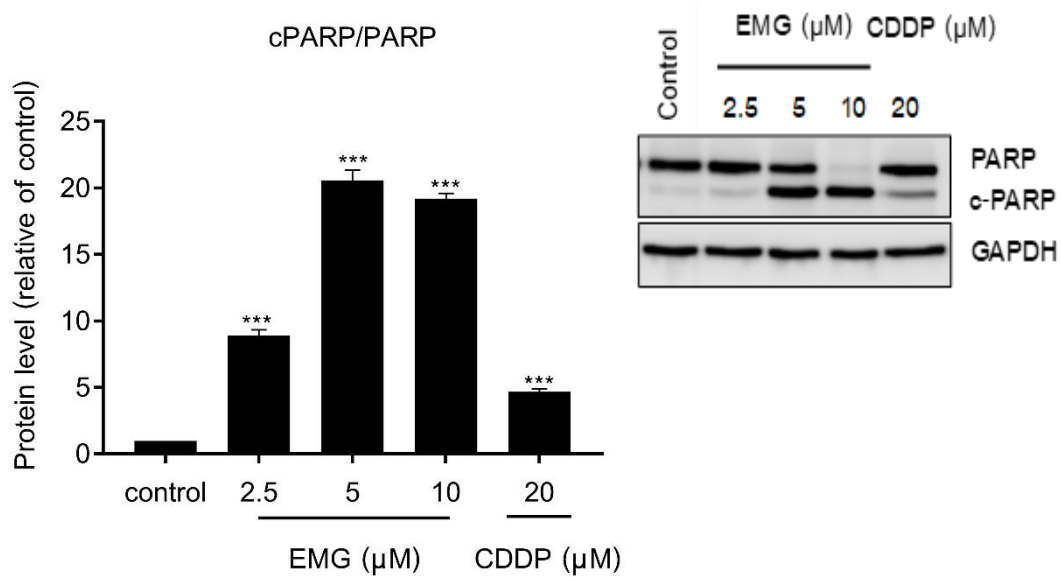


Figure 20 Effect of EMG on PARP cleavage in H1975 cells. The cells were treated with EMG at 2.5, 5 and 10 μM, CDDP at 20 μM, or 0.2% DMSO for 24 h. The protein levels of cleaved PARP and PARP were determined by western blotting. Each value is expressed as the mean \pm SEM (n=3). ***P<0.001 compared with vehicle control (0.2% DMSO).

4.11 Effect of EMG on the expression of Bcl-2 family proteins in H1975 cells

To determine the effects of EMG on the expression of apoptosis-related proteins, cells were treated with 2.5, 5 and 10 μM of EMG, 20 μM of CDDP or 0.2% DMSO for 24 h and the expression of pro-apoptotic proteins (BAK, BAX), anti-apoptotic proteins (Bcl-2, Bcl-X_L) in H1975 cells was evaluated. The results showed that the protein expression of BAK was significantly increased after treatment with EMG at 10 μM and CDDP at 20 μM , compared with vehicle control. Moreover, EMG at 2.5, 5 and 10 μM significantly upregulated the expression of BAX proteins in a concentration-dependent manner in H1975 cells (Figures 21A and 21B, $P < 0.05$). Similarly, the expression of BAX protein was significantly increased after treatment with CDDP at 20 μM . In addition to increases in pro-apoptotic proteins, EMG significantly downregulated the expression of antiapoptotic proteins. The expression of Bcl-X_L was significantly decreased after treatment with EMG at 20 μM and CDDP at 20 μM . Notably, EMG at 5 and 10 μM and CDDP at 20 μM also significantly decreased the expression of Bcl-2 in H1975 cells (Figure 22A and 22B, $P < 0.05$). These results suggest that apoptosis-inducing effect of EMG is likely mediated through upregulation of BAK and BAX and downregulation of Bcl-X_L and Bcl-2 in H1975 cells.

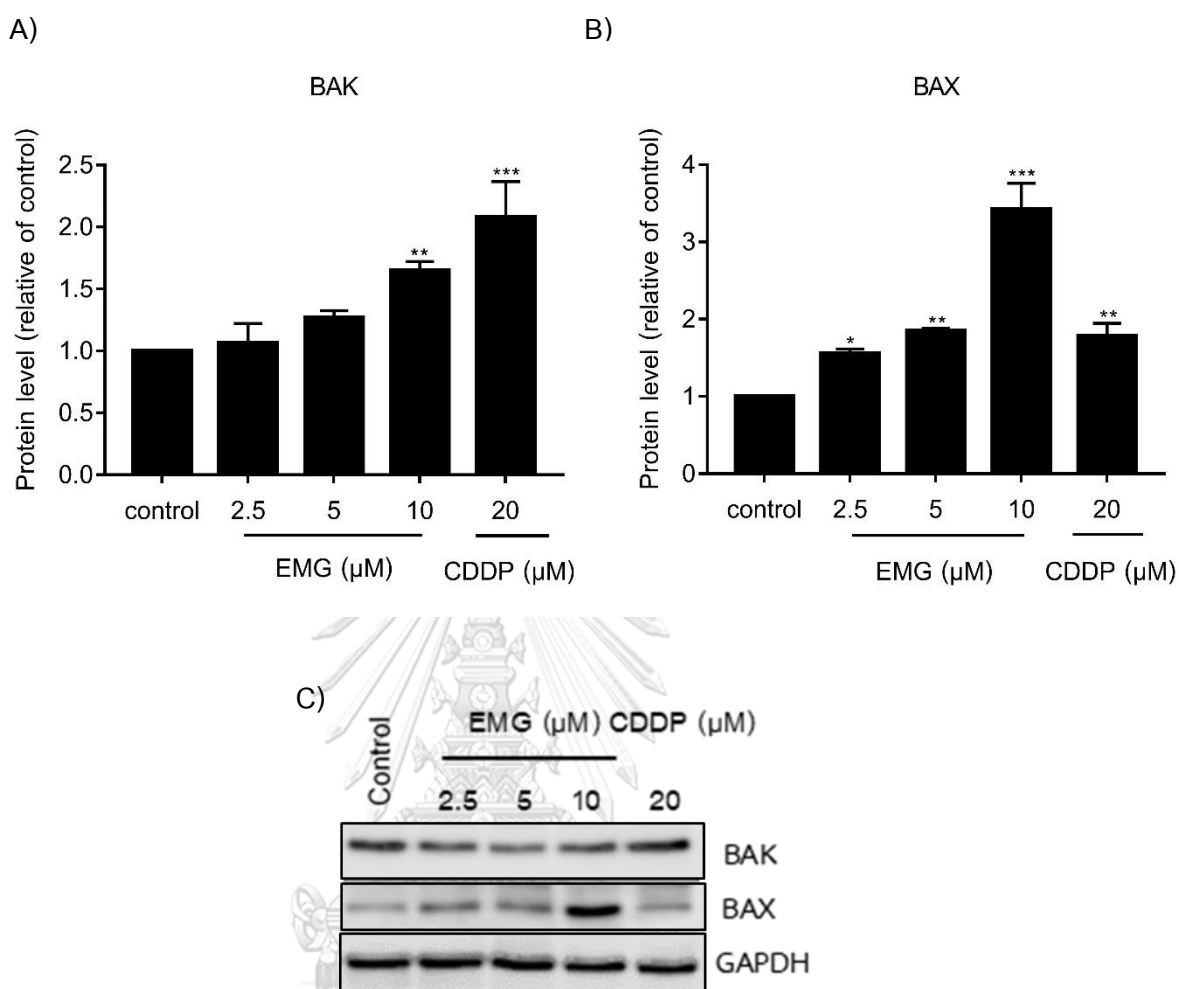


Figure 21 Effect of EMG on the expression of pro-apoptotic Bcl-2 family proteins in H1975 cells. Cells were treated with EMG at 2.5, 5 and 10 μ M and CDDP at 20 μ M for 24 h. The levels of pro-apoptotic proteins, including (A) BAK and (B) BAX, were determined by western blotting. (C) Representative immunoblot images of BAK and BAX. The values are shown as fold change relative to the vehicle control. Each value is expressed as the mean \pm SEM (n=3). *P<0.05, **P<0.01, ***P<0.001 compared with vehicle control (0.2% DMSO).

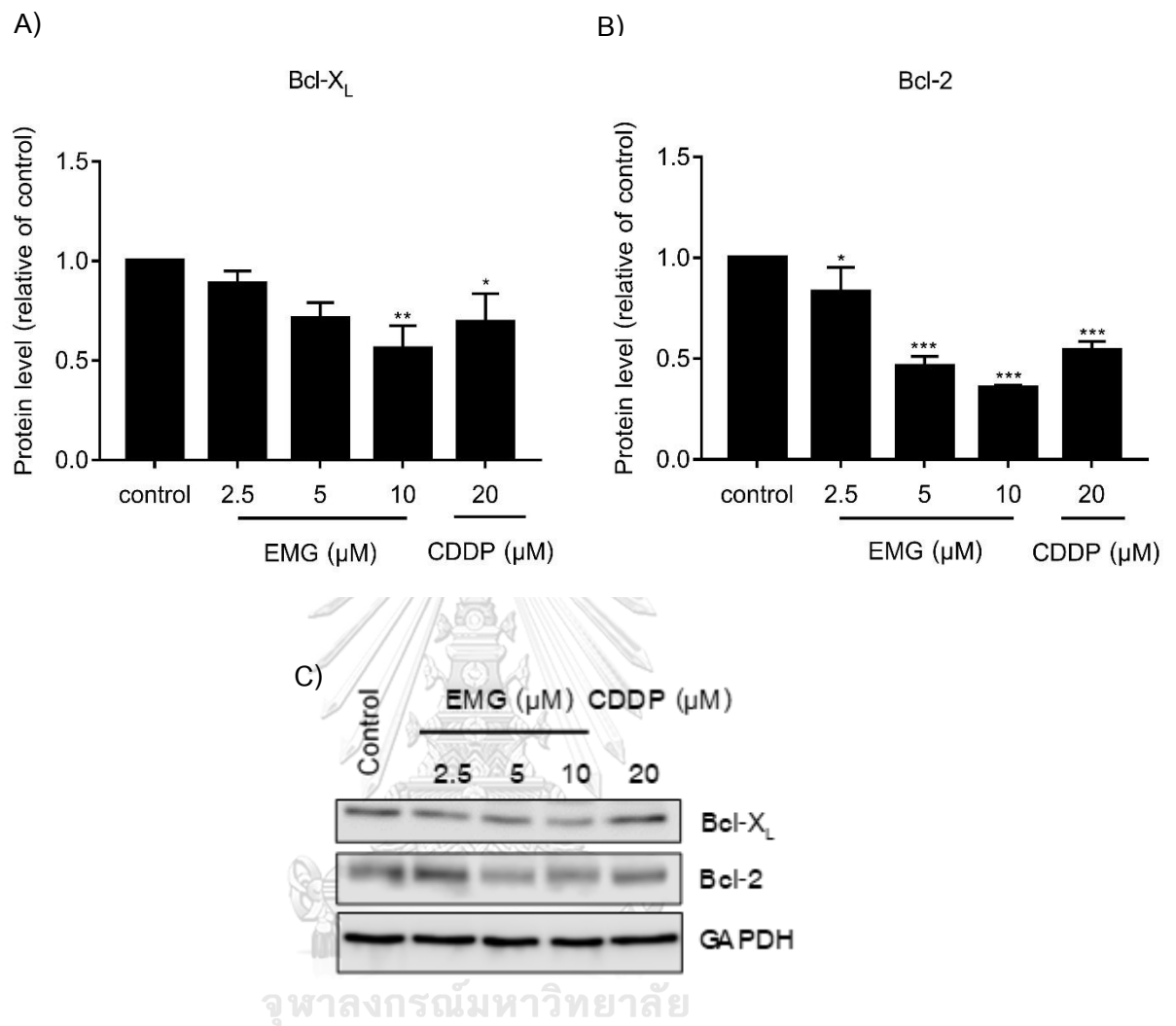


Figure 22 Effect of EMG on the expression of anti-apoptotic Bcl-2 family proteins in H1975 cells. Cells were treated with EMG at 2.5, 5 and 10 μM and CDDP at 20 μM for 24 h. The levels of anti-apoptotic proteins including (A) Bcl-X_L and (B) Bcl-2 were determined by western blotting. (C) Representative immunoblot images of Bcl-X_L and Bcl-2. The values are shown as fold change relative to the vehicle control. Each value is expressed as the mean ± SEM (n=3). *P<0.05, **P<0.01, ***P<0.001 compared with vehicle control (0.2% DMSO).

4.12 Apoptosis-inducing effect of EMG through ROS generation in H1975 cells

To determine whether apoptosis-inducing effect of EMG is associated with ROS generation in H1975 cells, the cells were treated with NAC for 2 h before treatment with EMG at 5, 10 and 20 μM , CDDP at 20 μM , or 0.2% DMSO for 24 h. Then, apoptotic and necrotic cells were identified by flow cytometry analysis of annexin V-FITC/PI-stained cells. As shown in Figure 23, pretreatment with NAC for 2 h significantly prevented apoptosis in H1975 cells. The percentage of apoptotic cells significantly decreased by 1.5, 1.6 and 1.4 folds when pre-treated with NAC, compared with treatment with EMG at 5, 10 and 20 μM alone, respectively ($P < 0.05$). These results suggest that ROS is likely involved in EMG-induced apoptosis in H1975 cells.

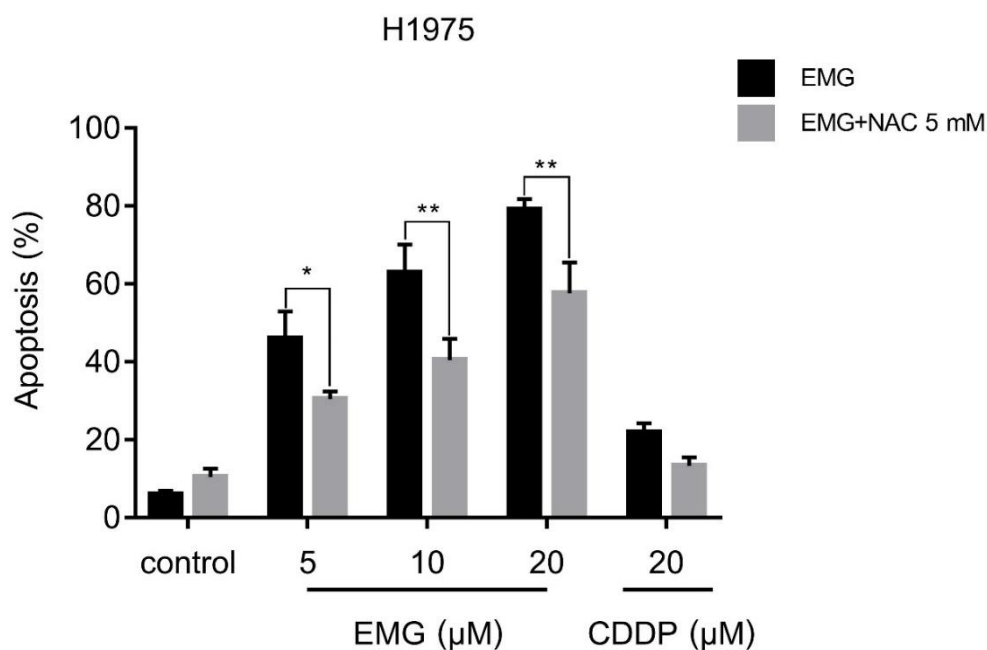


Figure 23 Apoptosis-inducing effect of EMG is mediated through ROS generation in H1975 cells. Cells were treated with EMG at 5, 10 and 20 μM or CDDP at 20 μM for 24 h, in the presence or absence of 5 mM NAC. Apoptotic cells were analyzed by flow cytometry analysis using annexin V-FITC/PI staining. Each value is expressed as the mean \pm SEM ($n=3$). * $P < 0.05$ and ** $P < 0.01$ compared with EMG-treated cells.

4.13 Effect of EMG on MAPK/ERK and PI3K/AKT signaling pathways in H1975 cells

To evaluate the effect of EMG on MAPK/ERK and PI3K/AKT signaling pathways in H1975 cells, the cells were treated with EMG at 2.5, 5 and 10 μM , CDDP at 20 μM , or 0.2% DMSO for 24 h and the levels of proteins involved in MAPK/ERK and PI3K/AKT signaling pathways, including, AKT, p-AKT, ERK1/2 and p-ERK1/2 were determined by western blotting. As shown in Figures 24A and 24B, EMG at 10 and 20 μM significantly decreased the phosphorylation of AKT and ERK1/2. Notably, CDDP at 20 μM significantly decreased the phosphorylation of AKT but increased the phosphorylation of ERK1/2 in H1975 cells ($P < 0.05$). These results suggest that cytotoxicity of EMG may be mediated via inhibition of MAPK/ERK and PI3K/AKT signaling pathways.



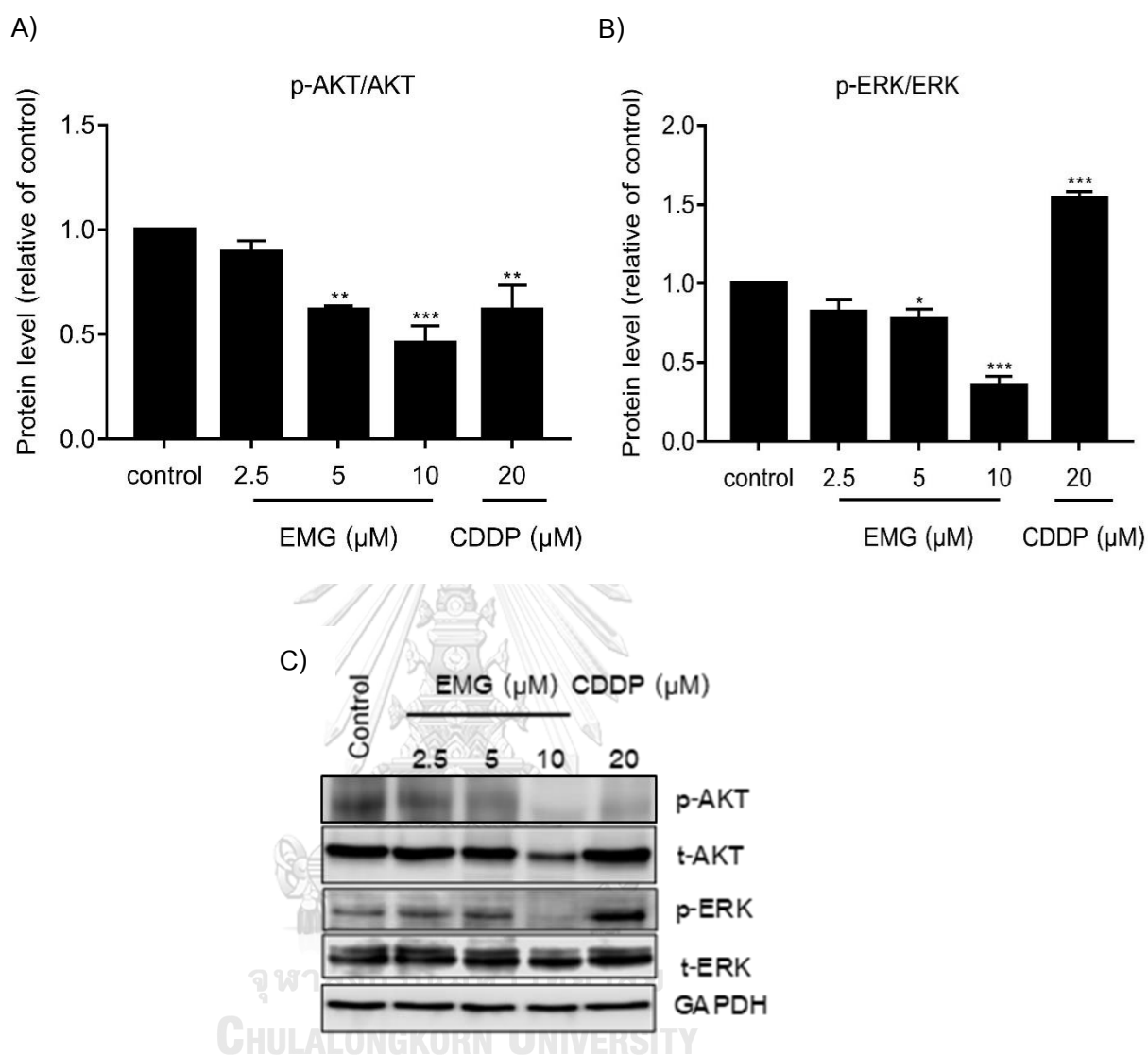


Figure 24 Effect of EMG on MAPK/ERK and PI3K/AKT signaling pathways in H1975 cells. Cells were treated with EMG at 2.5, 5 and 10 μ M, CDDP at 20 μ M or 0.2% DMSO for 24 h. The levels of proteins involved in MAPK/ERK and PI3K/AKT signaling pathways were determined by western blot. (A) The ratio of phospho-AKT/total-AKT (p-AKT/t-AKT) (B) The ratio of phospho-ERK1/2/total-ERK1/2 (p-ERK1/2/t-ERK) (C) Representative immunoblot images of p-AKT, AKT, p-ERK and ERK2. The values are shown as fold change relative to the vehicle control. Each value is expressed as the mean \pm SEM (n=3). *P<0.05, **P<0.01, ***P<0.001 compared with vehicle control (0.2% DMSO).

CHAPTER V

DISCUSSION AND CONCLUSION

Lung cancer is one of the most common human cancers and represents the leading cause of cancer mortality worldwide for both men and women. Surgery, radiation therapy, chemotherapy and targeted therapy are the standard cancer therapies (4, 95). For lung cancer patients with advanced stage, chemotherapy is the treatment of choice, which is mostly associated with severe adverse events. Therefore, new compounds with high anticancer activity and low toxicity are critically needed.

Mansonones are naphthoquinone-containing compounds extracted from the heartwood of *Mansonia gagei* (13). A previous study reported that mansonones E and F exhibited anticancer effects against various cancer cell lines such as breast cancer (MCF-7), cervical cancer (HeLa), lymphoma (U937) and melanoma (A375-S2) (18). Additionally, mansonone G (MG) exhibited anticancer activity against ovarian (A2780) and tamoxifen-resistant breast LCC2 cancer cell lines with IC_{50} values of 10.2 ± 0.9 and 26.19 ± 0.16 μ M, respectively (96, 97). In this study, the cytotoxicity of MG and its derivative, ethoxy mansonone G (EMG), were investigated on two non-small cell lung cancer cell lines, A549 expressing wild-type EGFR and H1975 expressing mutant EGFR. The result showed that both MG and EMG exhibited cytotoxicity against A549 and H1975 NSCLC cells. However, it should be noted that EMG displayed higher cytotoxicity than MG in both A549 and H1975 cells. Previously, it was reported that ether analogues of mansonone G displayed higher antiadipogenic activity higher than the parent MG (4). Moreover, ether analogues of MG were found to have higher antibacterial activity than the parent MG (3). It was suggested that increasing alkyl chain length on ether analogues of MG, made the compounds more hydrophobic which could facilitate the access of compounds to bacterial cells. Thus, it is likely that increasing number of carbon units of alkyl side chain enhances the cytotoxicity of EMG against NSCLC cell lines.

ROS levels are higher in cancer cells than normal cells. It is known that ROS can generate from dysregulated mitochondria and high level of ROS can cause the oxidative stress and damage the cellular components (98, 99). Therefore, inducing ROS generation in cancer cells has been considered a new strategy for anti-cancer therapy. Indeed, many chemotherapeutic drugs, including cisplatin, oxaliplatin and doxorubicin and natural compounds such as curcumin, lawsone, shikonin, juglone and plumbagin, have been known to induce various cancer cells to undergo apoptosis through ROS production (100-102). Similarly, this study found that EMG induced ROS production in NSCLC cells and *N*-acetylcysteine (NAC), a ROS scavenger, could prevent EMG-induced cell death in both A549 and H1975 cells. Moreover, NAC was able to prevent apoptosis-inducing effect of EMG in both cell lines. Taken together, these results suggest that ROS generation are partly involved in cytotoxicity and apoptosis-inducing effect of EMG in NSCLC cells.

Most chemotherapeutic agents cause DNA damage and activate a complex signaling network, resulting in cell cycle arrest and/or apoptosis (103). A previous study reported that EPDMNQ and ENDMNQ, 1,4-naphthoquinone derivatives, induced A549 cell cycle arrest at the G₁ phase (104). In this study, treatment of A549 cells with EMG at 5 and 10 μ M induced cell cycle arrest at G₁ phase while EMG at a higher concentration (20 μ M) induced apoptosis. In contrast to A549 cells, the result showed that EMG at 5 μ M did not induce cell cycle arrest at any phase of cell cycle in H1975 cells whereas EMG at 10 and 20 μ M induced accumulation of H1975 cells in the sub-G₁ phase. A previous study reported that CDDP induced G₂/M cell cycle arrest in A549 cells (105). Similarly, the present study found that cisplatin induced accumulation of A549 cells in the G₂/M phase whereas CDDP did not induce accumulation of H1975 cells in a certain phase. It is well established that induction of the p53 tumor suppressor protein in cells can lead to either cell cycle arrest or apoptosis (106) and loss of p53 lead to loss of cell cycle arrest after DNA damage or physiological stresses (107). Thus, it is possible that effect of EMG on cell cycle arrest may have been compromised by mutation of p53 in H1975 cells.

Several chemotherapeutic drugs and natural naphthoquinones induce cancer cells to undergo apoptosis via the mitochondrial pathway (91, 108, 109). A recent study

reported that mansonone E induced apoptosis in cervical cancer cells by downregulating expression of anti-apoptotic proteins, Bcl-X_L and Bcl-2 and upregulating expression of a proapoptotic protein, Bax (18). In the present study, EMG induced apoptosis in NSCLC cells. Western blotting demonstrated that EMG downregulated the expression of Bcl-X_L and Bcl-2 and upregulated the expression of BAK and BAX in both A549 and H1975 cells. Taken together, these results suggest that EMG-induced apoptosis by modulating Bcl-2 family proteins in NSCLC cells. The most common signaling cascades involved in apoptosis is the activation of caspases. Once activated, caspases initiate cell death by cleaving and activating effector caspases which drive the process of apoptosis (110, 111). PARP is a key nuclear enzyme involved in DNA repair (112-115) and cleavage of PARP is considered to be a hallmark of apoptosis (111). This study found that EMG induced PARP cleavage in both A549 and H1975 cells, highlighting the apoptosis-inducing effect of EMG. Studies in several cancer cell types such as melanoma, ovarian and small cell lung cancer cells have demonstrated that treatment of cells with CDDP induced PARP cleavage and apoptosis (64, 116-118). Similarly, this study found that in A549 cells, CDDP upregulated the expression of BAK and BAX and downregulated the expression of Bcl-2 whereas CDDP upregulated the expression of BAK and BAX and downregulated the expression of Bcl-X_L and Bcl-2 in H1975 cells. Moreover, CDDP also induced cleavage of PARP and apoptosis in both A549 and H1975 cells.

The PI3K/AKT and MAPK/ERK signaling pathways are frequently activated in NSCLC and play important roles in the oncogenesis through promoting cell survival, growth, proliferation and migration. These signal transduction cascades are also known to contribute to tumor progression and resistance to chemotherapeutic agents (119, 120). A previous study reported that artocarpin exhibited apoptosis-inducing effect by activating cellular protein kinases including Erk1/2, p38 and AKT in A549 cells (121). Moreover, ellipticine was shown to induce apoptosis cell death via activation of AKT signaling pathway in A549 cells (122). Similarly, the present study found that EMG increased AKT phosphorylation in A549 cells. In addition to PI3K/AKT pathway, EMG could increase ERK1/2 phosphorylation in A549 cells. These findings are consistent with

others that showed 1,2-Naphthoquinone increased EGFR phosphorylation, resulting in activation of MAPK/ERK signaling pathway in A549 cells (123). A recent evidence suggests that ERK can contribute to cell apoptosis through activation of caspase 3 (124). Taken together, it is likely that anticancer of EMG may be mediated through activation of PI3K/AKT and MAPK/ERK signaling pathways in A549 cells. Notably, in contrast to A549 cells, the present study found that EMG inhibited the phosphorylation of AKT and ERK1/2 in H1975 cells. This was in agreement with previous study reported that butoxy mansonone G significantly inhibited AKT signaling pathways in H1975 cells (125). Moreover, it was shown that isoliquiritigenin (ILQ) induced apoptosis and inhibited xenograft tumor growth of H1975 cells by inhibiting the phosphorylation of AKT and ERK1/2 (126). Thus, it is possible that anticancer activity of EMG may be mediated through modulation of PI3K/AKT and MAPK/ERK signaling pathways in NSCLC cells.

ROS are known to be involved in activation of PI3K/AKT and MAPK family members, including JNK, p38 and ERK1/2 (121, 127, 128). Previous study reported that some natural compounds such as resveratrol, EGCG and curcumin suppressed cancer cell growth by mediating apoptotic signaling components, including MAPKs (p38, ERK1/2 and JNK), PI3K/AKT, BAX/Bcl-2 ratio, cytochrome c, Apaf-1, caspase cascade (caspase 3, 8 and 9) and PARP via ROS production (129-131). Moreover, ROS have been shown to be upstream modulators of MAPK and PI3K/AKT signaling pathways during anticancer drugs-induced apoptosis (132-134). Therefore, it is likely that ROS-mediated PI3K/AKT and MAPK/ERK signaling pathways are involved in apoptosis-inducing effects of EMG. The role of ROS in PI3K/AKT and MAPK/ERK signaling pathways in EMG-treated NSCLC cells needs further investigation.

Conclusion

The present study demonstrated that EMG exerted a potent anticancer activity against two NSCLC cell lines, A549 expressing wild-type EGFR and H1975 expressing mutant EGFR. In A549 cells, EMG induced cell cycle arrest at G₁ phase and apoptosis through modulation of Bcl-2 family proteins, Bcl-2, BAK and BAX and accumulation of ROS level. Moreover, EMG activated PI3K/AKT and MAPK/ERK signaling pathways by upregulating the phosphorylation of ERK1/2 and AKT. In H1975 cells, treatment with EMG induced apoptosis through modulation of Bcl-2 family proteins, Bcl-X_L, Bcl-2, BAK and BAX and accumulation of ROS level and inhibited the phosphorylation of ERK1/2 and AKT. These findings suggest that EMG may potentially be used as a novel anticancer agent for NSCLC.



APPENDIX A

PREPARATION OF REAGENTS

1. DMEM stock solution (1 L)

DMEM powder	10.4 g
NaHCO ₃	3.7 g
ddH ₂ O	900 mL

Adjust pH to 7.4 with 1 N HCl or 1 N NaOH

Add ddH₂O to 1 L and sterilized by filtering through a 0.2 sterile membrane filter

Store at 4°C

2. RPMI 1640 stock solution (1 L)

RPMI powder	10.4 g
NaHCO ₃	1.5 g
Glucose	4.5 g
Sodium pyruvate	0.11 g
HEPES (1M)	10 mL
ddH ₂ O	900 mL

Adjust pH to 7.2 with 1 N HCl and 1 N NaOH

Add ddH₂O to 1 L and sterilized by filtering through a 0.2 sterile membrane filter

Store at 4°C

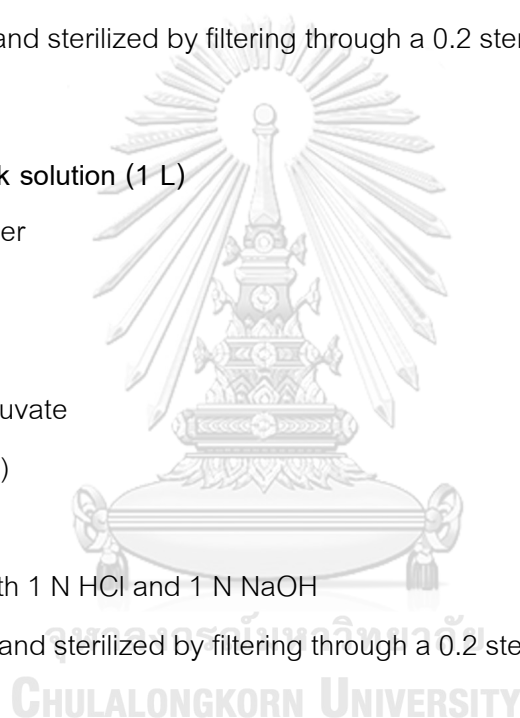
3. DMEM high glucose stock solution (1 L)

DMEM powder	10.4 g
NaHCO ₃	3.7 g
Glucose	4.5 g
ddH ₂ O	900 mL

Adjust pH to 7.4 with 1 N HCl or 1 N NaOH

Add ddH₂O to 1 L and sterilized by filtering through a 0.2 sterile membrane filter

Store at 4°C



4. 1X Phosphate Buffer Saline (PBS) (1 L)

NaCl	8.065 g
KCl	0.2 g
KH_2PO_4	0.2 g
Na_2HPO_4	1.15 g
ddH ₂ O	900 mL

Adjust pH to 7.4 with 1 N HCl or 1 N NaOH

Add ddH₂O to 1 L and sterilized by autoclaving

Store at room temperature

5. 1x Assay Buffer for Flow Cytometer (100 mL)

HEPES (1M)	1.0 mL
CaCl_2 (0.1M)	2.8 mL
NaCl (5M)	2.5 mL
ddH ₂ O	93.7 mL

Store at 4°C

6. Hank's buffered salt solution (HBSS) (1 L)

Hank balance salt powder	9.8 g
NaHCO_3	0.35 g
ddH ₂ O	850 mL

Adjust pH to 7.24 with 1 N HCl or 1 N NaOH

Add ddH₂O to 1 L and sterilized by filtering through a 0.2 sterile membrane filter

Store at room temperature

7. Separating buffer (500 mL)

Tris base	45.43 g
ddH ₂ O	350 mL

Adjust pH to 8.8 with 1 N HCl or 1 N NaOH

Add ddH₂O to 500 mL

Store at 4°C

8. Stacking buffer (500 mL)

Tris base	15.14 g
-----------	---------

ddH ₂ O	350 mL
--------------------	--------

Adjust pH to 6.8 with 1 N HCl or 1 N NaOH

Add ddH₂O to 500 mL

Store at 4°C

9. Sample diluting buffer (SDB) (225 mL)

Stacking buffer	31.25 mL
-----------------	----------

10% Sodium dodecyl sulfate (SDS)	50 mL
----------------------------------	-------

Pyronin Y (0.5% stock)	5 mL
------------------------	------

Bromophenol blue (0.5% stock)	5 mL
-------------------------------	------

Glycerol	50 mL
----------	-------

Add ddH₂O to 225 mL

Store at room temperature

10. 10X Laemli buffer (1L)

Tris base	30.25 g
-----------	---------

Glycine	144 g
---------	-------

Sodium dodecyl sulfate (SDS)	10 g
------------------------------	------

ddH ₂ O	700 mL
--------------------	--------

Add ddH₂O to 1 L

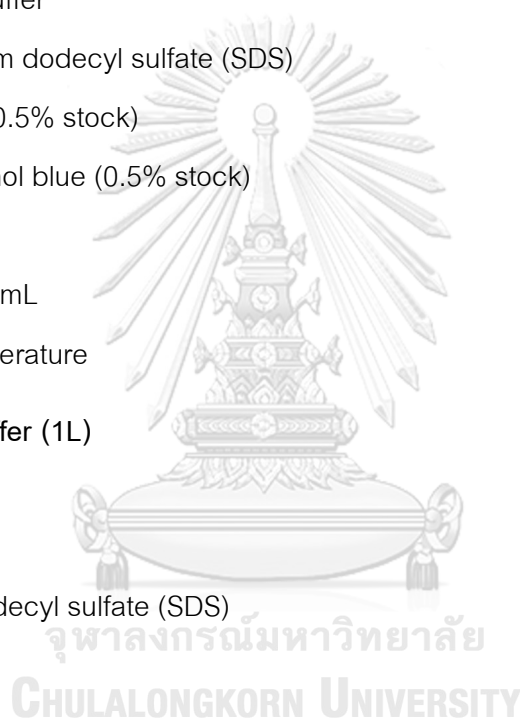
Store at 4°C

11. 1X Laemli buffer (1L)

10X Laemli buffer	100 mL
-------------------	--------

ddH ₂ O	900 mL
--------------------	--------

Store at 4°C



12. 10X Tris-Buffered Saline (TBS) (1L)

Tris base	12.1 g
NaCl	87.5 g
ddH ₂ O	800 mL

Adjust pH to 7.4 with 1 N HCl or 1 N NaOH

Add ddH₂O to 1 L

Store at 4°C

13. 1X Tris-Buffered Saline (TBS) (1L)

10X Tris-Buffered Saline (TBS)	100 mL
ddH ₂ O	900 mL

Store at 4°C

14. 1X Tris-Buffered Saline (TBS)/Tween buffer (1L)

Tween 20	0.5 mL
1X Tris-Buffered Saline (TBS)	999.5 mL

Store at 4°C

15. 10X Transfer buffer (1L)

Tris base	30 g
Glycine	144 g
Sodium dodecyl sulfate (SDS)	1 g
ddH ₂ O	700 mL

Add ddH₂O to 1 L

Store at 4°C

16. 1X Transfer buffer (1L)

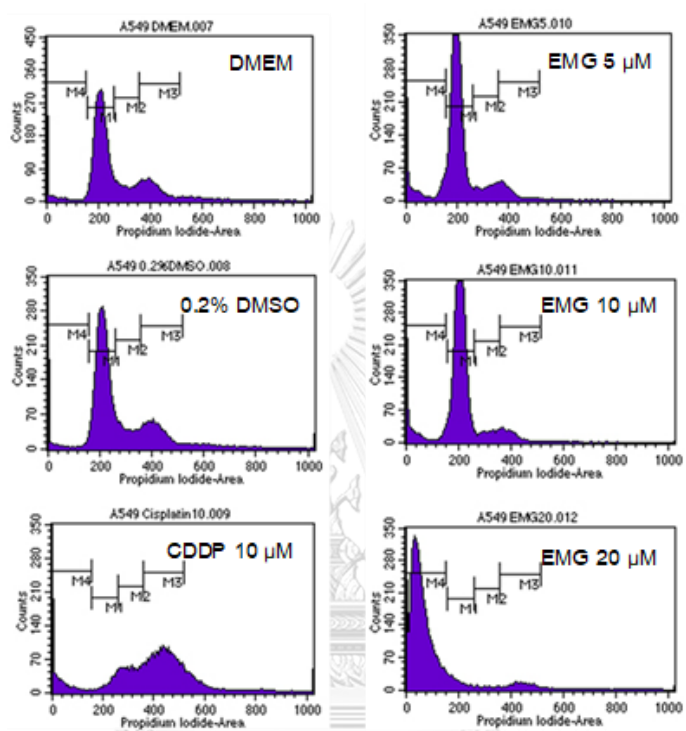
10X Transfer buffer	100 mL
Methanol	200 mL
ddH ₂ O	700 mL

Store at 4°C

APPENDIX B

RESULTS

Appendix B-1: The cytograms of cell cycle distribution in A549 cells (EGFR wild type) after treatment with 5, 10 and 20 μM of EMG and 10 μM of CDDP for 24 h

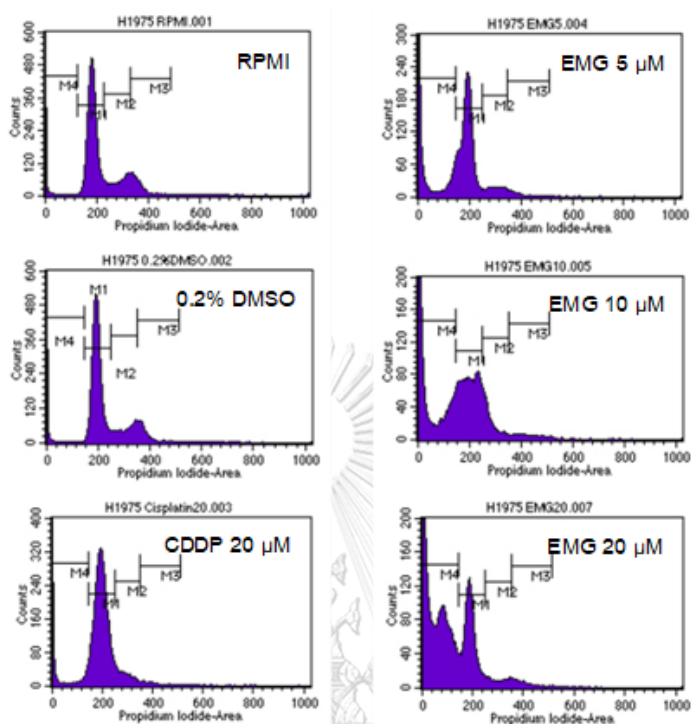


Appendix B-2: Distribution of A549 cells in the cell cycle phases after treatment with 5, 10 and 20 μM of EMG and 10 μM of CDDP for 24 h

Treatment	% Cell population			
	Sub-G ₁	G ₁	S	G ₂ /M
Untreated	3.26±0.75	53.97±1.38	16.29±1.65	17.27±0.75
0.2%DMSO	3.84±0.79	53.86±1.01	17.30±2.17	15.16±1.38
Cisplatin 10 μM	6.52±2.66	6.44±2.99	13.44±2.10	36.09±1.13
EMG 5 μM	5.45±1.86	64.21±0.43	11.53±1.63	11.01±2.23
EMG 10 μM	4.83±1.53	67.84±1.03	9.36±1.26	8.69±1.45
EMG 20 μM	65.99±7.01	3.86±1.15	1.72±0.11	7.28±2.57

Data represent mean±SEM from three independent experiments.

Appendix B-3: The cytograms of cell cycle distribution in H1975 cells (EGFR mutant) after treatment with 5, 10 and 20 μM of EMG and 20 μM of CDDP for 24 h

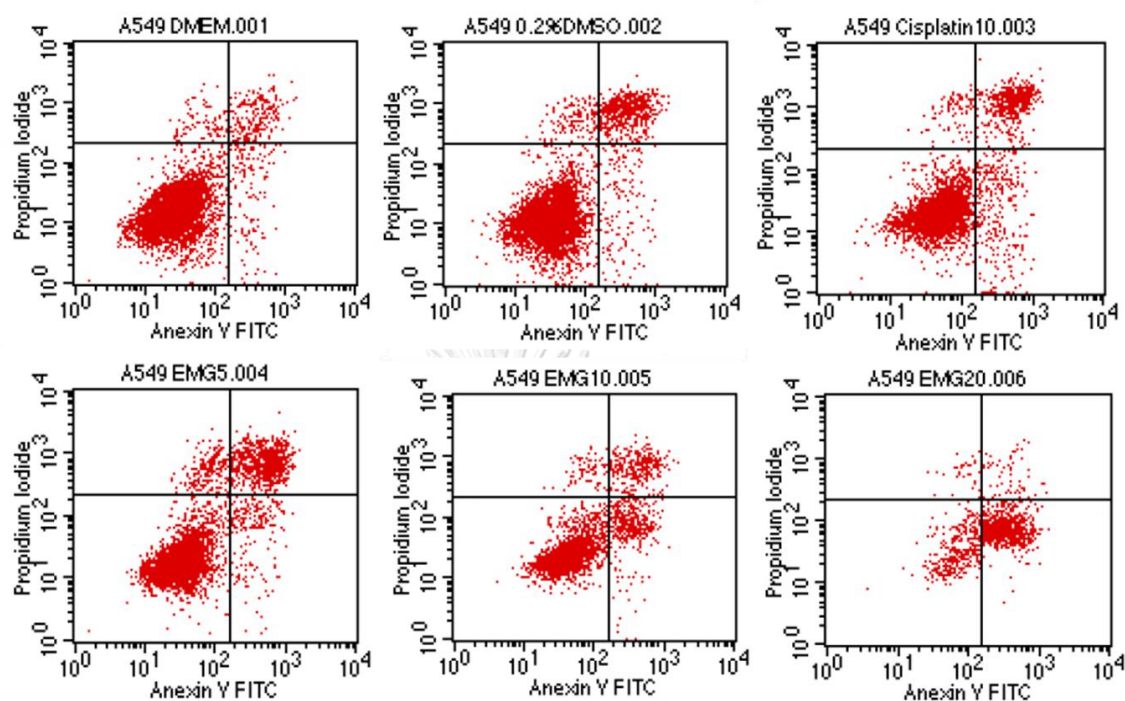


Appendix B-4: Distribution of H1975 cells in the cell cycle phases after treatment with 5, 10 and 20 μM of EMG and 20 μM of CDDP for 24 h

Treatment	% Cell population			
	Sub-G ₁	G ₁	S	G ₂ /M
Untreated	10.85±1.64	56.75±1.98	13.33±2.22	17.15±2.63
0.2%DMSO	8.94±3.52	59.14±1.98	14.31±1.68	13.64±2.27
Cisplatin 20 μM	6.55±1.02	60.11±1.93	8.85±0.42	2.78±0.53
EMG 5 μM	13.17±1.99	40.74±3.62	5.75±0.39	4.64±1.51
EMG 10 μM	29.00±1.65	28.43±2.73	5.41±0.77	3.41±0.56
EMG 20 μM	49.74±1.03	19.46±0.35	3.24±0.13	2.43±0.14

Data represent mean±SEM from three independent experiments.

Appendix B-5: Representative cytograms of cell apoptosis analysis of A549 cells after treatment with 5, 10 and 20 μM of EMG and 10 μM of CDDP for 24 h

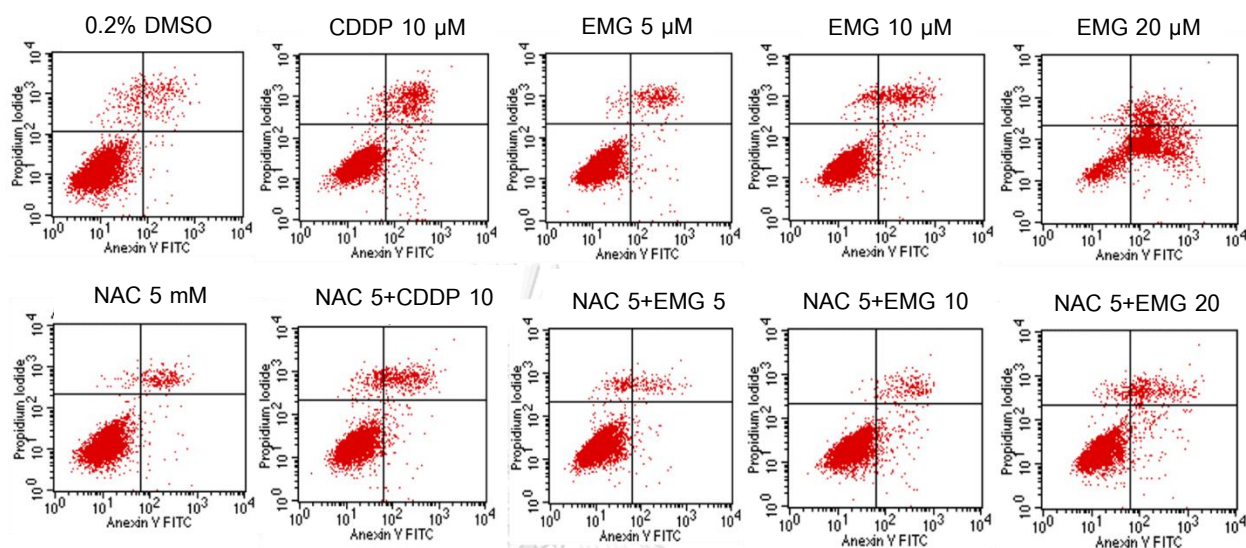


Appendix B-6: The percentage of apoptotic and necrotic cells of A549 cells after treatment with 5, 10 and 20 μM of EMG and 10 μM of CDDP for 24 h

Treatment	Cell population (%)		
	Alive	Apoptosis	Necrosis
Untreated	89.58±0.82	8.98±0.98	1.44±0.19
0.2%DMSO	84.69±0.69	13.36±0.35	1.96±0.41
Cisplatin 10 μM	76.78±0.97	21.71±0.99	1.51±0.56
EMG 5 μM	79.04±2.60	18.88±1.39	2.09±1.26
EMG 10 μM	74.91±1.51	24.07±1.37	1.35±0.71
EMG 20 μM	17.48±4.72	80.70±5.10	1.83±0.60

Data represent mean±SEM from three independent experiments.

Appendix B-7: Representative cytograms of cell apoptosis analysis of A549 cells after treatment with or without 5 mM of NAC for 1 h and then treated with 5, 10 and 20 μ M of EMG and 10 μ M of CDDP for 24 h

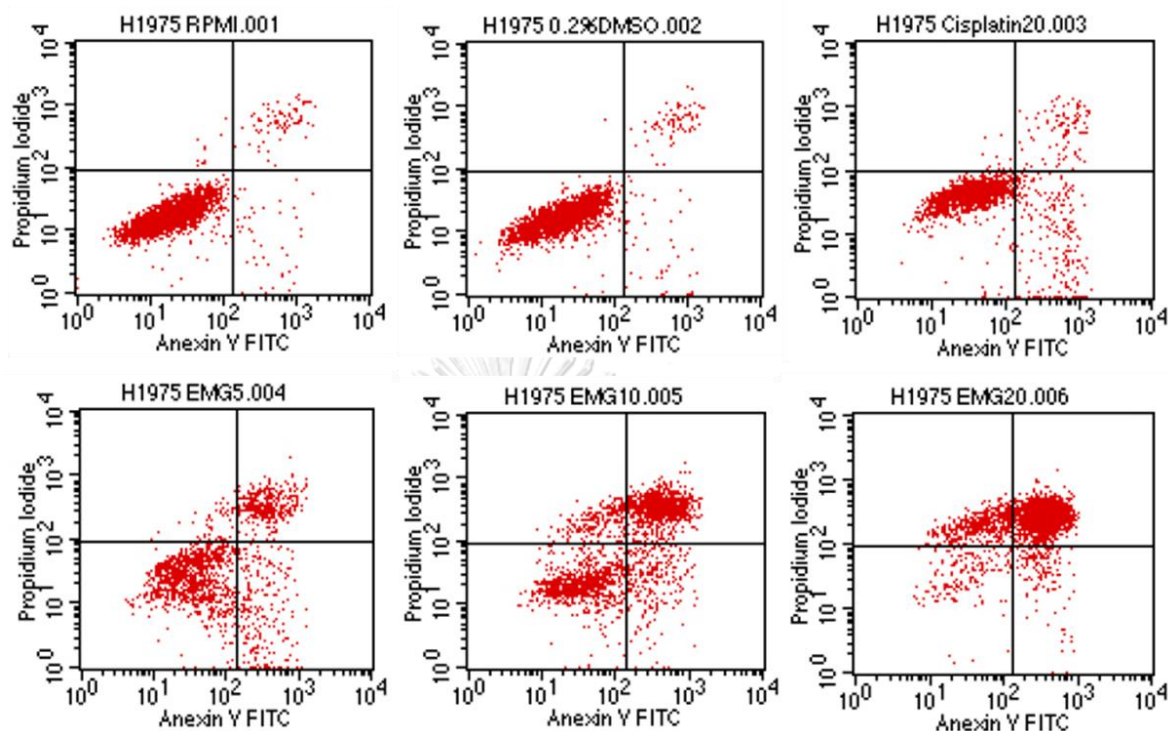


Appendix B-8: The percentage of apoptotic cells of A549 cells after treatment with or without 5 mM of NAC for 1 h and then treated with 5, 10 and 20 μ M of EMG and 10 μ M of CDDP for 24 h

Treatment	Cell population (%)	
	NAC 5 mM	
	+	-
0.2%DMSO	3.96±1.12	3.71±0.95
Cisplatin 10 μ M	6.86±1.93	23.62±5.86
EMG 5 μ M	3.52±1.18	7.89±2.44
EMG 10 μ M	6.66±1.50	9.63±1.97
EMG 20 μ M	23.33±11.56	75.24±5.88

Data represent mean±SEM from three independent experiments

Appendix B-9: Representative cytograms of cell apoptosis analysis of H1975 cells after treatment with 5, 10 and 20 μM of EMG and 20 μM of CDDP for 24 h

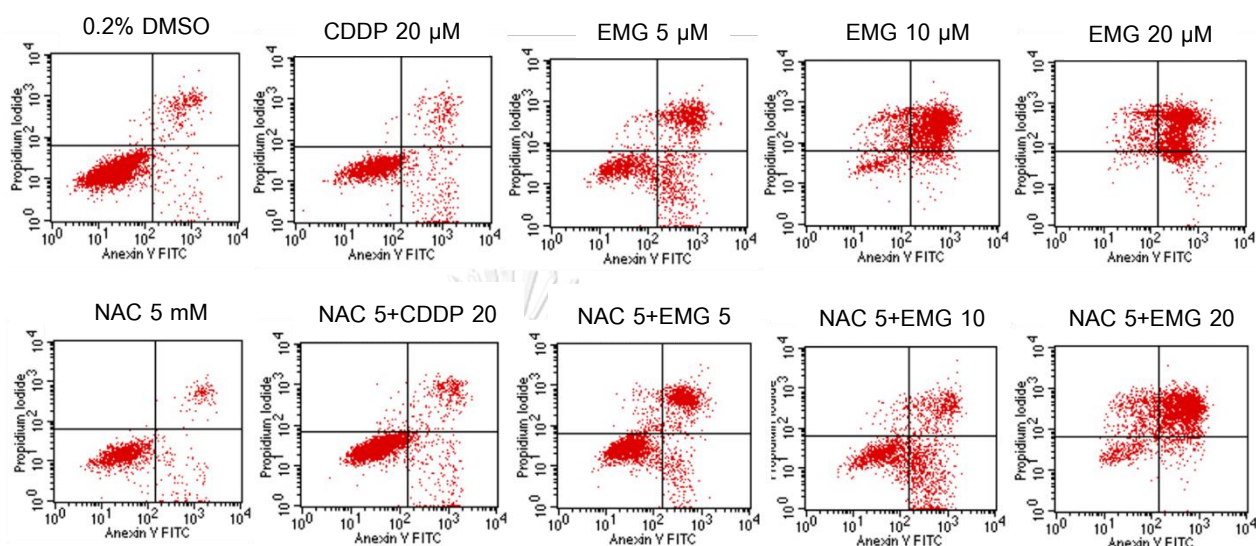


Appendix B-10: The percentage of apoptotic and necrotic cells of H1975 cells after treatment with 5, 10 and 20 μM of EMG and 20 μM of CDDP for 24 h

Treatment	Cell population (%)		
	Alive	Apoptosis	Necrosis
Untreated	93.96±0.85	5.64±0.72	0.40±0.17
0.2%DMSO	93.75±1.05	5.97±0.99	0.28±0.07
Cisplatin 20 μM	77.69±2.26	21.87±2.41	0.45±0.15
EMG 5 μM	51.58±7.05	45.85±7.10	2.57±0.23
EMG 10 μM	25.52±8.54	62.88±7.21	11.61±1.34
EMG 20 μM	5.44±1.40	79.16±2.61	15.40±1.34

Data represent mean±SEM from three independent experiments.

Appendix B-11: Representative cytograms of cell apoptosis analysis of H1975 cells after treatment with or without 5 mM of NAC for 1 h and then treated with 5, 10 and 20 μ M of EMG and 20 μ M of CDDP for 24 h



Appendix B-12: The percentage of apoptotic cells of H1975 cells after treatment with or without 5 mM of NAC for 1 h and then treated with 5, 10 and 20 μ M of EMG and 20 μ M of CDDP for 24 h

Treatment	Cell population (%)	
	NAC 5 mM	
	+	-
0.2%DMSO	10.49±2.13	5.97±0.99
Cisplatin 20 μ M	13.41±2.15	21.87±2.41
EMG 5 μ M	30.42±2.07	45.94±7.01
EMG 10 μ M	40.49±5.44	62.88±7.21
EMG 20 μ M	57.61±7.96	79.16±2.61

Data represent mean±SEM from three independent experiments

REFERENCES

1. Siegel RL, *et al.* Cancer statistics, 2019. CA: A Cancer Journal for Clinicians. 2019;69(1):7-34.
2. GC O. Lung cancer fact sheet. International Agency for Reserch on Cancer. 2018:1-2.
3. Imsamran W, *et al.* Hospital-based cancer registry annual report 2017. J Natl Cancer Inst. 2018;32:1-94.
4. Lemjabbar-Alaoui H, *et al.* Lung cancer: Biology and treatment options. Biochimica et biophysica acta. 2015;1856(2):189-210.
5. Hensing T, *et al.* A Personalized Treatment for Lung Cancer: Molecular Pathways, Targeted Therapies, and Genomic Characterization. In: Maltsev N, Rzhetsky A, Gilliam TC, editors. Systems Analysis of Human Multigene Disorders. New York, NY: Springer New York; 2014. p. 85-117.
6. Bethune G, *et al.* Epidermal growth factor receptor (EGFR) in lung cancer: an overview and update. J THORAC DIS. 2010;2(1):48-51.
7. Sosa Iglesias V, *et al.* Drug Resistance in Non-Small Cell Lung Cancer: A Potential for NOTCH Targeting? Front Oncol. 2018;8:267-.
8. Shigematsu H and Gazdar AF. Somatic mutations of epidermal growth factor receptor signaling pathway in lung cancers. International Journal of Cancer. 2006;118(2):257-62.
9. Wu S-G and Shih J-Y. Management of acquired resistance to EGFR TKI-targeted therapy in advanced non-small cell lung cancer. Mol Cancer. 2018;17(1):38-.
10. Jorge SEDC, *et al.* Epidermal growth factor receptor (EGFR) mutations in lung cancer: preclinical and clinical data. Brazilian Journal of Medical and Biological Research. 2014;47:929-39.
11. Ray PD, *et al.* Reactive oxygen species (ROS) homeostasis and redox regulation in cellular signaling. Cell Signal. 2012;24(5):981-90.

12. Yang H, *et al.* The role of cellular reactive oxygen species in cancer chemotherapy. *J Exp Clin Cancer Res.* 2018;37(1):266-.
13. Hairani R, *et al.* Allyl and prenyl ethers of mansonone G, new potential semisynthetic antibacterial agents. *Bioorg Med Chem Lett.* 2016;26(21):5300-3.
14. Kim HK, *et al.* CBMG, a novel derivative of mansonone G suppresses adipocyte differentiation via suppression of PPAR γ activity. *Chem Biol Interact.* 2017;273(Supplement C):160-70.
15. Tiew P, *et al.* Antifungal, antioxidant and larvicidal activities of compounds isolated from the heartwood of *Mansonia gagei*. *Phytother Res.* 2003;17(2):190-3.
16. El-Halawany AM, *et al.* Anti-estrogenic activity of mansonins and mansonones from the heartwood of *Mansonia gagei* DRUMM. *Chemical & pharmaceutical bulletin.* 2007;55(9):1332-7.
17. Wang D, *et al.* Cytotoxic effects of mansonone E and F isolated from *Ulmus pumila*. *Biol Pharm Bull.* 2004;27(7):1025-30.
18. Wang D, *et al.* Cytotoxic effects of mansonone E and F isolated from *Ulmus pumila*. *Biol Pharm Bull.* 2004;27(7):1025-30.
19. Boonsri S, *et al.* Cytotoxic and Antibacterial Sesquiterpenes from *Thespesia populnea*. *Journal of Natural Products.* 2008;71(7):1173-7.
20. Hairani R, *et al.* CBMG, a novel derivative of mansonone G suppresses adipocyte differentiation via suppression of PPAR γ activity. *Chemico-Biological Interactions.* 2017;273:160-70.
21. Siegel RL, *et al.* Cancer statistics, 2019. *CA: a cancer journal for clinicians.* 2019;69(1):7-34.
22. Malhotra J, *et al.* Risk factors for lung cancer worldwide. *The European respiratory journal.* 2016;48(3):889-902.
23. Akhtar N and Bansal JG. Risk factors of Lung Cancer in nonsmoker. *Current Problems in Cancer.* 2017;41(5):328-39.
24. Zappa C and Mousa SA. Non-small cell lung cancer: current treatment and future advances. *Transl Lung Cancer Res.* 2016;5(3):288-300.

25. Chemotherapy in non-small cell lung cancer: a meta-analysis using updated data on individual patients from 52 randomised clinical trials. Non-small Cell Lung Cancer Collaborative Group. *BMJ (Clinical research ed)*. 1995;311(7010):899-909.
26. Souhami R. Lung Cancer. *BMJ: British Medical Journal*. 1992;304(6837):1298-301.
27. Wang D and Lippard SJ. Cellular processing of platinum anticancer drugs. *Nat Rev Drug Discov*. 2005;4(4):307-20.
28. Boulikas T and Vougiouka M. Cisplatin and platinum drugs at the molecular level. (Review). *Oncology reports*. 2003;10(6):1663-82.
29. Fong CW. Platinum anti-cancer drugs: Free radical mechanism of Pt-DNA adduct formation and anti-neoplastic effect. *Free radical biology & medicine*. 2016;95:216-29.
30. Astolfi L, *et al*. Correlation of adverse effects of cisplatin administration in patients affected by solid tumours: a retrospective evaluation. *Oncology reports*. 2013;29(4):1285-92.
31. Oun R, *et al*. The side effects of platinum-based chemotherapy drugs: a review for chemists. *Dalton transactions (Cambridge, England : 2003)*. 2018;47(19):6645-53.
32. Kampan NC, *et al*. Paclitaxel and Its Evolving Role in the Management of Ovarian Cancer. *BioMed research international*. 2015;2015:413076.
33. George J, *et al*. Molecular Mechanisms of Taxol for Induction of Cell Death in Glioblastomas. 2010. p. 283-98.
34. Mukherji SK. Bevacizumab (Avastin). *American Journal of Neuroradiology*. 2010;31(2):235.
35. Kazazi-Hyseni F, *et al*. Bevacizumab. *The oncologist*. 2010;15(8):819-25.
36. Sun S, *et al*. New molecularly targeted therapies for lung cancer. *The Journal of Clinical Investigation*. 2007;117(10):2740-50.
37. Chan BA and Hughes BGM. Targeted therapy for non-small cell lung cancer: current standards and the promise of the future. *Translational Lung Cancer Research*; Vol 4, No 1 (February 2015): *Translational Lung Cancer Research*. 2014.
38. Shtivelman E, *et al*. Molecular pathways and therapeutic targets in lung cancer. *Oncotarget*. 2014;5(6):1392-433.

39. Kiyohara Y, *et al.* Erlotinib-related skin toxicities: Treatment strategies in patients with metastatic non-small cell lung cancer. *Journal of the American Academy of Dermatology.* 2013;69(3):463-72.
40. Ding S, *et al.* Acute myocardial infarction following erlotinib treatment for NSCLC: A case report. *Oncology letters.* 2016;11(6):4240-4.
41. Johnson DG and Walker CL. CYCLINS AND CELL CYCLE CHECKPOINTS. *Annual Review of Pharmacology and Toxicology.* 1999;39(1):295-312.
42. Blackstone Neil W. *Molecular Biology of the Cell.* Fourth Edition. By Bruce Alberts, Alexander Johnson, Julian Lewis, Martin Raff, Keith Roberts, and Peter Walter. *The Quarterly Review of Biology.* 2003;78(1):91-2.
43. Schafer KA. The Cell Cycle: A Review. *Veterinary Pathology.* 1998;35(6):461-78.
44. Collins K, *et al.* The cell cycle and cancer. *Proc Natl Acad Sci U S A.* 1997;94(7):2776-8.
45. Eymin B and Gazzeri S. Role of cell cycle regulators in lung carcinogenesis. *Cell Adh Migr.* 2010;4(1):114-23.
46. King KL and Cidlowski JA. CELL CYCLE REGULATION AND APOPTOSIS. *Annual Review of Physiology.* 1998;60(1):601-17.
47. García-Reyes B, *et al.* The Emerging Role of Cyclin-Dependent Kinases (CDKs) in Pancreatic Ductal Adenocarcinoma. *International Journal of Molecular Sciences.* 2018;19(10).
48. Simone F and Klaus-Michael D. Targeting Apoptosis Pathways in Cancer Therapy. *Current Cancer Drug Targets.* 2004;4(7):569-76.
49. Fulda S and Debatin KM. Extrinsic versus intrinsic apoptosis pathways in anticancer chemotherapy. *Oncogene.* 2006;25(34):4798-811.
50. Locksley RM, *et al.* The TNF and TNF receptor superfamilies: integrating mammalian biology. *Cell.* 2001;104(4):487-501.
51. Kumar R, *et al.* An introduction to death receptors in apoptosis. *International Journal of Surgery.* 2005;3(4):268-77.

52. Schultz DR and Harrington WJ. Apoptosis: Programmed cell death at a molecular level. *Seminars in Arthritis and Rheumatism*. 2003;32(6):345-69.
53. Elmore S. Apoptosis: a review of programmed cell death. *Toxicologic pathology*. 2007;35(4):495-516.
54. Blanco A and Blanco G. Chapter 32 - Apoptosis. In: Blanco A, Blanco G, editors. *Medical Biochemistry*: Academic Press; 2017. p. 791-6.
55. Opferman JT and Kothari A. Anti-apoptotic BCL-2 family members in development. *Cell Death Differ*. 2018;25(1):37-45.
56. Chapter 10 - Programmed Cell Death. In: Goodman SR, editor. *Medical Cell Biology (Third Edition)*. San Diego: Academic Press; 2008. p. 291-307.
57. Tait SWG and Green DR. Mitochondria and cell death: outer membrane permeabilization and beyond. *Nature Reviews Molecular Cell Biology*. 2010;11:621.
58. Covarrubias L, *et al*. Function of reactive oxygen species during animal development: Passive or active? *Developmental Biology*. 2008;320(1):1-11.
59. Brieger K, *et al*. Reactive oxygen species: from health to disease. *Swiss medical weekly*. 2012;142:w13659.
60. Kehrer JP and Klotz LO. Free radicals and related reactive species as mediators of tissue injury and disease: implications for Health. *Critical reviews in toxicology*. 2015;45(9):765-98.
61. Redza-Dutordoir M and Averill-Bates DA. Activation of apoptosis signalling pathways by reactive oxygen species. *Biochimica et Biophysica Acta (BBA) - Molecular Cell Research*. 2016;1863(12):2977-92.
62. Navaneetha Krishnan S, *et al*. ROS-Mediated Cancer Cell Killing through Dietary Phytochemicals. *Oxidative Medicine and Cellular Longevity*. 2019;2019:16.
63. Yokoyama C, *et al*. Induction of oxidative stress by anticancer drugs in the presence and absence of cells. *Oncol Lett*. 2017;14(5):6066-70.
64. Wu YJ, *et al*. The Chemoprotective Agent &emdash;N&emdash;Acetylcysteine Blocks Cisplatin-Induced Apoptosis through Caspase Signaling Pathway. *Journal of Pharmacology and Experimental Therapeutics*. 2005;312(2):424.

65. Conklin KA. Chemotherapy-associated oxidative stress: impact on chemotherapeutic effectiveness. *Integrative cancer therapies*. 2004;3(4):294-300.
66. Srinivas P, *et al.* Plumbagin induces reactive oxygen species, which mediate apoptosis in human cervical cancer cells. *Molecular Carcinogenesis*. 2004;40(4):201-11.
67. Liang W, *et al.* Shikonin induces ROS-based mitochondria-mediated apoptosis in colon cancer. *Oncotarget*. 2017;8(65):109094-106.
68. Mazumder A and Diederich M. *Natural Compound-Generated Oxidative Stress: From Bench to Bedside*. 2016.
69. Sznarkowska A, *et al.* Inhibition of cancer antioxidant defense by natural compounds. *Oncotarget*. 2017;8(9):15996-6016.
70. Wee P and Wang Z. Epidermal Growth Factor Receptor Cell Proliferation Signaling Pathways. *Cancers (Basel)*. 2017;9(5):52.
71. Brambilla E and Gazdar A. Pathogenesis of lung cancer signalling pathways: roadmap for therapies. *The European respiratory journal*. 2009;33(6):1485-97.
72. Katz M, *et al.* Regulation of MAPKs by growth factors and receptor tyrosine kinases. *Biochimica et biophysica acta*. 2007;1773(8):1161-76.
73. Cargnello M and Roux PP. Activation and function of the MAPKs and their substrates, the MAPK-activated protein kinases. *Microbiol Mol Biol Rev*. 2011;75(1):50-83.
74. Molina JR and Adjei AA. The Ras/Raf/MAPK Pathway. *Journal of Thoracic Oncology*. 2006;1(1):7-9.
75. Meister M, *et al.* Mitogen-Activated Protein (MAP) Kinase Scaffolding Proteins: A Recount. *International Journal of Molecular Sciences*. 2013;14(3).
76. Hemmings BA and Restuccia DF. PI3K-PKB/Akt pathway. *Cold Spring Harb Perspect Biol*. 2012;4(9):a011189-a.
77. Liu P, *et al.* Targeting the phosphoinositide 3-kinase pathway in cancer. *Nature reviews Drug discovery*. 2009;8(8):627-44.
78. Hemmings BA and Restuccia DF. PI3K-PKB/Akt Pathway. *Cold Spring Harb Perspect Biol*. 2012;4(9).

79. Yu JSL and Cui W. Proliferation, survival and metabolism: the role of PI3K/AKT/mTOR signalling in pluripotency and cell fate determination. *Development*. 2016;143(17):3050.
80. Garcia-Echeverria C and Sellers WR. Drug discovery approaches targeting the PI3K/Akt pathway in cancer. *Oncogene*. 2008;27:5511.
81. Pongboonrod S. *Mai Tet Muang Thai*. 1976:162-3.
82. Tiew P, *et al.* Coumarins from the heartwoods of *Mansonia gagei* Drumm. *Phytochemistry*. 2002;60(8):773-6.
83. Tiew P, *et al.* Four new sesquiterpenoid derivatives from the heartwood of *Mansonia gagei*. *J NAT PROD*. 2002;65(9):1332-5.
84. Mongkol R and Chavasiri W. Antimicrobial, herbicidal and antifeedant activities of mansonone E from the heartwoods of *Mansonia gagei* Drumm. *Journal of Integrative Agriculture*. 2016;15(12):2795-802.
85. Tiew P, *et al.* Antifungal, antioxidant and larvicidal activities of compounds isolated from the heartwood of *Mansonia gagei*. *Phytotherapy Research*. 2003;17(2):190-3.
86. El-Halawany AM, *et al.* Anti-estrogenic activity of mansonone G and mansorin A derivatives. *Pharmaceutical Biology*. 2013;51(8):948-54.
87. Hairani R, *et al.* Allyl and prenyl ethers of mansonone G, new potential semisynthetic antibacterial agents. *Bioorganic & Medicinal Chemistry Letters*. 2016;26(21):5300-3.
88. Qiu HY, *et al.* Naphthoquinones: A continuing source for discovery of therapeutic antineoplastic agents. *Chemical biology & drug design*. 2018;91(3):681-90.
89. Bai J, *et al.* Cell cycle regulation and anticancer drug discovery. *Cancer Biol Med*. 2017;14(4):348-62.
90. Dasari S and Tchounwou PB. Cisplatin in cancer therapy: molecular mechanisms of action. *European journal of pharmacology*. 2014;740:364-78.
91. Hassan M, *et al.* Apoptosis and molecular targeting therapy in cancer. *BioMed research international*. 2014;2014:150845-.
92. Ricci MS and Zong W-X. Chemotherapeutic approaches for targeting cell death pathways. *The oncologist*. 2006;11(4):342-57.

93. Morales J, *et al.* Review of poly (ADP-ribose) polymerase (PARP) mechanisms of action and rationale for targeting in cancer and other diseases. *Crit Rev Eukaryot Gene Expr.* 2014;24(1):15-28.
94. Sharma SV, *et al.* Epidermal growth factor receptor mutations in lung cancer. *Nature reviews Cancer.* 2007;7(3):169-81.
95. Wu C-Y, *et al.* Anticancer activity of Astragalus polysaccharide in human non-small cell lung cancer cells. *Cancer Cell International.* 2017;17(1):115.
96. El-Halawany AM, *et al.* Anti-estrogenic activity of mansonone G and mansorin A derivatives. *Pharm Biol.* 2013;51(8):948-54.
97. Dai Y, *et al.* Isolation and synthesis of two antiproliferative calamenene-type sesquiterpenoids from *Sterculia tavia* from the Madagascar Rain Forest. *Bioorganic & Medicinal Chemistry.* 2012;20(24):6940-4.
98. Chonsut P, *et al.* Ethoxy mansonone G as an anticancer agent in estrogen receptor-positive and endocrine-resistant breast cancer. *Journal of Pharmacy and Pharmacology.* 2019.
99. Amanullah A, *et al.* Indomethacin elicits proteasomal dysfunctions develops apoptosis through mitochondrial abnormalities. *Journal of cellular physiology.* 2018;233(2):1685-99.
100. Galadari S, *et al.* Reactive oxygen species and cancer paradox: To promote or to suppress? *Free radical biology & medicine.* 2017;104:144-64.
101. Qiu H-Y, *et al.* Naphthoquinones: A continuing source for discovery of therapeutic antineoplastic agents. *Chemical biology & drug design.* 2018;91(3):681-90.
102. Tafani M, *et al.* The Interplay of Reactive Oxygen Species, Hypoxia, Inflammation, and Sirtuins in Cancer Initiation and Progression. *Oxid Med Cell Longev.* 2016;2016:3907147.
103. Wu H-Y, *et al.* Ergosterol peroxide from marine fungus *Phoma* sp. induces ROS-dependent apoptosis and autophagy in human lung adenocarcinoma cells. *Scientific Reports.* 2018;8(1):17956.

104. Alimbetov D, *et al.* Pharmacological Targeting of Cell Cycle, Apoptotic and Cell Adhesion Signaling Pathways Implicated in Chemoresistance of Cancer Cells. *Int J Mol Sci.* 2018;19(6).
105. Zhang Y, *et al.* The design of 1,4-naphthoquinone derivatives and mechanisms underlying apoptosis induction through ROS-dependent MAPK/Akt/STAT3 pathways in human lung cancer cells. *Bioorganic & Medicinal Chemistry.* 2019;27(8):1577-87.
106. Sarin N, *et al.* Cisplatin resistance in non-small cell lung cancer cells is associated with an abrogation of cisplatin-induced G2/M cell cycle arrest. *PLoS One.* 2017;12(7):e0181081-e.
107. Kruse JP and Gu W. Modes of p53 regulation. *Cell.* 2009;137(4):609-22.
108. Reisman D, *et al.* Transcriptional Regulation of the p53 Tumor Suppressor Gene in S-Phase of the Cell-Cycle and the Cellular Response to DNA Damage. *Biochem Res Int.* 2012;2012:808934-.
109. Hsu Y-L, *et al.* Plumbagin (5-Hydroxy-2-methyl-1,4-naphthoquinone) Induces Apoptosis and Cell Cycle Arrest in A549 Cells through p53 Accumulation via c-Jun NH2-Terminal Kinase-Mediated Phosphorylation at Serine 15 in Vitro and in Vivo. *The Journal of pharmacology and experimental therapeutics.* 2006;318:484-94.
110. Pereyra CE, *et al.* The diverse mechanisms and anticancer potential of naphthoquinones. *Cancer Cell International.* 2019;19(1):207.
111. Li J and Yuan J. Caspases in apoptosis and beyond. *Oncogene.* 2008;27(48):6194-206.
112. Chaitanya GV, *et al.* PARP-1 cleavage fragments: signatures of cell-death proteases in neurodegeneration. *Cell Commun Signal.* 2010;8:31-.
113. Herceg Z and Wang Z-Q. Failure of Poly(ADP-Ribose) Polymerase Cleavage by Caspases Leads to Induction of Necrosis and Enhanced Apoptosis. *Molecular and Cellular Biology.* 1999;19(7):5124.
114. Gobeil S, *et al.* Characterization of the necrotic cleavage of poly(ADP-ribose) polymerase (PARP-1): implication of lysosomal proteases. *Cell Death & Differentiation.* 2001;8(6):588-94.

115. Tian R-H, *et al.* Involvement of poly(ADP-ribose) polymerase and activation of caspase-3-like protease in heat shock-induced apoptosis in tobacco suspension cells. *FEBS Letters*. 2000;474(1):11-5.
116. Lyakhovich A and Surrallés J. Constitutive Activation of Caspase-3 and Poly ADP Ribose Polymerase Cleavage in Fanconi Anemia Cells. *Molecular Cancer Research*. 2010;8(1):46.
117. Del Bello B, *et al.* Role of caspases-3 and -7 in Apaf-1 proteolytic cleavage and degradation events during cisplatin-induced apoptosis in melanoma cells. *Experimental Cell Research*. 2004;293(2):302-10.
118. Henkels KM and Turchi JJ. Cisplatin-induced Apoptosis Proceeds by Caspase-3-dependent and -independent Pathways in Cisplatin-resistant and -sensitive Human Ovarian Cancer Cell Lines. *Cancer Research*. 1999;59(13):3077.
119. Gonzalez VM, *et al.* Is cisplatin-induced cell death always produced by apoptosis? *Molecular pharmacology*. 2001;59(4):657-63.
120. Paraiso KHT, *et al.* Measurement of constitutive MAPK and PI3K/AKT signaling activity in human cancer cell lines. *Methods Enzymol*. 2010;484:549-67.
121. Cheng H, *et al.* Targeting the PI3K/AKT/mTOR pathway: potential for lung cancer treatment. *Lung Cancer Manag*. 2014;3(1):67-75.
122. Tsai M-H, *et al.* Artocarpin, an isoprenyl flavonoid, induces p53-dependent or independent apoptosis via ROS-mediated MAPKs and Akt activation in non-small cell lung cancer cells. *Oncotarget*. 2017;8(17):28342-58.
123. Wang J-P, *et al.* The collective nuclear migration of p53 and phosphorylated S473 of Akt during ellipticine-mediated apoptosis in human lung epithelial cancer cells. *Molecular and Cellular Biochemistry*. 2015;407(1):123-33.
124. Zhuang S and Schnellmann RG. A Death-Promoting Role for Extracellular Signal-Regulated Kinase. *Journal of Pharmacology and Experimental Therapeutics*. 2006;319(3):991.

125. Mahalapbutr P, *et al.* Butoxy Mansonone G Inhibits STAT3 and Akt Signaling Pathways in Non-Small Cell Lung Cancers: Combined Experimental and Theoretical Investigations. *Cancers (Basel)*. 2019;11(4).
126. Jung SK, *et al.* Isoliquiritigenin induces apoptosis and inhibits xenograft tumor growth of human lung cancer cells by targeting both wild type and L858R/T790M mutant EGFR. *J Biol Chem*. 2014;289(52):35839-48.



VITA

NAME Arachawipa Wannachote

DATE OF BIRTH 18 March 1993

INSTITUTIONS ATTENDED Bachelor of Science in Biology, Chulalongkorn University

